DETAILED THERMAL ANALYSIS OF A THIN-SHELL, SPHERICAL RADIOMETER IN EARTH ORBIT

by

John Oliver Passwaters, III

Thesis submitted to the Graduate Faculty of the
Virginia Polytechnic Institute and State University
in partial fulfillment of the requirements for the degree of

MASTER OF SCIENCE

in

Mechanical Engineering

APPROVED:

J. R. Mahan, Chairman

W. C. Thomas

F. J. Pierce

May, 1976

Blacksburg, Virginia

ACKNOWLEDGEMENTS

The author would like to express his appreciation to Dr. J. R. Mahan for his encouragement, guidance, patience and assistance in this work.

The author is also indebted to Dr. W. C. Thomas and Dr. F. J. Pierce for their help and for serving on the author's graduate committee.

The author wishes to thank his wife, , for her patience, cooperation and typing.

Appreciation is extended to the National Aeronautics and Space Administration whose financial assistance made this work possible.

Finally, the author wishes to thank Dr. J. B. Jones for his encouragement and guidance.

TABLE OF CONTENTS

LIST OF FIGURES

LIST OF FIGURES (Continued)

NOMENCLATURE

English

Capital

ABSIR	long wavelength absorptance (dimensionless)
ABSORB	the long wavelength absorptance for each incident source of radiant power to each node on the detector as a function of wavelength, temperature, and angle of incidence (dimensionless)
ABSUV	the average short wavelength absorptance for each point in orbit (dimensionless)
ALBEDO	the earth reflected solar power (watts)
ALW	the average long wavelength absorptance for the detector (dimensionless)
ANGLE	the angle for the angle of incidence for the earth emitted power to each node on the detector (radians)
AREATH	the area on the earth viewed by the detector in orbit (M^2)
ASQURD	an intermediate step in the solution of Fresnel's equation
ASW	the short wavelength absorptance averaged for the entire orbit (dimensionless)
AVGALW	the average emittance of the detector for the entire orbit (dimensionless)
AVG	the average short wavelength absorptance of the detector for the orbit (dimensionless)
BNDENG	the amount of energy in a given wavelength interval, based on a Plankian distribution ($W/m^2\mu m$)
BPAR	a variable that defines the position of each subpoint in the earth radiation field
BUF	a variable that defines the season, starting point and other orbital parameters for earth radiation field

BSQURD	an intermediate step in the solution of Fresnel's equation
CBB	the cosine of the angle between the negative of the earth vector and satellite normal vector
CE	the correction factor for the earth-emitted component of the storage array for the Plankian distribution of each source of the earth
CONTAN	emitted flux incident to each node (W/m^2)
CO	the velocity of light in a vacuum (mm/sec)
COUNT	the number of point sources of long wavelength flux incident to the detector surface
CR	the correction factor for the earth reflected solar flux
CS	the correction factor for the solar flux
CSS	the cosine of the angle between the negative of the solar unit vector and the unit normal vector at the point on the detector being considered
DENOM	the denominator in the ratio for the component reflected normal to the direction of progation
DCCOND	the d.c. electrical conductivity of aluminum as a function of temperature (ohm^{-1})
DTM	time increment between each orbital subpoint (sec)
DT	computational time increment used in the energy equation (sec)
E	the charge of an electron, $4{,}80 \times 10^{-10}$ esu
ELW	the long wavelength absorptance for each node on the detector as a function of the nodal temperature (dimensionless)
ENERGY	the long wavelength power absorbed in each wavelength interval ($W/\mu m$)
ENRIN	the total long wavelength power incident to each detector node (W/m^2)

FE	the ratio of the long wavelength absorptance for each node on the detector as a function of temperature, wavelength, and angle of incidence to the average for the orbit
FO	the ratio of the emittance for each node on the detector, as a function of temperature, to the average emittance for the orbit
FR	the ratio of the earth reflected solar absorptance for each detector node as a function of incident angle, to the average absorptance for the orbit
FS	the ratio of the solar absorptance, as a function of angle of incidence to the average solar absorptance for the entire orbit
GETVEC	the subroutine that provides the earth radiation field
HIN	the total flux incident to the point on the detector being investigated (W/m^2)
HS	the incident solar flux to the point on the detector being investigated (W/m^2)
KKKK	number of twenty second intervals in the orbit, ranges from 1 to 325
LCHECK	a command statement to determine the desired solution technique
LIMIT	the number of point sources of radiant energy incident to each node on the detector
NPOINT	the number given each node on the detector
NPS	the number of nodal divisions in the ϕ direction of the satellite
NTS	the number of nodal divisions in the Θ direction of the satellite
NVECTOR	the variable given to each point source of radiant energy that is incident to each node on the detector
PART	an intermediate step in the solution of the Fresnel equations
POMEGA	the plasma frequency for the free electrons (sec^{-1})

P2	2π
PRCNT	the per cent of the total power contained in specific wavelength intervals for a Plankian distribution (%)
PROD	an intermediate step in the solution of the Fresnel equations
RADICL	an intermediate step in the solution of the Fresnel equations
RADSQT	an intermediate step in the solution of the Fresnel equations
RAT, RAT1, RAT2, RAT3, RAT4	terms in determining the emittance of the metallic surface, as a function of surface temperature
REFLEX	the name of the subroutine that determines the absorbed power for the earth reflected solar flux, as a function of angle of incidence
REFMNL	the component of the reflected flux polarized normal to the plane of propagation
REFPAR	the component of the reflected flux polarized parallel to the direction of propagation
RELAXT	the relaxation time of the conduction electrons (sec)
RS	the number of satellites in orbit
RSAT	radius of the satellite (M)
SIG	Stefan-Boltzman constant (5.668×10^{-8} W/m^2 - K^4)
SIGO	the reference d.c. electrical conductivity (at 273 K) of the metal (esu)
SOLAB	the name of the subroutine that determines the short wavelength absorptance as a function of angle of incidence
SOLAR	the storage array for the angle of incidence (radians) for the incident solar flux to each node on the detector

SOURCE	the storage array for the angle of incidence (in radians) for each point source incident to each node point on the detector
SQRPRD	an intermediate step in the solution of Fresnel's equation
STIX	the absorbed earth reflected solar power for each node on the detector (W)
SULABS	the total absorbed earth reflected solar power incident to the entire detector (W)
SUMENT	the total emitted power for the detector at each orbital position (W)
SUMIN	the total long wavelength power absorbed by the entire detector surface (W)
SUMSOL	the total solar power incident to the detector (W)
SUMSQD	an intermediate step in the solution of the Fresnel equations (dimensionless)
SUN	the total solar power incident to the detector at each orbital position (W)
T	temperature distribution of the detector surface (K)
TAU2	the inverse of the relaxation time squared (sec^{-2})
TINCID	the total long wavelength power incident to the detector (W)
TINIT	the initial temperature distribution of the nodes on the detector (K)
TLAM	the blackbody radiation function as prepared by Dunkle are expressed as the product of wavelength and temperature (m/K)
TOTABS	the total long wavelength power absorbed by each detector node point (W)
TOTHIN	the sum of the total absorbed solar, earth emitted and earth reflected solar power (W)
TOTIN	the total earth reflected solar power incident to the entire detector surface (W)

TOTINC	the total earth reflected solar power incident to each node point on the detector surface (W)
TOTREF	the average of the normal and parallel polarized components of reflectance from the Fresnel equations (dimensionless)
TOTSTK	the total earth reflected solar power absorbed by each node point on the detector surface (W)
TTALW	the sum of the long wavelength absorptances for each detector node point (dimensionless)
VECTOR	the storage array for the direction cosines, and the radiant flux originating from each point in the earth radiation field (dimensionless)
VERC	the storage array for the emittance of each point on the detector surface, as a function of temperature (dimensionless)
XLAMDA	the array of wavelength intervals established to decompose the incident long wavelength flux into the Plankian distribution
XMNEFF	the number of electrons per atom involved in the reflecting process
XNK	the product of the extinction coefficient and the index of refraction for use in solving the Fresnel equations
XNORML	the fraction of the reflected flux polarized perpendicular to the direction of propagation
XNUMER	the numerator in the ratio for the component reflected normal to the direction of propagation
XN2K2	the difference between the square of the index of refraction (n^2) and the square of the extinction coefficient (k^2), utilized in the Fresnel equations
XOMEGA	the frequency of the specific wavelength intervals (sec^{-1})
XOMEG2	the square of the frequency of the specific wavelength interval (sec^{-2})
XPARAL	the fraction of the reflected flux polarized parallel to the direction of propagation

XXH	the interior irradiance of the detector for each node point in orbit (W/m^2)
XINFRA	the total earth emitted power incident to the detector for each point in orbit

Lower Case

c_s	specific heat (W-sec/kg-k)
dS	differential surface area on the detector (m^2)
f_e	the nodal correction factor for the absorptance of the earth emitted component
f_i	the nodal correction factor for the absorptance of the interior irradiance
f_o	the nodal correction factor for the emittance of the exterior irradiance
f_I	the nodal correction factor for the emittance on the detector interior
f_s	the nodal correction factor for the absorptance of the solar component
f_r	the nodal correction factor for the absorptance of the earth reflected solar component
i	index for node definition in the Θ direction
j	index for node definition in the ϕ direction
$\dot{q}_e$	the earth emitted flux incident to a node on the detector (W/m^2)
$\dot{q}_s$	the solar flux incident to a node on the detector (W/m^2)
$\dot{q}_r$	the earth reflected solar flux incident to a node on the detector (W/m^2)
$\dot{q}_o$	the long wavelength flux emitted by the exterior surface of the detector (W/m^2)
$\dot{q}_I$	the long wavelength flux emitted by the interior surface of the detector (W/m^2)

t	time (sec)
Δt	incremental time (sec)

Greek

α	radiant absorptance
α_e	long wavelength earth-emitted absorptance
$\bar{\alpha}_e$	the average long wavelength earth-emitted absorptance for the orbit
α_s	the solar absorptance
$\bar{\alpha}_s$	average solar radiant absorptance for the orbit
ε	radiant emittance
ε_k	dielectric constant
ε_i	interior radiant emittance
$\bar{\varepsilon}_o$	satellite exterior radiant emittance
$\bar{\varepsilon}$	the average emittance for the orbit
$\Delta\Theta$	angular increment between nodal centers in the direction (radians)
Θ	the angle of incidence
λ	the wavelength of the radiant power (μm)
ρ	reflectance
σ	Stefan-Boltzmann constant (5.668×15^8 W/m^2-K^4)
σ_o	the reference d.c. conductivity at 273 K
τ	the relaxation time between collisions of the conduction electrons
$\Delta\phi$	angular increment between nodal centers in the ϕ direction (radians)
$d\omega$	the differential solid angle (stereradian)

ω_p	plasma frequency (sec^{-1})
ω	circular frequency (sec^{-1})

I. INTRODUCTION

The material needs of a rapidly growing world population have stimulated a significant rate of increase in industrial and agricultural growth. There is concern that pollution of the air and water concomitant with the levels of industrialization needed to meet these needs could lead to inadvertent climate modification [1]. For example, pollutants in the air are responsible for altering the fractions of atmospheric water vapor, ozone, carbon dioxide, and particulates. Possible consequences of slight variations in these constituents extend from the melting of the polar ice caps, to precipitation of another ice age [2] because climate changes are known to be sensitive to the earth's radiative energy budget, which in turn is sensitive to the composition of the atmosphere in a way presently understood only qualitatively. Thus, a clear need exists for developing monitoring tools for the qualitative assessment of its local and temporal variations of the earth's radiative energy budget for extended periods of time. This presumably would permit correlations to be established with concurrently observed climatic changes, and hopefully would lead to a long-range predictive ability.

One proposed method of obtaining a quantitative measure of the earth's radiative energy budget would utilize man-made satellites in earth orbit to measure the solar flux incident on earth, the earth-emitted long wavelength radiation, and the short wavelength radiation reflected away from the earth. The monitoring effort would have to extend over a ten to thirty year period in order to correlate the

results with observed variations in the earth's climate. An absolute accuracy in measuring the earth's radiative energy budget on the order of plus or minus one per cent may be needed for the results to be useful [1,3,4]. Present satellite data, such as obtained from Nimbus and ESSA, are inadequate for this purpose. These measurements were obtained for limited areas of the earth's surface, did not obtain the earth's energy budget with the required accuracy, and were conducted over a relatively short time period.

A system of economical, accurate earth orbiting instruments for monitoring the earth's energy budget has been proposed [4]. The Long Term Zonal Earth Energy Budget Experiment (LZEEBE) system would utilize a fleet of satellites each consisting of a central hub and three one and one-half meter diameter detectors for monitoring earth-emitted, direct solar, and the earth-reflected solar radiation. The three spherical detectors, one black, one white, and one aluminum, would be spaced at 120 degree intervals on booms 35 to 40 meters from the central hub, which would house electronic and telemetry equipment. The satellite configuration is shown in Fig. 1.

The inflatable sphere as a radiation detector incorporates three important features. Because the spherical detector is light in weight, the launch cost is significantly reduced. The material and fabrication techniques are state-of-the-art and economical. The sphere is also an omnidirectional sensor of radiation, so that expensive orientation equipment with respect to the earth is not required.

The principle of the system is described by Sweet and Mahan [5]. Because the interior of the spherical detector is an integrating sphere, the irradiance is uniform across the interior surface. That is, the interior surface receives a uniform radiative heat flux even though the surface may not be isothermal. This characteristic is the basis for the omnidirectional sensing capability of the detector.

The concept of Sweet and Mahan is based on several assumptions. They are:

(1) the temperature difference distributions on the interior and exterior surfaces of the detector are identical,

(2) conduction along the detector shell is negligible,

(3) the spherical detector is opaque to all incident radiation,

(4) the interior and exterior surfaces of the detector are optically gray, and

(5) the thermal response time of the detector is significantly more rapid than the variations in the radiation field incident to the exterior surface, thus allowing such variations to be detected.

The interior surface irradiance of the detectors will be measured by one or more radiometers mounted on the interior wall. Two detectors having different surface optical properties will provide different values of interior irradiance in the same exterior radiation field. If energy balances are performed on two such spherical detectors, the results will be

$$H_{I,a} = I_e + (\alpha/\varepsilon)_a \frac{H_s}{4} + (\alpha/\varepsilon)_a I_r \tag{1-1}$$

and

$$H_{I,b} = I_e + (\alpha/\varepsilon)_b \frac{H_s}{4} + (\alpha/\varepsilon)_b I_r, \tag{1-2}$$

where

$$I_e = \frac{1}{S} \int_S H_e dS \tag{1-3}$$

and

$$I_r = \frac{1}{S} \int_S H_r dS, \tag{1-4}$$

the area-weighted average earth-emitted and earth-reflected components. H_I is the interior surface irradiance of the two spherical detectors whose surface optical properties are denoted by the subscript a and b.

Equations (1-1) and (1-2) show that the interior surface irradiance of a spherical detector is a function of three distributions; H_e, the earth-emitted component of irradiance, H_r, the earth-reflected short wavelength component, and H_s, the direct solar component. It is possible to determine the area-weighted average earth-emitted and the earth-reflected components if the solar component, H_s, is known. The two components can be determined by exposing two detectors with known but different surface optical property ratios, α/ε, and measuring the interior surface irradiance with wall-mounted radiometers. The measured values of the interior irradiance combined with the known quantities, allow the two equations to be solved simultaneously. The technique of

using two detectors having different surface optical properties was pioneered by Dr. V. E. Suomi in 1958 [6]. The use of three detectors having different optical properties will allow a cross check of results while providing maximum sensitivity in each of the two spectral ranges of interest.

An idealized thermal model of the spherical detector was developed by R. L. Rasnic [7] and later improved by M. R. Luther [9]. This model accurately predicts the behavior of an ideal detector when exposed to a realistic earth radiation field. Luther has carried out investigations into the influence that parameters such as materials, shell thickness, detector diameter, and uniformity of surface radiative properties using this model. The earth radiation field utilized in Rasnic's original simulation was an arbitrary field not based on satellite data.

A simulation of the earth radiation field was developed by G. G. Campbell and T. H. Vonder Haar [8] at Colorado State University. The computer simulation is based on radiometer measurements taken from the Nimbus III meterological satellite. The computer program utilizes 172 Nimbus III measurements to define the earth radiation field as viewed from the satellite. The simulation allows the detector to orbit the earth at different altitudes and polar orbits of various inclinations and permits the choice of summer or winter radiation fields.

The present work includes the integration of Rasnic's detector simulation with the CSU earth radiation field to provide the most

accurate simulation possible. The composite simulation has subsequently been further modified to provide the first and second derivatives of the detector surface temperature. These derivatives were required and utilized by Luther [9] for studies of calibration of the surface radiative properties.

The detector simulation is valueless unless it responds precisely as the actual detector would in earth orbit. The actual interchange of radiant energy with real surfaces is marked by dependence on the temperature of the surface, the angle of incidence, and the wavelength of the incident radiative flux [10]. The radiative properties of metallic surfaces are also a function of the surface roughness and preparation. However, all previous simulations assume the detector surface to be optically gray and independent of temperature.

The primary objective of the present study is the development and evaluation of a detailed simulation that incorporates the interaction of radiative heat fluxes with a realistic aluminum surface. The study includes suitable models that define the surface radiative properties of aluminum as functions of surface temperature and the wavelength and angle of incidence of the incident radiative flux. The analysis establishes the departure of the surface from the assumed gray behavior.

II. LITERATURE REVIEW

Calculation of the interaction of radiant energy with surfaces requires that the absorptance, emittance, and reflectance characteristics of the surface be known. The degree of accuracy attained in determining the radiation heat transfer is limited by the detail with which the radiation properties are specified. Since the present study requires high accuracy, the most detailed descriptions of properties available are employed.

The blackbody is by definition a perfect absorber, and consequently a perfect emitter, of radiant energy. The spectral, or monochromatic, emissive power of a blackbody is given by Planck's blackbody distribution function as

$$e_{b\lambda}(T) = C_1/n^2\lambda^5[e^{C_2/n\lambda T} - 1] \qquad (2\text{-}1)$$

where n is the index of refraction, λ is the wavelength, and

$$C_1 = 3.740 \times 10^{-12} \text{ W-cm}^2$$

$$C_2 = 1{,}438 \text{ cm-degree.}$$

The total blackbody emissive power, which is the energy emitted per unit time and area by a blackbody over all wavelengths, is given by the Stefan-Boltzmann Law as

$$e_b(T) = n^2\sigma T^4, \qquad (2\text{-}2)$$

where σ is the Stefan-Boltzmann constant. The angular distribution of radiation emitted from a blackbody is given by Lambert's Cosine

Law as

$$I_\Theta = I_0 \cos \Theta \tag{2-3}$$

where I_Θ is the directional intensity of a plane source in the direction Θ with respect to the surface normal and I_0 is the intensity of the source in a direction normal to its surface. Also, by utilization of Kirchoff's Laws [11] it can be shown that the monochromatic absorptance equals the monochromatic emittance for a system in thermodynamic equilibrium.

When a body is irradiated, part of the incident radiant energy is reflected, part is absorbed, and the rest is transmitted. The incident radiant energy E_I is equal to the sum of the reflected radiant energy E_R, the absorbed energy E_A, and the transmitted energy E_T;

$$E_A + E_R + E_T = E_I. \tag{2-4}$$

Dividing both sides of Eq. (2-4) by E_I gives

$$\frac{E_A}{E_I} + \frac{E_R}{E_I} + \frac{E_T}{E_I} = 1 \tag{2-5}$$

or

$$\alpha + \rho + \tau = 1. \tag{2-6}$$

The reflectance ρ is the ratio of the reflected energy to the incident energy; the absorptance α is the ratio of the absorbed energy to the incident energy; and the transmittance τ is the ratio of the transmitted energy to the incident energy.

In describing radiant interchange with solids it is necessary to deal with two sets of parameters, optical properties and thermal

radiative properties. The optical properties describe the interaction of an electromagnetic wave with matter in terms of phase and amplitude, while the thermal radiative properties describe the energy transfer during the interaction. Of course, the two types of properties, optical and thermal radiative, are intimately related.

The thermal radiative properties of the opaque metallic materials are strongly influenced by surface effects arising from methods of preparation, surface finish, thermal history, and interaction with the environment. Oxide films in particular may significantly affect the thermal radiative properties.

Essential to this investigation is the need to understand the behavior of real materials. Fulfillment of this requirement would manifest itself as a rigorous definition of the thermal radiative properties and their dependency upon wavelength, temperature, and geometric direction.

The emittance of metallic surfaces as a function of wavelength and temperature has been the subject of several studies. The influence of temperature on the monochromatic emittance of metals has been investigated by Seban [12], Hagen and Rubens [13], Sadykov [14], Zholev and Sidorenko [15], and by Jack and Spisz [16]. The general behavior observed was a slight increase in monochromatic emittance with an increase in temperature. The variation of emittance with wavelength was investigated by Hagen and Rubens [13]. The behavior of metals exhibits a sharp decrease in emittance with an increase in wavelength.

The influence of temperature on the total emittance of several metals has been investigated by Davisson and Weeks [17]. The general trends observed in the investigation point to an increase in total emittance with an increase in temperature. The same investigation determined that the total hemispherical emittance is greater than the total normal emittance because of deviation from Lambert's Cosine Law.

Evaluation of the heat transfer process for surfaces exhibiting specular reflectance has been carried out and reported by several authors [18,19,20]. The majority of these investigations were concerned with the effect of specular surfaces visible to each other and the influence on the temperature distribution on the surfaces [21,22, 23,24]. The majority of investigations utilize the reflectance model developed by Sparrow and Lin [25] that deals with the non-diffuse character of surface reflectance as the sum of diffuse and specular components. The formulation by Hering and Bobco [21] employs a two-band, or semigray, model to approximate the spectral dependence of surface properties for high-temperature solar radiation and low-temperature surface emission.

The significance of directional reflectance on the radiation heat transfer to a surface has been investigated by Houchens and Hering [27], Clausen and Neu [28], and Hering [29]. These investigators found that the directional property effects for short wavelength incident radiation are most important for materials which are specularly reflecting and have low shortwave absorptance.

The evaluation of monochromatic reflectances may also be determined from electromagnetic theory. Various investigators have evaluated monochromatic reflectances of surfaces using the Fresnel equations [30], and one of several models for the surface optical properties. Rolling and Tien [31] utilized a single electron model to determine monochromatic behavior at low temperatures with good results. Hering and Fischer [32] employed the Roberts model to determine the monochromatic and temperature dependent radiative properties. Their analysis revealed that the gray body assumptions adequately predict the general non-gray behavior.

The Influence of Surface Conditions On Surface Optical Properties

The surface condition of metallic specimens is the dominant factor in determining the magnitude of the measured radiative properties. The literature reflects numerous examples of test surfaces shown to be very sensitive to methods of preparation, thermal history, and the local environment. Despite this knowledge, the descriptions of test surfaces are usually inadequate because of the lack of understanding of the important mechanisms of real surface effects and of how to sufficiently define a surface.

The fact that the reflection process is greatly influenced by the surface condition is predictable through utilization of plane wave theory. The depth of penetration of an incident electric field can range from very small to very large values depending upon the absorption

and scattering properties of the material. Absorption dominates the process for metals since the extinction coefficient is large in the thermal spectrum [33]. The extinction coefficient characterizes the ability of the material to absorb radiation which has entered through the surface. Consequently, incident radiant energy which penetrates the surface layer of a metal will not travel more than a few hundred angstroms before being completely absorbed. However, this behavior is not observed in nonmetallic or dielectric materials, which consequently are less sensitive to surface conditions [34]. In the emission process, internally generated electromagnetic radiation which reaches the surface originates from atomic and molecular thermal vibrations. For metals these vibrations are characteristic of the composition and physical state in a very thin surface layer occupying approximately the first 1,000 angstroms of depth.

The three different types of parameter which influence the properties of a surface are topographical, chemical, and physical in nature. The topographical characteristics define the geometry of the surface on a microscopic level. The chemical characteristics describe the composition of the surface layer including such features as contaminants. The physical characteristics describe the structure of the surface such as orientation of the crystal lattice, cell size, and strain. It is impossible to separate the effects of individual surface characteristics. For most materials, it is not possible to alter one characteristic without changing another.

The most influential factors which bear on the radiative properties of metals are those associated with surface roughness and oxide films. In some situations a thin dielectric film has more impact on emittance properties than does surface roughness of the same dimension. The impact is most pronounced when the characteristic profile variation or film thickness is of the same magnitude as the wavelength of interest, as might be anticipated. The influence of surface characteristics on a particular surface property can be dependent upon the spectral interval of relevance. In particular, the description of a surface meant to behave as an absorber of room temperature source radiation will be different than that of a surface meant to be an absorber of solar source radiation.

The profiles of a metal surface appear as an irregular pattern of peaks and valleys. Several parameters are commonly used to describe the topography of a surface including root mean square (RMS) height, center line average (CLA) height, lay, and average slope, to name a few. These parameters are obtained primarily by mechanical measurement and to some extent by interferometry techniques.

The effect of surface roughness on the optical properties of surfaces was first studied by Lord Rayleigh in 1901. If the size of the irregularities is of the order of the wavelength or larger, the interaction can be described by geometrical optics [35]. The orientation of the facets, which reflect in various directions, must be described by some statistical process in order to explain the optical behavior of the surface. On the other hand, if the surface irregulari-

ties are much smaller than the wavelength, the optical behavior is explainable only as a diffraction phenomenon.

The diffraction theory was studied by Daview [36], and his work was extended by Bennet and Porteus [37]. The expression developed by Bennet and Porteus for the measured reflectance from a "rough" surface reflectance; R, to the "smooth" surface reflectance, R_0, at normal incidence is given as

$$\frac{R}{R_0} = e^{[-(4\pi\mu/\lambda)^2]} + 32\,\pi^4[\mu/\lambda]^4\,[\Delta\psi]^2/M \qquad (2\text{-}7)$$

where μ is the RMS roughness, M is the RMS slope, and $\Delta\psi$ is the angle of acceptance of the optical system. The first term represents the coherently or specularly reflected fraction and the second term the incoherent or diffusely reflected term. The magnitude of the second term is proportional to $(\mu/\lambda)^4$. Porteus [38] showed that when the second term is important, an increasingly exact statistical description of the surface is required.

For very rough surfaces and short wavelengths, geometrical optical effects predominate. The combination of μ and λ as the ratio μ/λ allows the two limiting cases of geometrical and diffraction effects to be studied separately. In the range of geometrical effects, only regular shaped asperities can be handled without resorting to elaborate statistical tools.

Clearly, the variations in monochromatic reflectance must be understood before a meaningful total reflectance can be obtained for a surface. The factor that most influences the variations of mono-

chromatic reflectance is surface roughness. The parameter μ_0/λ, where μ_0 is the RMS deviation of the surface and λ the wavelength of the incident radiant flux, is important in determining the ratio of total specular reflectance of a surface. This relation was developed by Davies [36] and utilized by Birkebak and Eckert [39]. As the ratio of the roughness to wavelength decreases, the reflection characteristic approaches specular behavior.

Models For Optical Property Behavior

An acceptable description of emittance and reflectance characteristics is required in order to analyze the interchange of radiant energy among surfaces. Considerable detail is required in describing the surface optical properties in any study in which an attempt is made to evaluate the effect of their variation on heat transfer results. The intent of the present study is to utilize quantitatively correct functional forms which represent the behavior of the surface properties with variations in wavelength, temperature, and direction to assess the possible effects of such variations on the scientific results obtained from the measurement system.

The directional reflectance and emittance of optically smooth and chemically clean surfaces may be predicted from classical electromagnetic theory [10,30]. When unpolarized radiation is incident on a surface, it can be resolved into two equal components, one component polarized parallel to the plane of incidence and one component polarized perpendicular to the plane of incidence (see Fig. 2).

The expressions for the two components of polarization, $\rho_{||}(\theta)$ for parallel and $\rho_{\perp}(\theta)$ for perpendicular, are given by Fresnel's equations [10,30]

$$\rho_{\perp}(\theta) = \frac{a^2 + b^2 - 2a \cos\theta + \cos^2\theta}{a^2 + b^2 + 2a \cos\theta + \cos^2\theta} \qquad (2\text{-}8)$$

and

$$\rho_{||}(\theta) = \rho_{\perp}(\theta) \frac{a^2 + b^2 - 2a \sin\theta \tan\theta + \sin^2\theta \tan^2\theta}{a^2 + b^2 + 2a \sin\theta \tan\theta + \sin^2\theta \tan^2\theta}, \qquad (2\text{-}9)$$

where the quantities a and b are related to the angle of incidence, θ, the index of refraction n and the extinction coefficient k by

$$2a^2 = \sqrt{(n^2 - k^2 - \sin^2\theta)^2 + 4n^2k^2} + (n^2 - k^2 - \sin^2\theta) \qquad (2\text{-}10)$$

and

$$2b^2 = \sqrt{(n^2 - k^2 - \sin^2\theta)^2 + 4n^2k^2} - (n^2 - k^2 - \sin^2\theta) . \qquad (2\text{-}11)$$

The form of the Fresnel equations given by Eq. (2-8) and Eq. (2-9) is limited to the case where the reflecting surface is bounded by a medium with a refractive index of unity and an extinction coefficient of zero. The Fresnel equations are also a function of wavelength of the incident radiation and the temperature of material, since the index of refraction n and the extinction coefficient k vary with temperature and wavelength.

The influence of polarization on the theoretical value of reflectance has been investigated by Edwards and Tobin [40] and Edwards and Bevans [41]. The investigations were directed at the importance

of the heat transfer associated with specular reflection. The investigation revealed that when both reflector and absorber are irradiated at angles greater than 60 deg the heat transfer calculation will be in error by more than a factor of ten. However, in this investigation it was assumed that the two components of polarization in the incident beam were of equal intensity.

The optical properties of a material, n and k, define the complex index of refraction,

$$N = n - ik. \tag{2-12}$$

For most metals and semiconductors $k \neq 0$; however, for electric nonconductors $k = 0$. Both the index of refraction, n, and the extinction coefficient, k, are functions of both wavelength and temperature.

The complex index of refraction can be related to the electrical constants of the material by

$$N = n - ik = \sqrt{\varepsilon_k - i\left(\frac{4\pi\sigma}{\omega}\right)} \quad , \tag{2-13}$$

where ε_k is the dielectric constant, σ the conductivity, and ω the frequency of the oscillating electric field. Since Eq. (2-13) is a complex equation it may be reduced to two equations,

$$n^2 - k^2 = \varepsilon_k \tag{2-14}$$

and

$$nk\omega = 2\pi\sigma. \tag{2-15}$$

The earliest attempts to predict the optical properties of metals were made by Lorentz [42], Drude [43], Kronig [44], and Mott and Zener [45]. These investigators assumed the metal to contain electrons which were essentially free to move under the influence of the electric field induced by the incident electromagnetic wave. These free electrons are the valence electrons in the outer shell of the atoms constituting the metal. When an electromagnetic wave is incident upon the metal surface, an oscillating electric field parallel to the surface is induced in the metal causing the free electrons to oscillate at the frequency of the wave. There is a phase difference between the oscillation of the electrons and that of the incident electromagnetic wave caused by a viscous damping force arising from collisions between accelerated electrons and the atomic lattice [46]. Two parameters are required to describe the optical behavior of the material. One parameter is the number density of free electrons, N, being excited by the induced field, and the other is the average time, τ, called the relaxation time, between collisions of the electron with the atomic lattice. These two parameters can be estimated from the number of valence electrons per unit volume, the d.c. electrical conductivity, and the assumption of a spherical Fermi surface. The resulting model is called the Drude Free Electron Model [47].

The model describing the optical behavior of the material is greatly simplified if the phase change arising from electronic collisions can be neglected. This situation occurs when the relaxation time is zero or when the time between electronic collisions

is much less than the period of the induced electric field. For this condition, the optical behavior can be completely described by the d.c. electrical conductivity [47].

This simplified model for the optical constants serves as the basis for relations used to compute the thermal radiative properties of materials from a knowledge of the electrical conductivity (or resistivity) as a function of the temperature. If the appropriate relation between the complex dielectric constant and the monochromatic normal emittance is used with the Drude Model, the emittance can be expressed

$$\varepsilon_{n\lambda} = 0.365\ (r/\lambda)^{0.5} - 0.0464(r/\lambda), \qquad (2\text{-}16)$$

where r is the d.c. electrical resistivity in ohm-meters and λ is the wavelength in meters. This celebrated relation is frequently referred to as the Hagen-Rubens relation [13].

The Hagen-Rubens relation for long wavelengths,

$$n = k = \sqrt{\frac{2\pi\sigma_0}{\omega}} = \sqrt{\frac{\sigma_0}{\nu}}\ , \qquad (2\text{-}17)$$

was developed theoretically by Drude [43] and confirmed experimentally by Hagen-Rubens. This relation is arrived at by assuming that the conductivity σ_0 has the value of the d.c. conductivity and the currents in the metal are in phase with the electric field. The latter assumption is equivalent to assuming that the dielectric constant is unity ($\varepsilon_k = 1$). When these conditions are utilized,

$$n^2 - k^2 = \varepsilon_k, \qquad (2\text{-}14)$$

and

$$nk\omega = 2\pi\sigma$$

now becomes

$$n^2 - k^2 = 1 \tag{2-18}$$

and

$$nk\omega = 2\pi\sigma, \tag{2-15}$$

respectively. If n^2 and k^2 are large compared to unity, then they are approximately equal. Substituting the above values of n and k into Eqs. (2-8) and (2-9) for the case of normal incidence yields,

$$\rho_n = \frac{(n-1)^2 + k^2}{(n+1)^2 + k^2} \quad [48]. \tag{2-19}$$

Further, taking into account the fact that $1 << \sigma_0/\nu$, the expression for the reflectivity becomes

$$\rho_n = 1 - 2\sqrt{\frac{\nu}{\sigma_0}} \quad . \tag{2-20}$$

This is the form of the relation tested experimentally by Hagen and Rubens.

The assumptions used to derive this basic model limit the Hagen-Rubens relation to long wavelengths (usually beyond 10 mm) and high temperatures for metals in which the electronic structure can be approximated by only free electrons as the current carriers. This relationship has found extensive use in engineering applications.

The Hagen-Rubens relation has led to the development of various models for expressing total and angular property values for metals. Table I shows several of these relations expressed in terms of emittance. Aschkinass [49] obtained an expression for the normal total emittance $\varepsilon_n(T)$, by normalization of the first term of the

Hagen-Rubens relation with the Planck blackbody distribution,

$$\varepsilon_n(T) = \frac{\int_{\lambda=0}^{\lambda=\infty} \varepsilon_\lambda(T)\ e_{b\lambda}(T)d\lambda}{\int_{\lambda=0}^{\lambda=\infty} e_{b\lambda}(T)\ d\lambda}, \qquad (2\text{-}21)$$

which after integration yields

$$\varepsilon_n(T) = 0.5736[rT]^{0.5} - 0.1769[rT]. \qquad (2\text{-}22)$$

Foote [50] improved the usefulness of the Aschkinass relation by including the second term of the Hagen-Rubens relation in the integration, yielding

$$\varepsilon_n(T) = 0.578[rT]^{0.5} - 0.178[rT] + 0.0584[rT]^{1.5}. \qquad (2\text{-}23)$$

The relations so far have considered only the case of emission normal to the surface. The classical electromagnetic wave theory can describe the angular variation in the optical behavior of the material. Fresnel's equations relate the two polarization components of reflectance to the angle of incidence as measured from the surface normal in terms of the optical constants n and k. In the simple Drude theory, n and k are determined by the electrical resistivity. Davisson and Weeks [17] were the first to treat the problem of determining the total hemispherical emittance by integrating Fresnel's relations for angular dependency for the hemispherical space, yielding

$$\varepsilon_t(T) = 0.751(rT)^{0.5} - 0.633(rT). \qquad (2\text{-}24)$$

Although the limitation that the product of temperature and resistivity

be less than 0.1 is imposed on the Davisson and Weeks model, this limitation is usually no more restrictive than the assumptions utilized in developing the basic model itself.

Schmidt and Eckert [49] removed the limitation on the product of rT and also developed relations for spectral hemispherical emittance,

$$\varepsilon_\lambda(\lambda) = 0.476(r/\lambda)^{0.5} - 0.148(r/\lambda) \text{ for } 0 < r/\lambda < 0.5 \qquad (2\text{-}25)$$

and

$$\varepsilon_\lambda(\lambda) = 0.442(r/\lambda)^{0.5} - 0.0995(r/\lambda) \text{ for } 0.5 < r/\lambda < 2.5; \qquad (2\text{-}26)$$

and the total hemispherical emittance,

$$\varepsilon_t(T) = 0.751(rT)^{0.5} - 0.396(rT) \text{ for } 0 < rT < 0.2 \qquad (2\text{-}27)$$

and

$$\varepsilon_t(T) = 0.698(rT)^{0.5} - 0.266(rT) \text{ for } 0.2 < rT < 0.5. \qquad (2\text{-}28)$$

These four relations constitute the conventional and basic equations used to estimate the radiative properties of metals.

The previously mentioned models all assume that the phase difference between the imposed electric field and the induced electron current is negligible. The relaxation time of the electron carriers is small compared to the period of the applied electric field. Parker and Abbott [51] have developed a relation for the emittance which accounts for a finite relaxation time. The utilization of this equation requires that the parameters of relaxation time τ and the free electron density n be known. This particular model does not find widespread use because of the difficulty in evaluating τ and N as functions of

temperature.

In a recent experimental study by Bennett and Bennett [52] regarding the validity of the Drude theory, the infrared reflectance of carefully prepared ultra high-vacuum-deposited silver, gold, and aluminum films is shown to be in excellent agreement with the theoretical predictions. This work demonstrates the importance of proper specimen preparation if the appropriate theoretical models are to be in agreement.

The failure of the free-electron models to agree with experimental data in the wavelength regions of interest should be interpreted as a consequence of over-simplification of the absorption process mechanism. The absorption process actually involves several types of free electrons each characterized by different relaxation times and densities. Contributions to the absorption process also are made by electrons bound to the lattice, further complicating the process.

The contribution of the bound electrons to the optical properties has been investigated by several authors. The problem has been investigated by Roberts [53,54,55] who has limited the bound electron contribution to the visible or very near infrared wavelength region. Other authors have expanded Roberts' initial work. Seban [12] studied the emittance of the transition metals using Roberts' model and has attempted to determine their high temperature behavior. Edwards and De Volo [56] developed a complicated but realistic model that is restricted to research studies due to the complexity of the model.

The short wavelength absorptance of aluminum as a function of angle of incidence has been determined by Douglas [57] and Hoke [58]. Douglas [57] utilized Fresnel's equations [30] to calculate the solar absorptance. The theoretical values of solar absorptance obtained are based on an index of refraction (n) of 0.75 and extinction coefficient (k) of 4.8. The theoretical value of absorptance for angles up to 85 deg were found with an uncertainty of four to eight per cent. Hoke [58] measured the solar absorptance as a function of angle of incidence out to 75 deg. The findings were extrapolated out beyond 75 deg to 90 deg, as shown in Fig. 3, with a probable error of less than three per cent. The average hemispherical solar absorptance was obtained by mechanical integration of the absorptance curve with a result of $\bar{\alpha}_H = 0.0926$ which was within two per cent of the theoretical value obtained by utilizing the Fresnel equations [30].

III. ANALYSIS AND SIMULATION

Definition of Correction Factor

Evaluation of the departure of the surface from a diffuse, gray receiver and emitter of thermal radiation is initiated by first properly non-dimensionalizing the energy balance expression for the detector. An energy balance of an elemental volume of the detector skin, as shown in Fig. 4, yields

$$\dot{Q}_{in} - \dot{Q}_{out} = \dot{Q}_{\substack{increase \\ storage}}, \tag{3-1}$$

where

$$\dot{Q}_{in} = [\dot{q}_e + \dot{q}_r + \dot{q}_s + \dot{q}_i]dS, \tag{3-2}$$

where $\dot{q}_e$ is the absorbed earth-emitted radiant energy flux, $\dot{q}_r$ is the absorbed earth-reflected solar energy flux, $\dot{q}_s$ is the absorbed solar energy flux, and $\dot{q}_i$ is the absorbed energy from the interior flux, and

$$\dot{Q}_{out} = [\dot{q}_0 + \dot{q}_I]dS, \tag{3-3}$$

where $\dot{q}_0$ is the emitted radiant energy flux from the exterior of the detector, and $\dot{q}_I$ is the emitted radiant energy flux from the interior of the detector, and

$$\dot{Q}_{\substack{increase \\ storage}} = [\rho_S c_S \, \delta \, \partial T_S/\partial t]dS, \tag{3-4}$$

where ρ is the mass density of detector material, c is the specific heat of the detector material, and δ is the thickness of the detector.

The fluxes in the energy balance can be expressed by integral expressions which relate the temperature dependent, directional, monochromatic absorptance of the detector surface to the direction and wavelength of the incident radiant fluxes and the local surface temperature. The integral expressions for the radiant fluxes are:

$$\dot{q}_e = \int_{2\pi}\int_{\lambda} \alpha_\lambda(\theta_e,\phi_e,T_S)\, i_\lambda(\theta_e,\phi_e)d\lambda \cos\theta_e \, d\omega_e, \qquad (3\text{-}5)$$

$$\dot{q}_r = \int_{2\pi}\int_{\lambda} \alpha_\lambda(\theta_r,\phi_r,T_S)\, i_\lambda(\theta_r,\phi_r)d\lambda \cos\theta_r \, d\omega_r, \qquad (3\text{-}6)$$

$$\dot{q}_s = \int_{2\pi}\int_{\lambda} \alpha_\lambda(\theta_s,\phi_s,T_S)\, i_\lambda(\theta_s,\phi_s)d\lambda \cos\theta_s \, d\omega_s, \qquad (3\text{-}7)$$

$$\dot{q}_i = \int_{2\pi}\int_{\lambda} \alpha_\lambda(\theta_i,\phi_i,T_S)\, i_\lambda(\theta_i,\phi_i)d\lambda \cos\theta_i \, d\omega_i, \qquad (3\text{-}8)$$

$$\dot{q}_0 = \frac{1}{\pi}\int_{2\pi}\int_{\lambda} \varepsilon_\lambda(\theta_0,\phi_0,T_S)e_{b\lambda}(T_S) \, d\lambda \cos\theta_0 \, d\omega_0, \qquad (3\text{-}9)$$

and

$$\dot{q}_I = \frac{1}{\pi}\int_{2\pi}\int_{\lambda} \varepsilon_\lambda(\theta_I,\phi_I,T_S)e_{b\lambda}(T_S) \, d\lambda \cos\theta_I \, d\omega_I. \qquad (3\text{-}10)$$

Equations (3-5) through (3-10) identify the local energy per unit time and surface area that is absorbed and emitted by the detector. The earth-emitted long wavelength flux absorbed as a function of the temperature of the detector surface is given by Eq. (3-5), the earth-reflected short wavelength solar-flux absorbed is shown in Eq. (3-6), the short wavelength solar flux absorbed is shown in Eq. (3-7), and the long wavelength interior irradiance absorbed as a function of surface temperature is shown in Eq. (3-8). The total

hemispherical flux emitted by the exterior of the detector as a function of surface temperature is shown in Eq. (3-9) and the total hemispherical flux emitted by the interior of the detector as a function of surface temperature is shown in Eq. (3-10).

At this point it is convenient to define the non-dimensional parameters

$$\alpha_\lambda^* = \alpha_\lambda / \bar{\alpha}_\lambda , \tag{3-11}$$

$$\varepsilon_\lambda^* = \varepsilon_\lambda / \bar{\varepsilon}_\lambda , \tag{3-12}$$

$$i_\lambda^* = i_\lambda / (H/\pi) , \tag{3-13}$$

and

$$e_{b\lambda}^* = e_{b\lambda} / \sigma T_S^4 . \tag{3-14}$$

These parameters are ratios of the monochromatic values of the absorptance and emittance to the average values for the orbit. The average absorptance and emittance are determined by

$$\bar{\alpha}_j = \frac{1}{N} \sum_{i=1}^{N} \alpha_{ji} \tag{3-15}$$

and

$$\bar{\alpha} = \frac{1}{M} \sum_{j=1}^{M} \bar{\alpha}_j \tag{3-16}$$

where N is the number of discrete sources of irradiance incident on the detector, and M is the number of orbital positions. The monochromatic intensity and emitted power are non-dimensionalized by the assumed diffuse intensity and the blackbody emitted power. Since the radiative properties are a function of temperature as well as wavelength and angle of incidence, the average for the detector must

reflect the variation in the detector temperature distribution. The radiant fluxes, Eqs. (3-5) through (3-10), can then be expressed as

$$\dot{q}_e = \bar{\alpha}_e \, f_e(T_S) \, H_e, \tag{3-17}$$

$$\dot{q}_r = \bar{\alpha}_r \, f_r(T_S) \, H_r, \tag{3-18}$$

$$\dot{q}_s = \bar{\alpha}_s \, f_s(T_S) \, H_s, \tag{3-19}$$

$$\dot{q}_i = \bar{\alpha}_i \, f_i(T_S) \, H_i, \tag{3-20}$$

$$\dot{q}_0 = \bar{\varepsilon}_0 \, f_0(T_S) \, T_S^4, \tag{3-21}$$

and

$$\dot{q}_I = \bar{\varepsilon}_I \, f_I(T_S) \, T_S^4, \tag{3-22}$$

where H_e is the long wavelength earth-emitted irradiance, H_r is the short wavelength earth-reflected solar irradiance, H_s is the solar irradiance, and H_i is the interior irradiance.

The "f" factors employed in Eqs. (3-17) through (3-22) are defined by

$$f_e(T_S) = \frac{1}{\pi} \int_{2\pi} \int_{\lambda} \alpha_\lambda^*(\theta_e,\phi_e,T_S) \, i_\lambda^*(\theta_e,\phi_e) \, d\lambda \cos\theta_e \, d\omega_e \tag{3-23}$$

$$f_r(T_S) = \frac{1}{\pi} \int_{2\pi} \int_{\lambda} \alpha_\lambda^*(\theta_r,\phi_r,T_S) \, i_\lambda^*(\theta_r,\phi_r) \, d\lambda \cos\theta_r \, d\omega_r \tag{3-24}$$

$$f_s(T_S) = \frac{1}{\pi} \int_{2\pi} \int_{\lambda} \alpha_\lambda^*(\theta_s,\phi_s,T_S) \, i_\lambda^*(\theta_s,\phi_s) \, d\lambda \cos\theta_s \, d\omega_s \tag{3-25}$$

$$f_i(T_S) = \frac{1}{\pi} \int_{2\pi} \int_{\lambda} \alpha_\lambda^*(\theta_i,\phi_i,T_S) \, i_\lambda^*(\theta_i,\phi_i) \, d\lambda \cos\theta_i \, d\omega_i \tag{3-26}$$

$$f_0(T_S) = \frac{1}{\pi} \int_{2\pi} \int_{\lambda} \varepsilon_\lambda^*(\theta_0,\phi_0,T_S) e_{b\lambda}^*(T_S) \, d\lambda \cos\theta_0 \, d\omega_0 \tag{3-27}$$

and

$$f_I(T_S) = \frac{1}{\pi} \int_{2\pi} \int_{\lambda} \varepsilon^*_{\lambda}(\theta_I,\phi_I,T_S)\ e^*_{b\lambda}(T_S)\ d\lambda \cos\theta_I\ d\omega_I. \quad (3\text{-}28)$$

The dimensionless "f" factors are developed such that they are unity for diffuse, gray, and uniform radiation and surfaces. These quantities may then be considered as correction factors for use with Eqs. (3-17) through (3-22) for each node on the detector surface. The correction factors place a quantitative evaluation on the departure of the local radiation field and surface from diffuseness and uniformity.

Substitution of Eqs. (3-5) through (3-10) into Eqs. (3-1) through (3-4) yields

$$(\dot{q}_e + \dot{q}_r + \dot{q}_s + \dot{q}_i)dS - (\dot{q}_0 + \dot{q}_I)dS = \rho_S\ c_S\ \delta \frac{\partial T_S}{\partial t}\ dS, \quad (3\text{-}29)$$

or

$$(\dot{q}_e + \dot{q}_r + \dot{q}_s + \dot{q}_i - \dot{q}_0 - \dot{q}_I)\ dS = \rho_S\ c_S\ \delta \frac{\partial T_S}{\partial t}\ dS; \quad (3\text{-}30)$$

and introducing Eqs. (3-17) through (3-22) yields

$$[\bar{\alpha}_e H_e f_e(T_S) + \bar{\alpha}_r H_r f_r(T_S) + \bar{\alpha}_s H_s f_s(T_S) + \bar{\alpha}_i H_i f_i(T_S)$$
$$- \bar{\varepsilon}_0\ \sigma T_S^4 f_0(T_S) - \bar{\varepsilon}_I\ \sigma T_S^4 f_I(T_S)]dS = (\rho_S\ c_S\ \delta \frac{\partial T_S}{\partial t})dS. \quad (3\text{-}31)$$

If the assumption is made that the interior absorptance and emittance are equal,

$$\bar{\alpha}_i = \bar{\varepsilon}_I, \quad (3\text{-}32)$$

then Eq. (3-31) becomes

$$\{\bar{\alpha}_e H_e f_e(T_S) + \bar{\alpha}_r H_r f_r(T_S) + \bar{\alpha}_s H_s f_s(T_S) + \bar{\varepsilon}_I\ H_i\ f_i(T_S)$$

$$- \sigma T_S^4[\bar{\varepsilon}_I f_I(T_S) + \bar{\varepsilon}_I f_0(T_S)]\} \, dS = (\rho_S \, c_S \, \delta \frac{\delta T_S}{\delta t}) dS. \quad (3\text{-}33)$$

The energy balance for the entire detector is determined by integrating Eq. (3-33) over the interior and exterior surfaces of the sphere yielding

$$\int_S \sigma T_S^4 dS = (\frac{\bar{\alpha}_e}{\bar{\varepsilon}_0}) \int_S H_e f_e(T_S) dS + (\frac{\bar{\alpha}_r}{\bar{\varepsilon}_0}) \int_S H_r f_r(T_S) dS$$

$$(\frac{\bar{\alpha}_S}{\bar{\varepsilon}_0}) \int_S H_s f_s(T_S) + (\frac{\bar{\varepsilon}_I}{\bar{\varepsilon}_0}) \int_S H_i f_i(T_S) dS - (\frac{\bar{\varepsilon}_I}{\bar{\varepsilon}_0}) \int_S \sigma T_S^4 f_I(T_S) dS$$

$$- (\frac{1}{\bar{\varepsilon}_0}) \int_S (\rho_S \, c_S \, \delta \frac{\delta T_S}{\delta t}) \, dS. \quad (3\text{-}34)$$

It is now possible to determine overall correction factors applicable to the entire detector surface corresponding to anisotrophy of the radiation field visible to the detector; that is,

$$F_e = \int_S H_e f_e(T_S) dS / \int_S H_e dS, \quad (3\text{-}35)$$

$$F_r = \int_S H_r f_r(T_S) dS / \int_S H_r dS, \quad (3\text{-}36)$$

$$F_s = \int_S H_s f_s(T_S) dS / \int_S H_s dS, \quad (3\text{-}37)$$

$$F_i = \int_S H_i f_i(T_S) dS / \int_S H_i dS, \quad (3\text{-}38)$$

$$F_0 = \int_S \sigma T_S^4 f_0(T_S) dS / \int_S \sigma T_S^4 dS, \quad (3\text{-}39)$$

$$F_I = \int_S \sigma T_S^4 f_I(T_S) dS / \int_S \sigma T_S^4 dS, \quad (3\text{-}40)$$

$$F_M = \frac{1}{\bar{\varepsilon}_0} \int_S (\rho_S \, c_S \, \delta \frac{\delta T_S}{\delta t}) dS / \frac{1}{\bar{\rho}_S \, \bar{c}_S \, \delta} \int_S \frac{\delta T_S}{\delta t} \, dS. \quad (3\text{-}41)$$

A more tractable form for the overall energy balance of the detector is obtained if the above expressions are substituted into Eq. (3-34), yielding

$$F_0 \int \sigma T_S^4 \, dS = \left(\frac{\bar{\alpha}_e}{\bar{\varepsilon}_0}\right) F_e \int_S H_e \, dS + \left(\frac{\bar{\alpha}_r}{\bar{\varepsilon}_0}\right) F_r \int_S H_r \, dS +$$

$$\left(\frac{\bar{\alpha}_s}{\bar{\varepsilon}_0}\right) F_s \int_S H_s \, dS - \left(\frac{\bar{\varepsilon}_i}{\bar{\varepsilon}_0}\right) F_i \int_S H_i \, dS$$

$$- \left(\frac{\bar{\varepsilon}_I}{\bar{\varepsilon}_0}\right) F_I \int_S \sigma T_S^4 \, dS - F_M \left(\frac{\rho_S \, c_S \, \delta}{\bar{\varepsilon}_0}\right) \int_S \frac{\partial T_S}{\partial t} \, dS \qquad (3\text{-}42)$$

or,

$$\int_S \sigma T_S^4 \, dS = \left(\frac{\bar{\alpha}_e}{\bar{\varepsilon}_0}\right) \frac{F_e}{F_0} \int_S H_e dS + \left(\frac{\bar{\alpha}_r}{\bar{\varepsilon}_0}\right) \frac{F_r}{F_0} \int_S H_r dS + \left(\frac{\bar{\alpha}_s}{\bar{\varepsilon}_0}\right) \frac{F_s}{F_0} \int_S H_s dS$$

$$+ \left(\frac{\bar{\varepsilon}_I}{\bar{\varepsilon}_0}\right) \frac{F_i}{F_0} \int_S H_i dS - \left(\frac{\bar{\varepsilon}_I}{\bar{\varepsilon}_0}\right) \frac{F_I}{F_0} \int_S H_I \, dS - \frac{F_M}{F_0} \left(\frac{\bar{\rho}_S \, \bar{c}_S \, \delta}{\bar{\varepsilon}_0}\right) \int_S \frac{\partial T_S}{\partial t} \, dS. \qquad (3\text{-}43)$$

Finally, it is convenient to define dimensionless correction factors for the detector for each position in orbit,

$$C_e = F_e/F_0, \qquad (3\text{-}44)$$

$$C_r = F_r/F_0, \qquad (3\text{-}45)$$

$$C_s = F_s/F_0, \qquad (3\text{-}46)$$

and

$$C_M = F_M/F_0. \qquad (3\text{-}47)$$

It is also convenient to define

$$M_S = \frac{\bar{\rho}_S \, \bar{c}_S \, \delta}{\bar{\varepsilon}_0} . \qquad (3\text{-}48)$$

Sweet and Mahan [5] show that it is possible to obtain a second expression for the interior irradiance, H_i. The second expression is obtained by integrating the flux emitted over the interior of the sphere and dividing by the surface area of the sphere, yielding

$$H_I = \frac{1}{S} \int_S \sigma T_S^4 \, dS. \tag{3-49}$$

This expression implies that the interior irradiance for the sphere is uniform, thereby, independent of position.

Substitution of the correction factors defined by Eqs. (3-44) through (3-47) into Eq. (3-43) yields

$$H_I = C_e\left(\frac{1}{S}\right) \int_S H_e dS + C_r\left(\frac{\bar{\alpha}_r}{\bar{\varepsilon}_0}\right)\left(\frac{1}{S}\right) \int_S H_r dS + C_s\left(\frac{\bar{\alpha}_s}{\bar{\varepsilon}_0}\right)\left(\frac{1}{S}\right)\int_S H_s dS$$

$$- C_M M_S\left(\frac{1}{S}\right) \int_S \frac{\partial T_S}{\partial t} \, dS. \tag{3-50}$$

The assumption has been made in the present study that C_M is unity. All correction factors, C, for the detector would be unity for diffuse, gray radiation, and constant thermophysical properties. The equation in that case would reduce to

$$H_I = \frac{1}{S}\int_S H_e dS + \left(\frac{\alpha}{\varepsilon}\right)_0\left(\frac{1}{S}\right)\int_S H_r dS + \left(\frac{\alpha}{\varepsilon}\right)_0 \frac{H_s}{4} - M_S \frac{1}{S} \int_S \frac{\partial T_S}{\partial t} \, dS, \tag{3-51}$$

the radiative energy balance for an "ideal" spherical detector. The correction factors for the orbit can be obtained by a modification of the Rasnic simulation [7] which utilizes temperature dependent, monochromatic, directional surface optical properties.

The preceding analysis indicates that the behavior of a spherical thermal radiation detector subject to non-diffuse and non-gray radiation may differ from the "ideal" behavior based on the assumption of constant, uniform thermophysical properties and gray, diffuse radiation. The departure of the correction factors from unity indicates that the assumptions utilized in the "ideal" detector analysis are not valid. If the deviations of the correction factors from unity are significant, a more precise numerical analysis should be undertaken.

Simulation of the Thermal Radiation Detector Behavior

A numerical simulation of the proposed detector in earth orbit has been accomplished by coupling a simulated earth radiation field [8] with the appropriate surface optical property models applied to the detector. Utilization of the mathematical models of the surface optical properties is accomplished by locating the detector surfaces relative to the sources of incident radiant flux.

The method of solution is based on an earth-centered coordinate system. The position of the satellite and the position of the sun are defined in terms of their direction cosines relative to the center of the earth. The location of the satellite is given by its direction cosines EX, EY, EZ in cartesian coordinates and location of the sun by the direction cosines SX, SY, SZ.

The surface of the detector has been divided into a finite number of isothermal elements. The elements on the surface are determined by the intersection of N longitudinal segments and N lati-

tudinal segments. The number of node points formed by this method is $N^2 - (N - 2)$. The number of longitudinal and latitudinal segments utilized in the numerical simulation is ten, producing 92 node points. The node points on the detector surface are defined by the cartesian components XS, YS, and ZS in terms of a satellite-centered coordinate system. The unit vectors defining the node points are found by dividing XS, YS, and ZS respectively by the radius of the spherical detector. It is not necessary to transform the satellite-centered coordinate system into an earth-centered coordinate system since it is of no consequence how the node points on the detector surface are numbered, as long as the numbering system is consistent.

The simulated earth radiation field developed by Campbell and Vonder Haar [8] provides the direction cosines from a point on the surface of the earth to the detector, as well as the flux originating from the area. The direction cosines make it possible to determine the cosine of the angle formed by the negative of the earth-to-satellite vector and the unit normal vector of the node point on the detector. By convention, if the negative of the cosine is itself negative, the earth source is not visible to the node point in question. All sources of flux in the earth radiation field are checked in the same manner to determine the number of sources of flux incident on the node point in question. The solution routine now iterates over the remaining node points on the detector to determine the sources of flux from the simulated earth radiation field visible to the node in question. The sources of flux provided by the simulated earth radiation field contain

the earth-emitted and solar reflected components incident to the detector from a particular direction. The solar flux incident to the detector node points is determined in a similar fashion utilizing the sun-to-earth direction cosines. The sun-to-earth direction cosines may be used in the analysis instead of the sun-to-satellite direction cosines since the difference in the two is negligibly small.

The flux incident to each node is determined by finding the product of the incident flux and the projected area of the node in the direction of the incident flux. For a system of equal area nodes, this is accomplished by the product of the incident flux and the cosine of the angle formed by the earth-to-satellite vector (or sun-to-earth vector for the solar component) and the unit normal vector of the node point.

The completion of the iteration over all nodes on the detector surface provides the direct solar, earth-reflected solar and earth emitted sources of flux incident to the node.

The simulation of the flux incident to the detector surface will approach the integral over the surface of the detector when an infinite number of nodes are employed to define the surface and an infinite number of sources on the earth are used. The economics of computer simulation prohibits this level of accuracy since the time required to perform the necessary calculations would be excessive. The determination of the number of node points utilized is, therefore, a function of the acceptable accuracy of the simulation and the computer time required to accomplish the calculations. An analysis performed by

M. R. Luther has shown that a detector defined by 92 nodes provides an accuracy of approximately three per cent error [9]. The accuracy of the simulation is increased to less than one per cent error when the detector is simulated by twenty longitudinal and twenty latitudinal segments or 382 node points. However, the computer time required to provide this accuracy is not practical.

The information available at this point in the simulation is adequate to perform a complete determination of the surface optical properties of the detector. If the temperature of the node point is known, it is possible to determine the absorptance, reflectance, and emittance of the surface as a function of temperature, wavelength of the incident energy, and the angle of incidence.

For each node on the detector surface, for which the temperature of the surface is known, the direct and earth-reflected solar flux and the earth-emitted flux are known, as is their corresponding angle of incidence to the surface. This basic information in conjunction with the models used to simulate the surface optical properties allow the net heat transfer to the surface to be calculated.

As previously mentioned in Chapter II, the absorptance of a metallic surface is characterized by different values of absorptance according to the wavelength range of the incident flux. The wavelength dependence has been modeled depending on the wavelength interval; short wavelength (direct and earth-reflected solar) and long wavelength (earth-emitted). The determination of the heat transfer to the detector due to the direct solar flux is calculated by iterating over

all nodes defining the surface. If the node is visible to the sun, the absorptance of the surface is determined as a function of the incident angle by means of the experimental values reported by Marla G. Hoke [58]. The short wavelength absorptance as a function of incident angle is shown in Fig. 3. The rate of heat transfer associated with this value of solar absorptance is determined by the product of the solar constant, the value of the solar absorptance, and the area of the node point projected in the direction of the solar flux. The detector surface will have one-half of the node points visible to the sun, if it is not in the earth's shadow.

The contribution to the total heat transfer from the earth reflected solar flux is determined as a function of the angle of incidence. The short wavelength absorptance as a function of incident angle are the values reported by Hoke [58]. The short wavelength flux absorbed by each node from each source of earth-reflected solar flux is the product of the area of the node point projected in the direction of incident flux, the short wavelength absorptance associated with the particular angle of incidence, and the intensity of the incident flux. The total absorbed flux to each node is the summation of the flux absorbed from each source incident to the node and the total absorbed flux is the summation of the flux absorbed by each node.

The heat transfer to the detector surface from the earth-emitted component is determined as a function of the angle of incidence, temperature of the node, and wavelength of the incident flux. The temperature of the node and the wavelength of the incident energy

provides the basis of the determination of the optical constants by the Drude-Zener theory [47] for wavelengths greater than 3.8 mm. The energy content in the wavelength region greater than 3 mm is determined by utilization of the Planckian distribution, using a wavelength integration interval that is small at the shorter wavelengths and increasing in range at the longer wavelenths. The Drude-Zener theory [47] provides the optical constants of a metallic surface which are required by the Fresnel equation along with the angle of incidence to determine the reflectance of the surface. Assuming the surface to be opaque to the infrared radiation, the sum of the reflectance and the absorptance of the surface is unity, so that

$$\alpha = 1 - \rho. \tag{3-52}$$

The heat transfer to each node of the detector from each infrared source visible to the node is the summation of the product of the absorptance for the wavelength interval and the flux contained in the interval. The amount of energy contained in each wavelength band is a function of the temperature of that portion of the earth from which the infrared energy is eminating. It is possible to determine the temperature of the earth for each source of infrared energy incident to the detector if a Planckian distribution is assumed. Each source of infrared energy is decomposed into its constituent wavelength bands, which are treated individually. The absorptance of the energy within these wavelength increments is determined and summed to obtain the overall absorptance of the surface.

The long wavelength absorptance of aluminum as a function of surface temperature, angle of incidence, and wavelength of the incident radiative energy is computed using the Drude-Zener theory [47] in conjunction with Fresnel's equations. The long wavelength absorptance as a function of temperature and angle of incidence is shown in Fig. 5. The Drude-Zener theory is used to calculate the index of refraction n and the extinction coefficient k. The mathematical expressions are

$$n^2 - k^2 = 1 - \frac{\omega_p^2}{\omega^2 + 1/\tau^2} \tag{3-53}$$

and

$$nk = \frac{1}{2\omega\tau} \frac{\omega_p^2}{\omega^2 + (1/\tau^2)} \tag{3-54}$$

where ω is the angular frequency of the incident flux, τ the relaxation time. The plasma frequency ω_p is given by

$$\omega_p = \sqrt{\frac{4\pi N e^2}{M^*}} \tag{3-55}$$

where for a metal N is the free electron density, e the electron charge, and M^* the optical effective mass. However, the ratio N/M^* is equal to N_{eff}/M where M is the free electron density. The effective electron density N_{eff} has no physical significance and must not be associated with the actual electron density.

The relaxation time, τ, is based on the assumption that the electrons have a Fermi spherical velocity v_f. Therefore the relaxation time is defined as

$$\tau = \frac{\ell}{v_f} \tag{3-56}$$

where ℓ is the mean free path of the electrons between collisions. The d.c. conductivity can be determined from the Lorentz-Sommerfeld Relation [42] by

$$\sigma_0 = \frac{N e^2 \ell}{M^* v_f} . \tag{3-57}$$

The relaxation time can be determined by substituting into Eq. (3-56) obtaining

$$\tau = \frac{M^* \sigma_0}{N e^2} . \tag{3-58}$$

Using 3.178×10^{17} esu as the bulk d.c. conductivity and the number of effective electrons N_{eff} is

$$N_{eff} = N\left(\frac{M}{M^*}\right) = 2.6 \frac{\text{Free Electrons}}{\text{Atom}}. \tag{3-59}$$

The absorptance calculated by this technique was found by Bennett, Silver, and Ashley [59] to be within 0.6% of the actual absorptance for aluminum films evaporated in ultra high vacuum.

The shortcoming of this method of calculating the absorptance of an aluminum surface is that an allowance is not made for deterioration of the surface. The increase in absorptance for evaporated aluminum films as a function of time is documented by Madden and Canfield [60]. This investigation established that the increase in absorptance of aluminum which occurs on exposure to the atmosphere can be explained by the growth of aluminum oxide on the surface.

The determination of the thermal radiative properties on the detector surface defines the rate of energy incident to the exterior of the detector. The remaining quantities to be defined are related through the emittance of the particular node points on the detector surface. The radiant energy exchange from one node to the remaining nodes is determined by the emittance and absorptance of the interior surface, which in this analysis has been assumed constant.

The emittance of the exterior surface as a function of the temperature of the aluminum surface has been simulated by the equation for total hemispherical emittance developed by Davisson and Weeks [17], Eq. (2-24). This equation for the total hemispherical emittance is based on the Drude free electron theory, modified to include the d.c. conductivity as a function of temperature, the long wavelength emittance as a function of temperature is shown in Fig. 6.

The constituent parts of Eq. (3-30) defining the radiative energy balance at each node on the detector surface are now available, with the exception of the time increment Δt, which can be varied to meet stability criterian, and the unknown temperature at time $t + \Delta t$.

The determination of Δt was performed by a trial-and-error method. The initial desire was that $\Delta t = 20$ seconds, the time increment of change of the radiation field. However, the solution achieved for $\Delta t = 20$ seconds was unstable. As a consequence, the time increment was halved and the solution was calculated twice for each discrete radiation field. The solution for this value of Δt was stable and this value of Δt is utilized in the present simulation. The simulation

The iteration overall nodes on the detector surface at this point defines the rate of energy incident to the exterior of the detector. The remaining quantities to be defined are related through the emittance of the particular node points on the detector surface. The radiant energy exchange from one node to the remaining nodes is determined by the emittance and absorptance of the interior surface, which in this analysis has been assumed constant.

The emittance of the exterior surface as a function of the temperature of the aluminum surface has been simulated by the equation for total hemispherical emittance developed by Davisson and Weeks [17], Eq. (2-24). This equation for the total hemispherical emittance is based on the Drude free electron theory, modified to include the d.c. conductivity as a function of temperature, the long wavelength emittance as a function of temperature is shown in Fig. 6.

The constituent parts of Eq. (3-30) defining the radiative energy balance at each node on the detector surface are now available, with the exception of the time increment Δt, which can be varied to meet stability criterion, and the unknown temperature at time $t + \Delta t$.

The determination of Δt was performed by a trial-and-error method. The initial desire was that $\Delta t = 20$ seconds, the time increment of change of the radiation field. However, the solution achieved for $\Delta t = 20$ seconds was unstable. As a consequence, the time increment was halved and the solution was calculated twice for each discrete radiation field. The solution for this value of Δt was stable and this value of Δt is utilized in the present simulation. The simulation

would approach the exact solution consistent with the number of surface elements used if indefinitely small intervals of time were utilized. However, the increased cost in computer time prohibits a further decrease in Δt.

At the beginning of each simulation the detector is allowed to reach equilibrium with the earth radiation field for the initial position in the simulated earth orbit before "launch." Determination of the equilibrium condition of the detector corresponding to the radiation heat flux for the initial position allows the detector behavior to be assessed without the built-in starting transient that would modify the detector behavior. Otherwise, the response of the detector is such that the starting transient would require several orbital positions to damp out and provide realistic detector behavior.

IV. RESULTS AND CONCLUSIONS

The absorbed solar radiant power is constant and is the primary source of the total radiant power absorbed when the detector is visible to the sun. The maximum contribution of the solar component to the total absorbed power is 98.58 per cent. The maximum contribution occurs at 1660 seconds into the orbit, just prior to the loss of the earth-reflected solar component. The minimum contribution of the solar component to the total absorbed radiant power is 76.00 per cent. The minimum contribution of the absorbed solar component and the maximum contribution of the absorbed earth-reflected solar component occurs at 5300 seconds into the orbit, which corresponds to the detector pass over the polar ice cap. The maximum contribution of the absorbed earth-emitted component is only 1.68 per cent and occurs 360 seconds into the orbit as the detector passes over the equitorial zone.

The angular distributions of the earth-emitted and earth-reflected solar sources of irradiance incident to the detector are shown in Figs. (7) through (10). The angular distributions are shown for angles greater than 49 deg, because the long wavelength absorptance and the solar absorptance are nearly constant for angles less than 50 deg as is shown in Figs. (3) and (5). Figures (7) through (10) show that the number of sources incident to the detector increase with increasing angle of incidence. The significance of the angular distributions of the earth-emitted and earth-reflected solar sources is more apparent when the percentage of the total sources incident to the detector in each angular interval is known, as shown in Figs. (11) through (14). The percentages

of earth-emitted and earth-reflected solar sources with an angle of incidence greater than 50 deg., as shown in Fig. (15), is nearly constant at 65 per cent of the total sources incident to the detector. The impact of the angular distribution on the earth-emitted long wavelength absorptance and the earth-reflected solar absorptance, as shown in Figs. (3) and (5), will result in an increased absorptance in both cases. The maximum long wavelength absorptance of 0.00955 is produced by an average surface temperature of 400 K and the minimum absorptance of 0.00708 is produced by an average surface temperature of 257 K. The per cent change from the maximum to the minimum absorptance for the orbit corresponds to a 25.9 per cent change. The average absorptance for the orbit was 0.00919 which corresponds to the long wavelength absorptance for a temperature of 380 K and an angle of incidence of 63.5 deg. Unfortunately, the values of the long wavelength absorptance are in error. The vales are low because the analytical model utilized to determine the long wavelength absorptance does not account for any diffuse reflectance from the aluminum surface.

The absorbed long wavelength earth-emitted power is shown in Fig. 16. Specific features of the earth radiation field can be interpreted from the figure. The points in the polar orbit with lowest incident earth-emitted power are at the poles (1600 seconds and 48,000 seconds into the orbit). Conversely, the equitorial zones should have the warmest temperatures, therefore the highest incident power as can be seen at 200 seconds, 3200 seconds, and 6000 seconds in the orbit, corresponding to the detector passes over the equitorial zones. The

incident long wavelength power at 3,200 seconds in the orbit is not as high as that from the equitorial zones at 200 and 6000 seconds because the terrain is in darkness.

The long wavelength absorptance, ALW, for the detector is shown in Fig. 17. The absorptance follows the variations in the earth radiation field. The absorptance decreases rapidly with the loss of the direct solar power, since the detector cooled rapidly. This characteristic reveals the temperature dependence of the long wavelength absorptance.

The absorbed earth-reflected short wavelength power is shown in Fig. 18. The figure is dominated by the long absence of any reflected power while the detector is in the earth's shadow; however, there is an increase in incident power at 200 seconds and 3200 seconds. The increase in incident earth reflected power at 200 seconds can be attributed to heavy cloud cover in the equitorial zone. The sharp increase in reflected short wavelength power at 3200 seconds coincides with the pass over the polar ice cap. The snow and ice reflect very well and this sharp increase would be anticipated.

The short wavelength absorptance, ASW, for the detector surface as a function of incident angle for the orbit is shown in Fig. (19). The figure reveals two periods of increased short wavelength absorptance which coincide with the pass over the polar caps. The directional nature of the earth radiation field at the poles can be seen from Figs. (9) and (10). The earth-reflected solar absorptance increased 1.6 and 1.3 per cent as the detector passed over each pole. The

increased absorptance resulted from a sharp increase in the percentage of sources incident to the detector with an angle of incidence greater than 70° at these points.

The total power incident to the detector from the earth-reflected short wavelength and the earth-emitted long wavelength components is shown in Fig. (20). The figure contrasts the magnitude of the two components. The earth-reflected short wavelength component dominates the power incident to the detector. The disparity in magnitude is so large that the total incident power increases from 4200 seconds until 5200 seconds while the earth-emitted power decreases by twenty-five per cent.

The interior irradiance of the spherical detector is shown in Fig. (21). The figure shows that the interior irradiance is strongly influenced by the direct solar power and the earth-reflected short wavelength power. The slight decrease in the interior irradiance from the start until 1,600 seconds is a result in the decrease in the earth-reflected short wavelength power as can be seen from Fig. (18). The interior irradiance is constant after the loss of earth-reflected solar power at 2600 seconds, until the loss of solar power at 2280 seconds. The interior irradiance after the loss of solar power decreases sharply until the solar power is regained at 3320 seconds. The return of solar power increases the interior irradiance sharply and coupled with the return of the earth-reflected solar power at 3840 seconds continues to increase and follow the behavior of the earth-reflected power as can be seen by comparison with Fig. (16). The

sharp decrease in the interior irradiance after the loss of solar power, at 2280 seconds, is a result of the low level of absorbed earth-emitted long wavelength power. The reason for the low level of absorbed earth-emitted power is the long wavelength absorptance, which is low by a factor of ten. The reduced value of long wavelength absorptance yields a ratio of the long wavelength absorptance to the emittance which is 0.33 at 1720 seconds into the orbit and increases to 0.36 at 2280 seconds into the orbit. As a result, the detector loses radiative power by rapid cooling while in the earth's shadow.

The total hemispherical emittance, ELW, of an aluminum surface, as a function of temperature, for the orbit is shown in Fig. (22). The emittance behavior directly follows that of the interior irradiance since the emittance is a function of temperature. Since the emittance follows the interior irradiance behavior it is strongly influenced by the direct solar power, and the earth-reflected short wavelength power. The figure compared with Fig. (17), the long wavelength absorptance, shows that the emittance was from 3.13 to 2.60 times greater than the infrared absorptance. The theoretical value of the total hemispherical emittance, however, does agree with experimental values. The range of temperatures encountered in the orbit vary from a maximum of 410.5 K to a minimum of 248.7 K. This temperature difference produces a difference in long wavelength emittance of 0.0031. The variation from the maximum to minimum emittance over the orbit 43 per cent and the variation from the maximum to the minimum emittance on the detector at any one point in orbit is 11 per cent.

Figure (23) shows the ratio of solution techniques for the long wavelength component, FE. The ratio compares the power absorbed by utilizing an absorptance that is a function of temperature, wavelength and angle of incidence, and the power absorbed by the detector utilizing the precise absorptance averaged over the entire orbit. As can be seen from the figure, the behavior of the ratio is that of the actual long wavelength absorptance, as shown in Fig. (17). The product of time in orbit and the amount that the ratio is greater than unity equals the product of time in orbit and the amount that the ratio is less than unity.

Figure (24) shows the difference in the absorbed long wavelength power as a result of solution technique for the orbit. The absorbed power determined by the more detailed long wavelength absorptance was greater than the power determined by the average absorptance for 5000 of the 6,500 seconds in the orbit. The point in the orbit when the actual absorptance was the smallest coincides with the point in orbit when the detector was the coldest, at 3200 seconds. The point in orbit where the infrared absorptance was greatest, 5,200 seconds, was also the point in orbit where the detector was the warmest. These two points show the significance of the temperature dependence on the long wavelength absorptance.

Figure (25) shows the per cent difference in the two solution techniques for the power absorbed from the long wavelength earth emitted component for the orbit. The calculation at each point in orbit is based on the power absorbed based on the value of the actual

absorptance. The largest per cent difference in the two solution techniques occurred when the detector was the warmest and the coldest. The per cent difference between the two extreme conditions was 510.76 per cent. The behavior of the figure reveals the temperature dependence of the actual solution technique.

The ratio of solution techniques for the earth-reflected short wavelength power as a function of orbital position, FR, is shown in Fig. (26). The ratio is formed from the earth-reflected solar short wavelength absorptance that is a function of the angle of incidence to the average absorptance for the orbit. The behavior of the ratio is similar to that of the short wavelength absorptance (ASW) shown in Fig. (19). The figure reveals the dependence of the actual absorptance on the angle of incidence. The per cent difference between the maximum and minimum absorptance from Fig. (19) equals the per cent difference between the maximum and minimum ratio of solution techniques.

The actual difference in the absorbed earth-reflected short wavelength power is shown in Fig. (28). The positive values indicate where the actual absorptance is greater than the average for the entire orbit. As can be seen from the figure, the two points of maximum difference between the exact and average absorptance occurs as the detector passes over the poles (1200 seconds and 5000 seconds). The points in the orbit where the average absorptance for the orbit is greater than the exact absorptance occurs just before the loss of the earth-reflected component (1600 seconds) and the return of the earth-reflected component (4200 seconds). A characteristic of the earth radiation field is that just

prior to the loss and just after the return of the earth-reflected component it contributes less than one per cent of the total incident power. However, at 5,000 seconds into the orbit the earth-reflected power constitutes approximately fifteen per cent of the absorbed power.

The per cent difference in the absorbed earth-reflected solar power, as shown in Fig. (27), is the ratio of the difference in the absorbed earth-reflected solar power obtained by utilizing the actual and average values of absorptance to the actual absorbed power. The maximum per cent difference of 1.6 per cent and 1.3 per cent in the absorbed earth-reflected solar power coincides with the detector pass over the polar ice caps, at 1200 and 5000 seconds into the orbit. The general behavior of the per cent difference is the same as the earth-reflected solar absorptance, as seen from Fig. (19).

The ratio of solution techniques for the solar component, FS, is not shown since it is unity throughout the orbit. The ratio is unity throughout the orbit since the detector profile as viewed by the incident solar radiant flux is invariant. This characteristic is reflected by the constant absorbed solar power as mentioned on page 41.

The ratio of the exact emitted power to the average emitted power for the orbit, FO, is shown in Fig. (29). The behavior of the ratio follows the interior irradiance as shown in Fig. (21). The ratio follows the temperature dependence of the exact emittance, since the ratio decreases to less than unity after the loss of the solar component and the corresponding decrease in the interior irradiance. This

behavior indicates that the average emittance is greater than the exact emittance during this period. The ratio of the exact emittance to the average emittance reflects the error in computing the long wavelength absorptance more than any other ratio. The rapid cooling associated with the loss of the solar component resulted in extremely low temperatures and emittance values dependent on the temperature. The low emittance values when averaged over the orbit are again too low. The reduced value of the average emittance now increases the value of the ratio for the interval in the orbit where solar radiant flux is incident on the detector.

The earth-emitted correction factor, CE, for the orbit is shown in Fig. (30). This correction factor is the ratio of two other ratios. The two ratios are the ratio of the actual long wavelength absorptance to the average long wavelength absorptance and the ratio of the actual emitted power to the average emitted power. Values of the earth-emitted correction factor less than unity indicate that the emitted power as a function of temperature is more sensitive to temperature than is the long wavelength absorptance for the same temperature as can be seen from Fig. (29). The rapid increase in the correction factor, with the loss of solar power, is caused by the rapid decrease in the detector temperature and the resulting decrease in emitted power as a function of temperature. The extremes of the correction factor reflect a difference of twenty per cent from minimum to maximum.

The earth-reflected correction factor, CR, for the orbit is shown in Fig. (31). The correction factor, like the earth-emitted correction

factor, is a ratio of two other ratios. The denominator is again the ratio of the actual emittance to the average emittance for the orbit. The numerator is the ratio of the actual absorptance of the earth-reflected short wavelength to the average absorptance for the orbit. The correction factor is less than unity for all points in the orbit where solar power is incident to the detector. The ratio of the actual emittance to the average emittance for the orbit controls the correction factor. As an example, the correction factor at four hundred seconds into the orbit would be increased by seven-tenths of one per cent if the ratio of the actual earth-reflected solar absorptance to the average absorptance was unity versus the present 1.07. The dominance of the emittance ratio, FO, is the cause of the sharp increase and decrease in the correction factor from twenty-two thousand seconds until thirty-eight thousand seconds in the orbit, since the numerator of the ratio is unity during this time.

The solar correction factor, CS, is shown in Fig. (32). The solar correction factor as in the two previous correction factors is the ratio of the actual solar absorptance to the average solar absorptance for the orbit to the ratio fo actual to average emittance. The general behavior of the correction factor is dominated by the ratio of the actual to average emittance. The absorbed solar power is nearly constant, as mentioned on page 41; however, the correction factor, CS, varies nearly fifty per cent from maximum to minimum values.

V. CONCLUSIONS AND RECOMMENDATIONS

The following conclusions can be made as a result of the preceeding analysis:

(1) The assumption of a diffuse, gray earth-radiation field in the ideal simulation is invalid. This conclusion was arrived at from the specular peaks of earth-reflected solar irradiance encountered as the detector passed over the poles and equitorial zones.

(2) The assumption that the detector surface is a diffuse absorber of incident radiant flux is invalid. This conclusion is based on the sharp increase in the earth-reflected solar absorptance as the detector passed over the areas where specular reflectance was present.

(3) The assumption that the long wavelength absorptance and emittance may be treated as independent of surface temperature is also invalid. The variation in absorptance and emittance over the orbit is 37.4 per cent and 43 per cent, respectively.

(4) The spherical radiation detector is not capable of determining the earth energy budget to within one per cent. The maximum per cent difference between the actual and average absorbed earth-emitted power is 6.3 per cent.

(5) The ability of the non-dimensional correction factors to quantitatively assess the departure of the spherical detector from the assumed constant, uniform thermophysical properties, and gray, diffuse radiation behavior is inconclusive. The error in the long wavelength absorptance distorted the correction factors and consequently rendered the values obtained in the present study useless.

Recommendations

The following recommendations are made based on the finding of this study.

(1) The complex computer simulation of the spherical radiation detector should be executed again after the model for the long wavelength absorptance has been modified to more accurately predict actual aluminum behavior.

(2) An investigation of the actual emittance of an aluminum film as a function of temperature should be performed to verify the calculations performed here.

REFERENCES

1. Study of Man's Impact on Climate (SMIC), Inadvertant Climate Modification, M.I.T. Press, 1971.

2. Goody, R. M. and J. C. G. Walker, Atmospheres, Prentice Hall Inc., Englewood Cliffs, N.J., 1972, p. 132.

3. Atmospheric Radiation Working Group (ARWG), Major Problems in Atmospheric Radiation: An Evaluation and Recommendations for Future Efforts, Second Meeting of ARWG, NCAR, Boulder, Colorado, June 14-15, 1971.

4. House, F. B., and G. E. Sweet, Long Term Zonal Earth Energy Budget Experiment, NASA Proposal for the Advanced Applications Flight Experiment, 1973.

5. Sweet, G. E. and J. R. Mahan, Analysis of a Non-isothermal Spherical Detector for Monitoring the Earth's Radiative Energy Budget, Conference on Atmospheric Radiation, 1972.

6. Soumi, V. E., "The Radiation Balance of the Earth from a Satellite," Annals of the IGY, Vol. I, 1958, pp. 331-340.

7. Rasnic, R. L., A Thermal and Kinematic Model of a Thin Wall Spherical Shell Satellite, M.S. Thesis VPI&SU, Blacksburg, Va., Dec., 1975.

8. Campbell, G. C. and T. H. Vonder Haar, Satellite Earth Radiation Budget Measurement Simulation Program Gendat; NASA Contract NAS1-12106, Langley Research Center, Colorado State Univ., Fort Collins, Colorado, Dec., 1973.

9. Luther, M. R., Determination of Detector Mass Constant and Earth Long Wavelength Exitance from Transient Temperature Measurements After Earth Shadow Ingression, File V-19000/4NAS-063, LTV-Langley Research Center, Feb. 28, 1974.

10. Sparrow, E. M. and R. D. Cess, Radiation Heat Transfer, Brooks/Cole Publishing Co., Belmont, California, 1970, pp. 32 and 33.

11. Planck, M., The Theory of Heat, Macmillan and Co. Ltd., New York, N.Y., 1933, p. 189.

12. Seban, R. A. M. "The Emissivity of Transition Metals in the Infrared," Journal of Heat Transfer, May 1965, pp. 173-176.

13. Hagen, E. and H. Rubens, "Metallic Reflection," Annals Physik, Vol. 8, 1902, p. 1, and Vol. 11, 1903, p. 873.

14. Sadykov, B. S., "Temperature Dependence of the Radiating Power of Metals," Teplofizika Vysokikh Temperatur, Vol. 3, No. 3, May-June 1964, pp. 389-394.

15. Zhulev, Yu. G. and A. F. Sidorenko, "Investigation of Radiative Systems Taking Account of the Dependence of the Thermophysical Properties of the Material on the Temperature," Teplofizika Vysokikh Temperatur, Vol. 9, No. 4, July-August 1971, pp. 796-801.

16. Jack, J. R., and E. W. Spisz, "Solar Absorptance and Hemispherical Emittance of Various Metals at Space Conditions," 7th AIAA Aerospace Sciences Meeting, N.Y., N.Y., January 20-22, 1969, pp. 69-80.

17. Davisson, D. and J. R. Weeks, "The Relationship Between the Total Thermal Emissive Power of a Metal and Its Electrical Resistivity," Journal of the Optical Society of America, Vol. 8, 1929, pp. 581-605.

18. Bevans, J. T., and D. K. Edwards, "Radiation Exchange in an Enclosure with Directional Wall Properties," Journal of Heat Transfer, Transactions of ASME, August 1965, pp. 388-396.

19. Eckert, E. R. G. and E. M. Sparrow, "Radiative Heat Exchange Between Surfaces with Specular Reflection," International Journal of Heat and Mass Transfer, Vol. 3, 1961, pp. 42-54.

20. Hering, R. G., "Radiative Exchange Between Conducting Plates with Specular Reflection," Journal of Heat Transfer, Transactions of the ASME, Feb. 1966, pp. 29-36.

21. Houchens, A. F. and Hering, R. G., "Directional Property Effects on Radiant Heat Transfer and Equilibrium Temperatures," 9th Aerospace Science Meeting, Paper 71-76, January 25-27, 1971.

22. Bevans, J. T. and Edwards, D. K., "Radiation Exchange in an Enclosure with Directional Wall Properties," Journal of Heat Transfer, Transactions of the ASME, August 1965, pp. 388-396.

23. Hering, R. G., "Radiative Heat Exchange Between Conducting Plates with Specular Reflection," Journal of Heat Transfer, Transactions of the ASME, February 1966, pp. 29-36.

24. Eckert, E. R. G. and Sparrow, E. M., "Radiative Heat Exchange Between Surfaces with Specular Reflection," International Journal of Heat and Mass Transfer, Vol. 3, 1961, pp. 42-54.

25. Sparrow, E. M. and S. H. Lin, "Radiation Heat Transfer at a Surface Having Both Specular and Diffuse Reflectance Components," International Journal of Heat and Mass Transfer, Vol. 8, 1965, pp. 769-779.

26. Hering, R. G. and R. P. Bobco, "A Second Order Approximation for Local Radiant Flux and Temperature in Semi-gray Non-Diffuse Enclosures," Journal of Spacecraft, Vol. 5, No. 11, Nov. 1968, pp. 1271-1278.

27. Houchens, A. F. and R. G. Hering, "Directional Property Effects on Radiant Heat Transfer and Equilibrium Temperature," 9th Aerospace Science Meeting, Jan. 25-27, 1971, paper 71-76.

28. Clausen, O. W. and J. T. Neu, "The Use of Directional Radiation Properties for Spacecraft Thermal Control," Astonautica Acta, Vol. 11, No. 5, 1965, pp. 328-329.

29. Hering, R. G., "Radiative Heat Exchange Between Specularly Reflecting Surfaces with Direction Dependent Properties," Proceedings of the Third International Heat Transfer Conference, American Institute of Chemical Engineers, New York, 1966, pp. 200-206.

30. Wood, R. W., Physical Optics, McMillan and Co., Ltd, 1934, p. 547.

31. Rolling, R. E. and C. L. Tien, Radiant Heat Transfer for Non-Gray Metallic Surfaces at Low Temperature, AIAA Thermophysics Specialiat Conference, New Orleans, La., April 17-20, 1967, paper 67-335.

32. Hering, R. G. and Fischer, W. D., "Radiant Heat Transfer Between Non-Gray Surfaces," AIAA 6th Thermophysics Conference, Tullahoma, Tenn., April 26-28, 1971, paper 71-464.

33. Gaumer, R. E., A Generalized Physical Model of the Role of Surface Effects in Modifying Intrinsic Thermal Radiation Parameters, Symposium on Thermal Radiation of Solids (S. Katzoff, Ed.), NASA, SP-55, 1963, pp. 135-139.

34. Richmond, J. C., "Effect of Surface Roughness on Emittance of Non-metals," The Journal of the American Optical Society, Vol. 56, pp. 253-254, 1966.

35. Torrance, K. E. and Sparrow, E. M., "Off Specular Peaks in the Directional Distribution of Reflected Thermal Radiation," The Journal of Heat Transfer, Transactions of the ASME, Vol. 88, 1966, pp. 223-230.

36. Davies, H., "Reflection of Electromagnetic Waves from Rough Surfaces," Proceedings of the Institute of Electrical Engineers, Vol. 101, 1954, pp. 209-214.

37. Bennet, H. E., and J. O. Porteus, Relation Between Surface and Specular Reflectance at Normal Incidence, The Journal of the Optical Society of America, Vol. 51, No. 2, Feb., 1961, pp. 123-129.

38. Porteus, J. O., Relation Between the Height Distribution of a Rough Surface and the Reflectance at Normal Incidence, The Journal of the Optical Society of America, Vol. 53, No. 12, Dec. 1963, pp. 1394-1402.

39. Birkebak, R. C. and E. R. G. Eckert, "Effects of Roughness of Metal Surfaces on Angular Distribution of Monochromatic Reflected Radiation," Journal of Heat Transfer, Transactions of the ASME, Vol. 87C, 1965, pp. 85-94.

40. Edwards, D. K. and R. D. Tobin, Effect of Polarization on Radiant Heat Transfer Through Long Passages, Journal of Heat Transfer, Transactions of the ASME, May 1967, pp. 132-138.

41. Edwards, D. K. and J. T. Bevans, Effect of Polarization on Spacecraft Radiation Heat Transfer, AIAA Journal, Vol. 3, 1965, pp. 1323-1329.

42. Lorentz, H. A., The Theory of Electrons and its Application to the Phenomena of Light and Radiant Heat, New York, Dover Press, 1959.

43. Drude, P. K. L., Theory of Optics, New York, Dover Press, 1959.

44. Kronig, R. L., "The Auantum Theory of Dispersion in Metallic Conductors," Proceedings of the Royal Society, Vol. 133A, 1931, p. 255.

45. Mott, N. F. and C. Zener, Optical Properties of Metals, Cambridge Philosophical Society Proceedings, Vol. 30, April 30, 1934, pp. 249-270.

46. Givens, M. P., "Solid State Physics," Advances in Research and Applications, Editors Seitz, F. and Turnbull, D., Vol. 6, 1958, p. 320.

47. Mott, N. F. and Jones, H., The Theory of the Properties of Metals and Alloys, Oxford University Press, 1936, p. 112.

48. Sparrow, E. M. and Cess, R. D., Radiation Heat Transfer, Brooks/Cole Publishing Co., Belmont, California, 1970, p. 66.

49. Wiebelt, J. A., Engineering Radiation Heat Transfer, Holt, Rinehart, and Winston Publishing Co., New York, N.Y., 1966, pp. 45-46.

50. Foote, P. D., The Emissivity of Metals and Oxides, Bulletin National Bureau of Standards, Vol. 11, 1914-1915, pp. 607-612.

51. Parker, W. J. and Abbott, G. C., "Total Emittance of Metals," Symposium on Thermal Radiation of Solids, (S. Katzoff, Ed.) NASA Sp. 55, 1963, pp. 11-28.

52. Bennett, H. E. and Bennett, J. M., Validity of the Drude Theory for Silver, Gold, and Aluminum in the Infrared, Optical Properties and Electronic Structure of Metals and Alloys, (Abele, Ed.) North Holland Publishing Co., Amsterdam, 1966, pp. 175-186.

53. Roberts, S., Interpretation of the Optical Properties of Metal Surfaces, Physical Review, Vol. 100, No. 6, 1055, pp. 1667-1671.

54. Roberts, S., Optical Properties of Nickel and Tungsten and Their Interpretation According to Drude's Formula, Physical Review, Vol. 114, No. 1, 1959, pp. 104-115.

55. Roberts, S., Optical Properties of Copper, Physical Review, Vol. 118, 1960, p. 1509.

56. Edwards, D. K. and deVolo, B. N., Useful Approximations for the Spectral and Total Emissivity of Smooth Bare Metals, Advances in Thermophysical Properties at Extreme Temperatures and Pressures (S. Gratch, Ed.), ASME, 1965, pp. 174-188.

57. Douglas, N. J., Directional Solar Absorptance Measurements, Symposium on Thermal Radiation of Solids, (S. Katzoff, Ed.), NASA, Sp-55, 1963, pp. 293-301.

58. Hoke, M. G., A Thermal Vacuum Technique for Measuring Solar Absorptance of Satellite Coatings as a Function of Angle of Incidence, Symposium on Thermal Radiation of Solids, (S. Katzoff, Ed.), NASA, Sp-55, 1963, pp. 303-311.

59. Bennett, H. E., Silver, M. and Ashely, E. J., Infrared Reflectance of Aluminum Evaporated in Ultra High Vacuum, The Journal of the Optical Society of America, Vol. 53, No. 9, 1963, pp. 1089-1095.

60. Madden, R. P. and Canfield, L. R., Apparatus for the Measurement of Vacuum Ultraviolet Optical Properties of Freshly Evaporated Films before Exposure to Air, The Journal of the Optical Society of America, Vol. 51, No. 8, 1961, pp. 838-845.

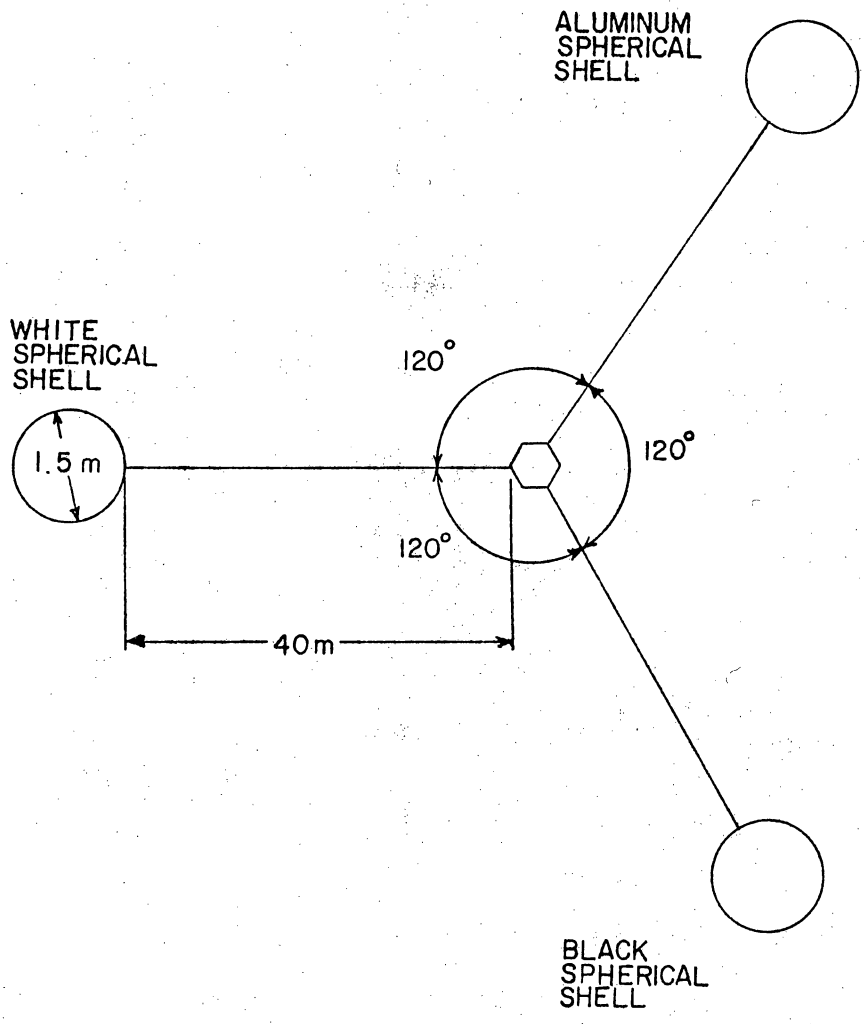

Figure 1. Configuration of the Radiation Detector

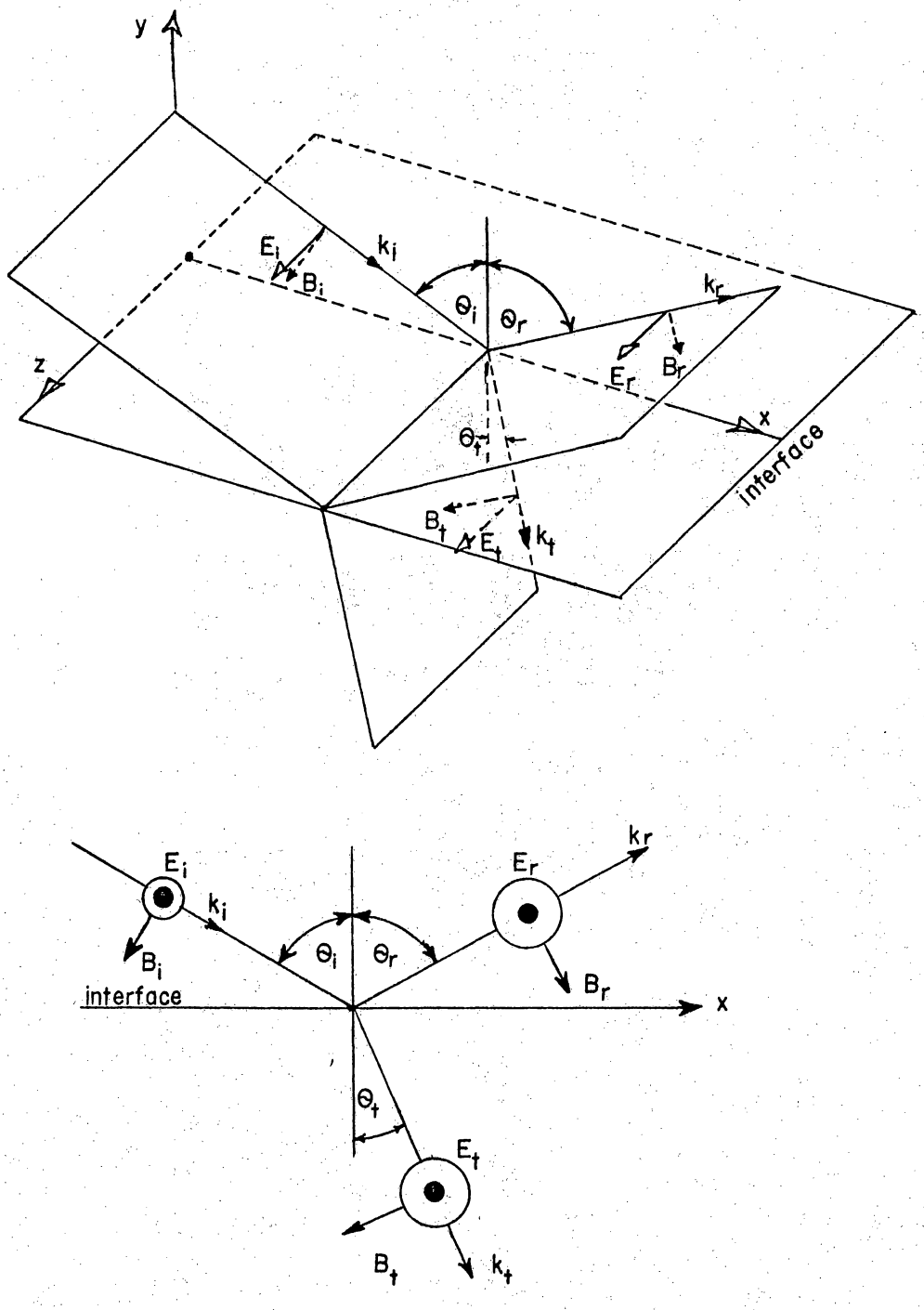

Figure 2. Reflection of an Electromagnetic Wave

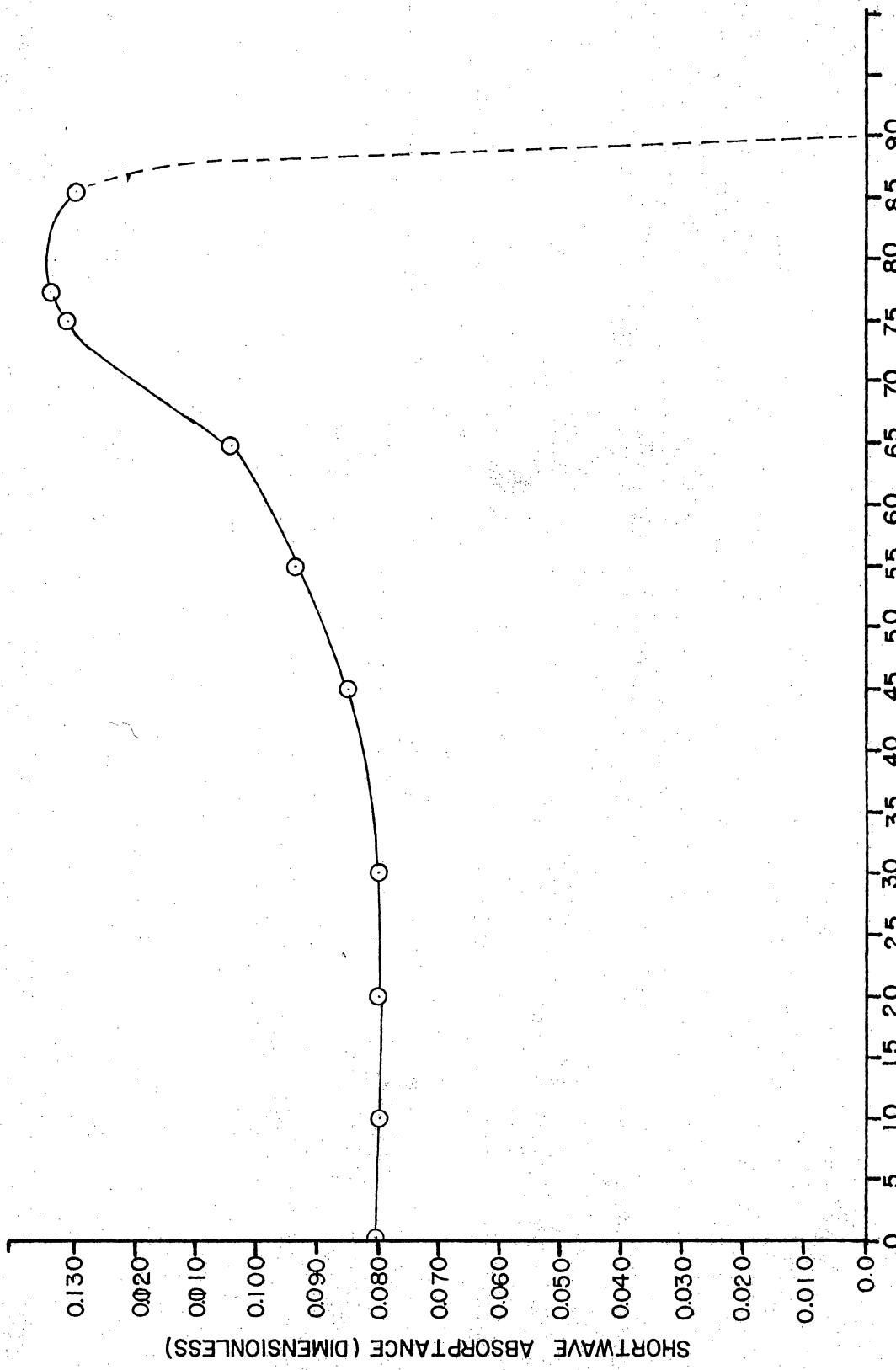

Figure 3. Solar Absorptance as a Function of Incident Angle

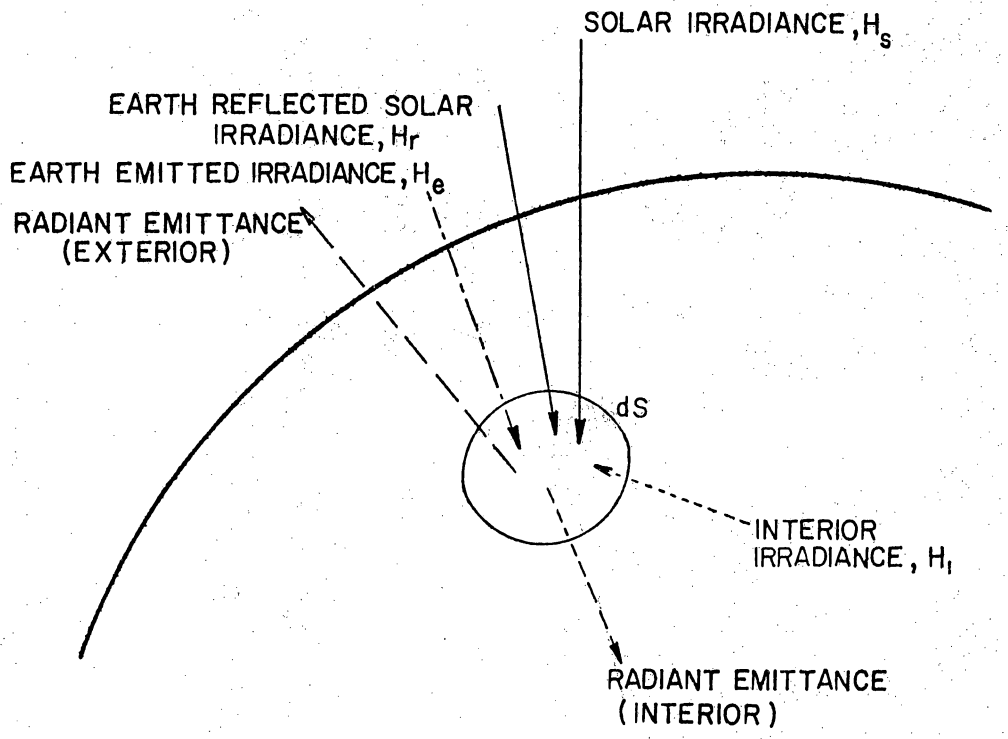

Figure 4. A Volume Element of the Radiation Detector

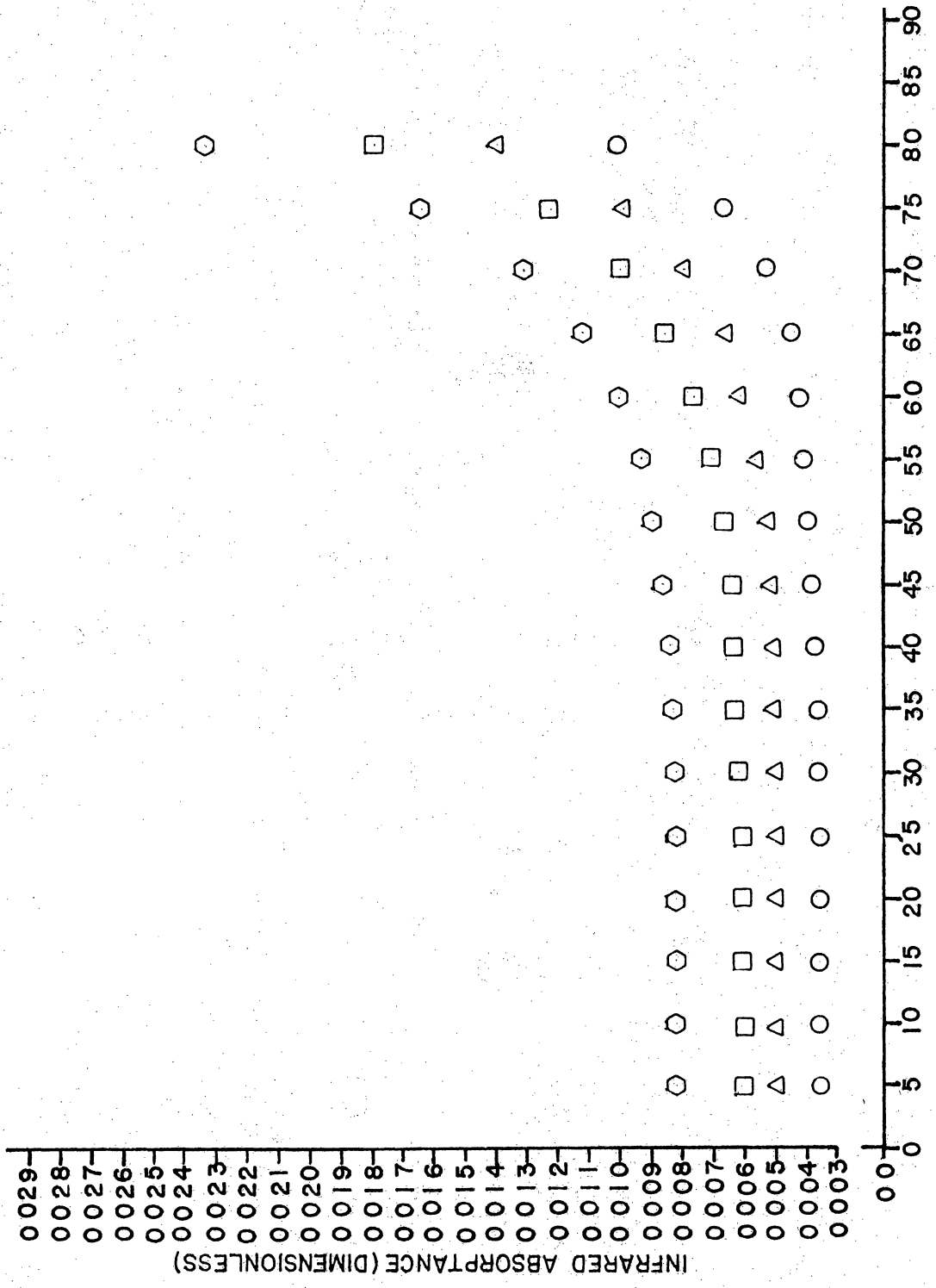

Figure 5. Long Wavelength Absorptance as a Function of Temperature and Incident Angle

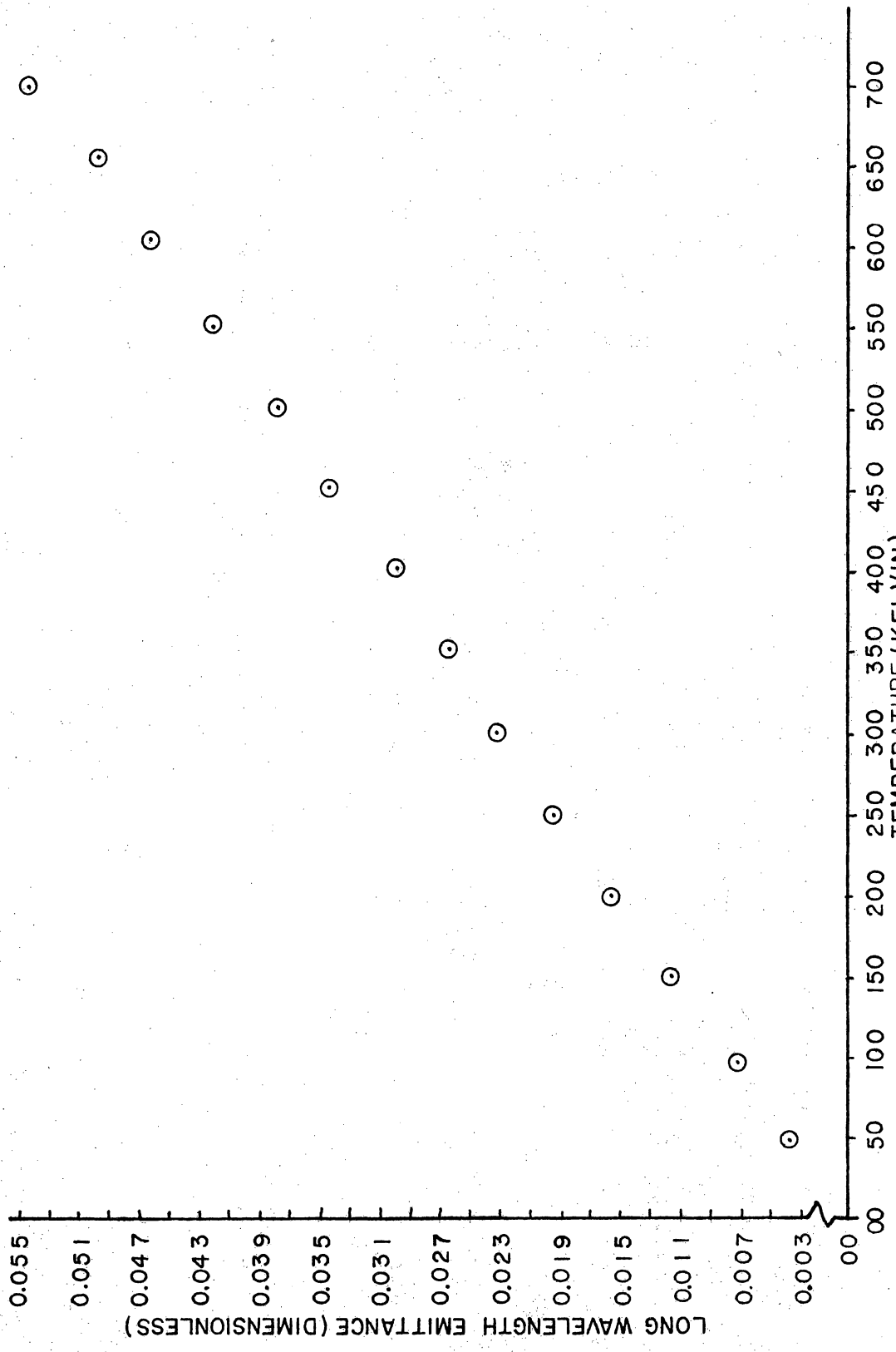

Figure 6. Emittance as a Function of Temperature

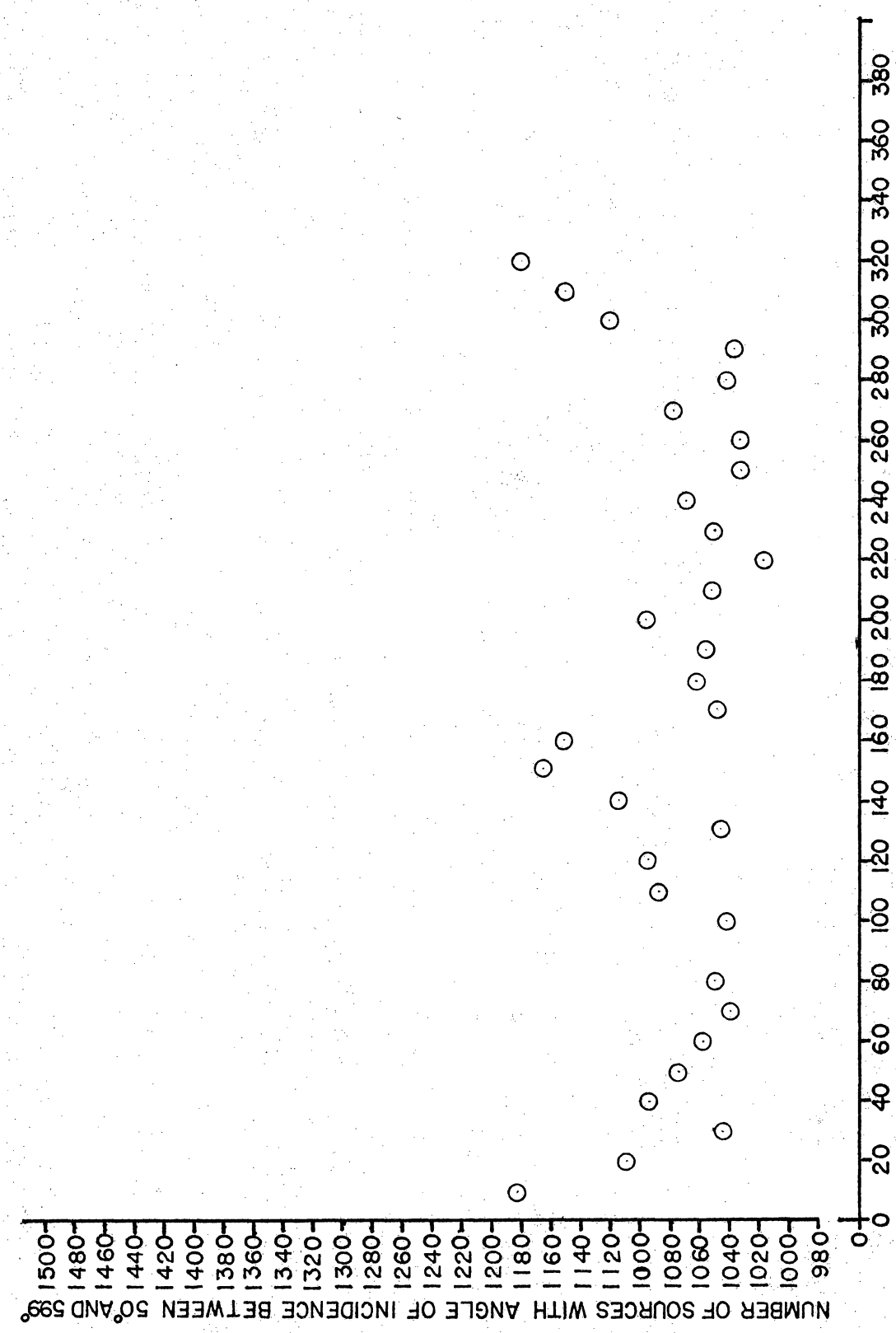

Figure 7. Number of Discrete Earth-Emitted Sources with Angle of Incidence Between 50 deg. and 59 deg.

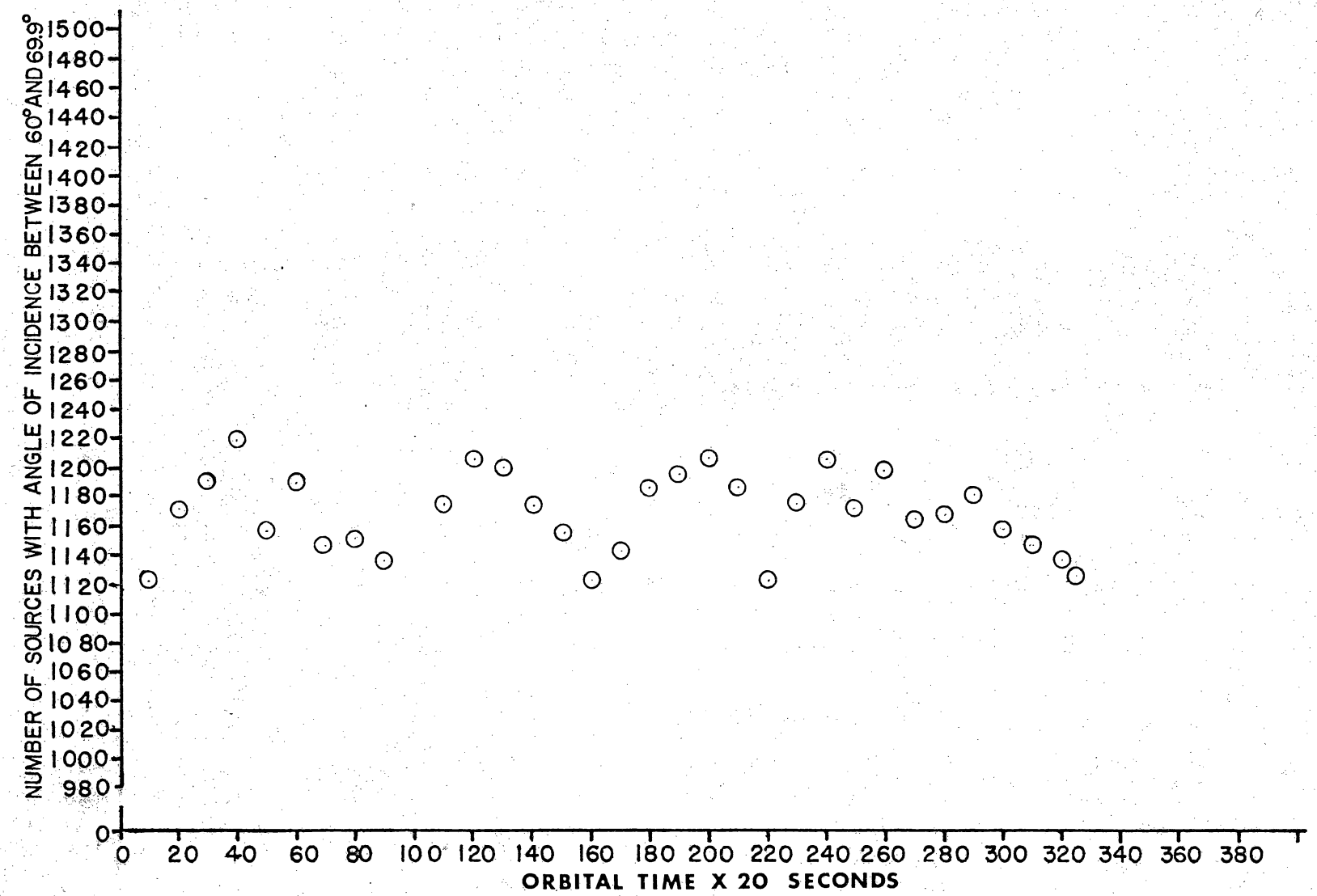

Figure 8. Number of Discrete Earth-Emitted Sources with Angle of Incidence Between 60 deg. and 69 deg.

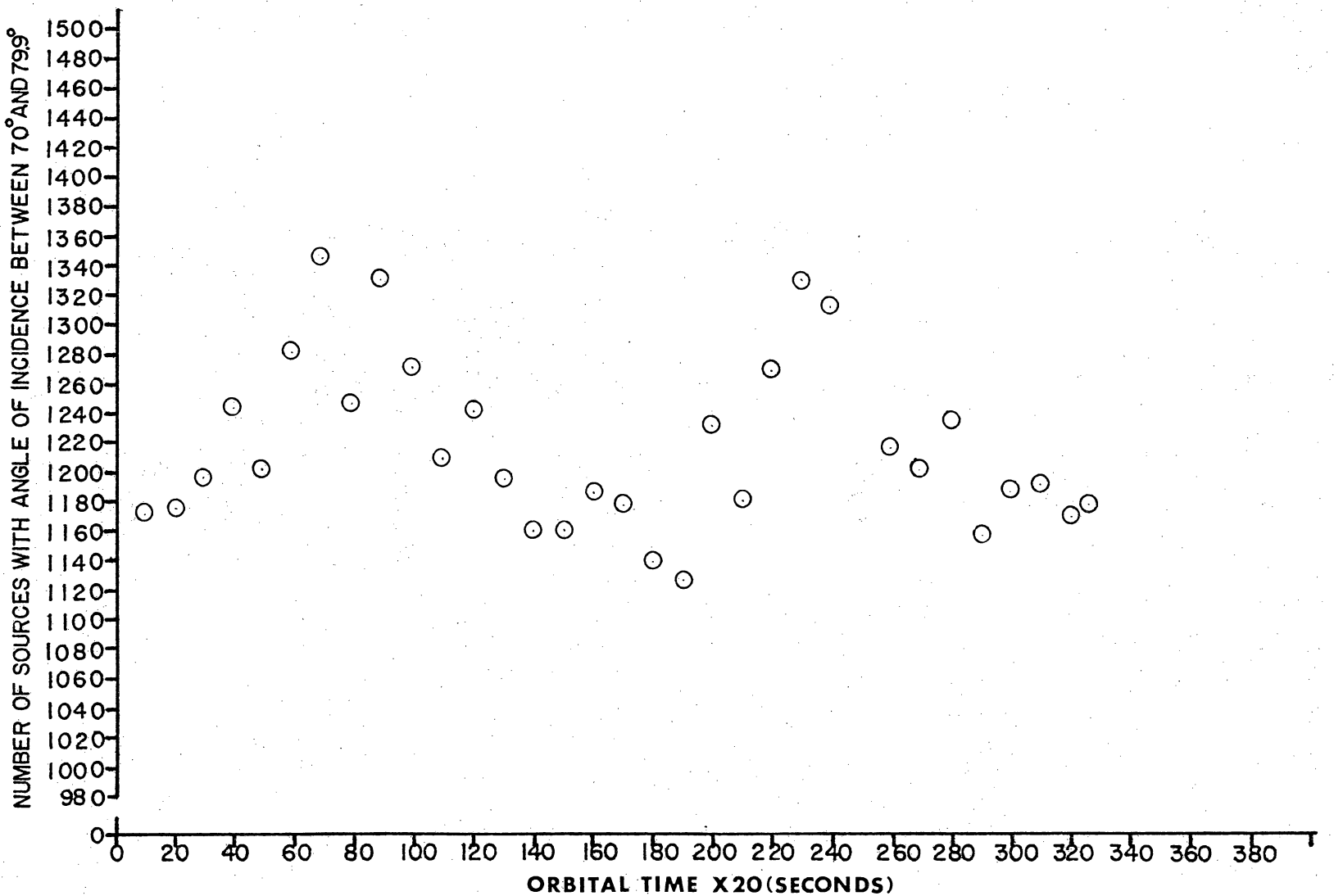

Figure 9. Number of Discrete Earth-Emitted Sources with Angle of Incidence Between 70 deg. and 79 deg.

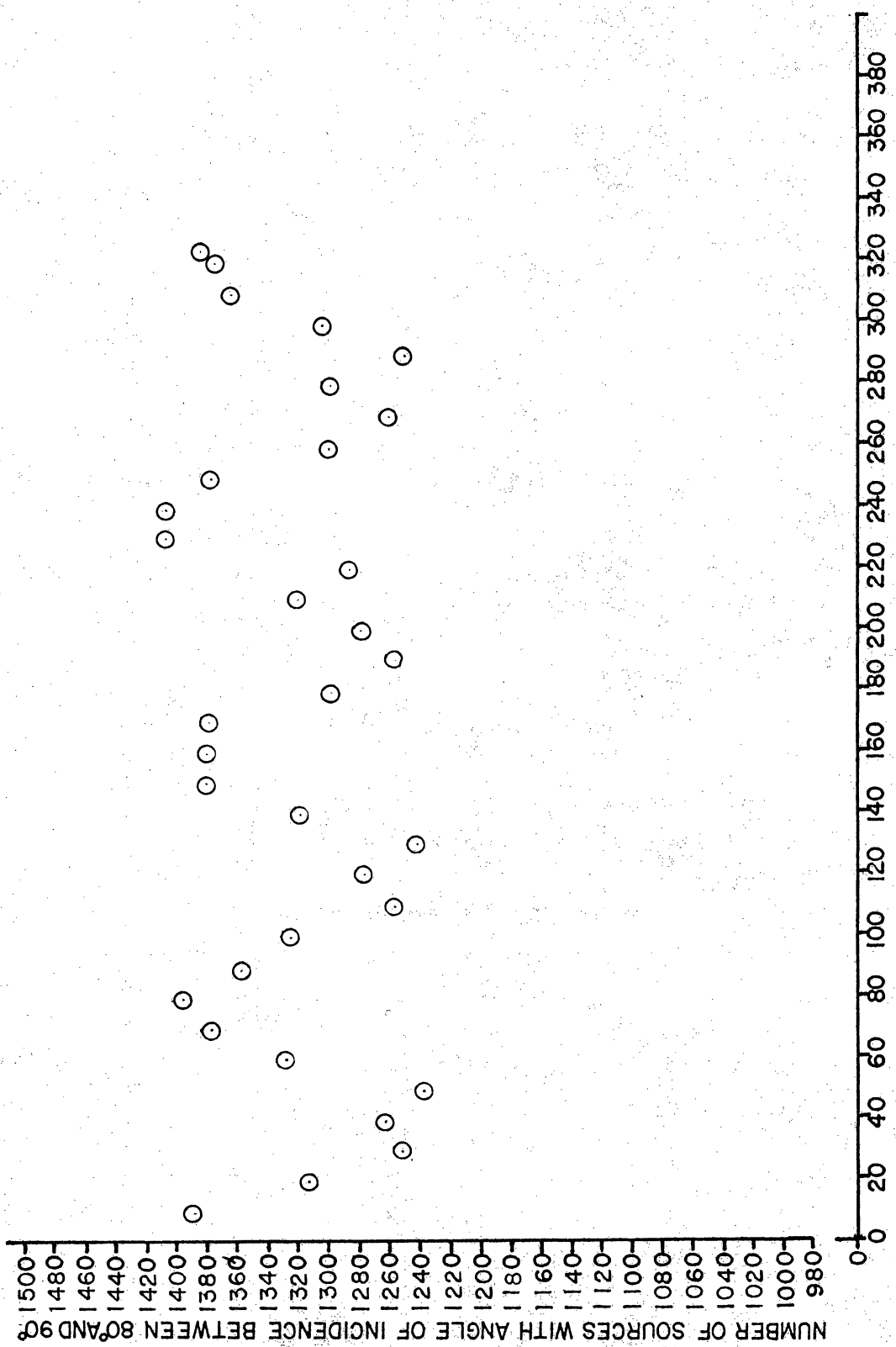

Figure 10. Number of Discrete Earth-Emitted Sources with Angle of Incidence Between 80 deg. and 90 deg.

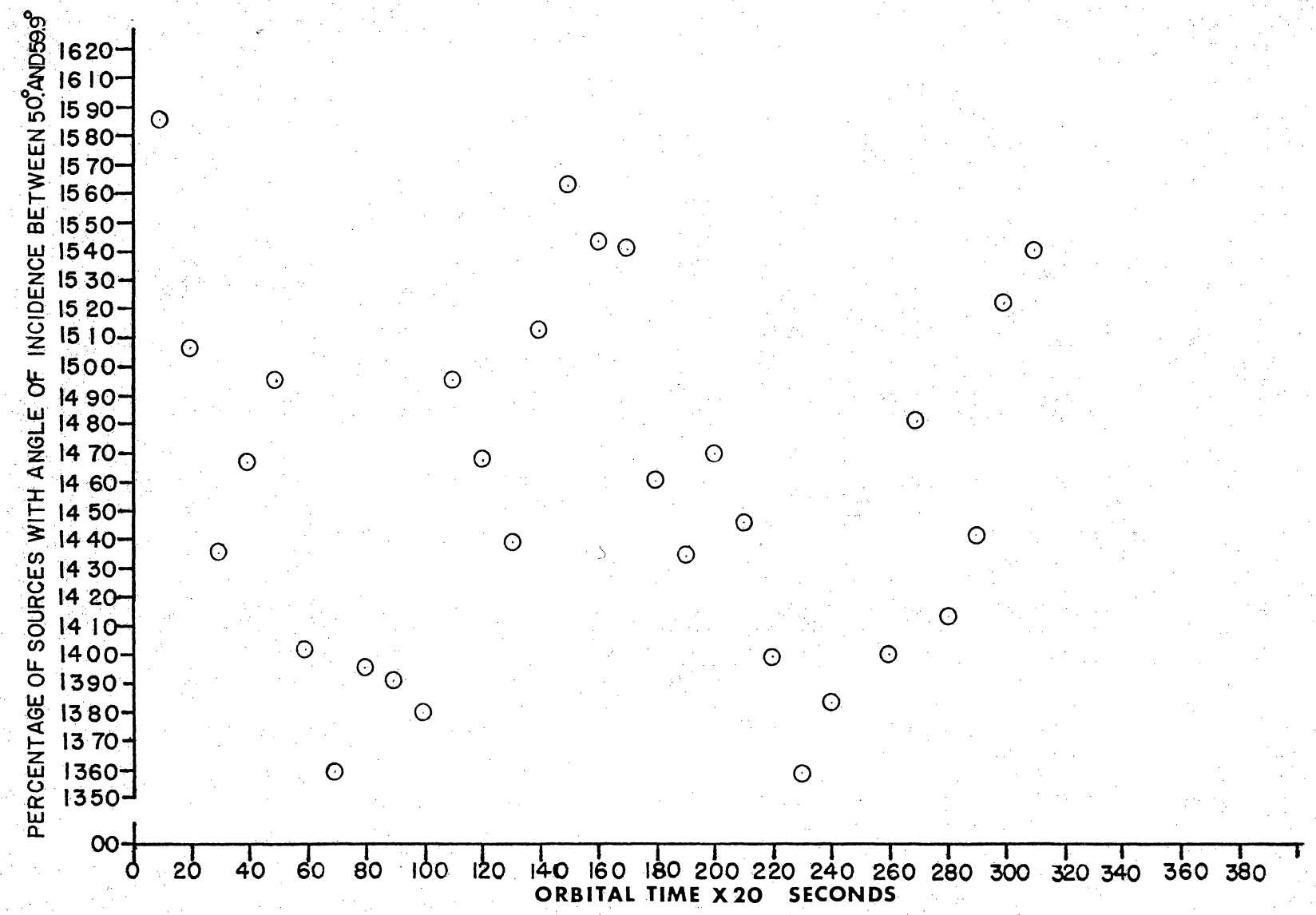

Figure 11. Percentage of all Earth-Emitted Sources with Angle of Incidence Between 50 deg. and 59 deg.

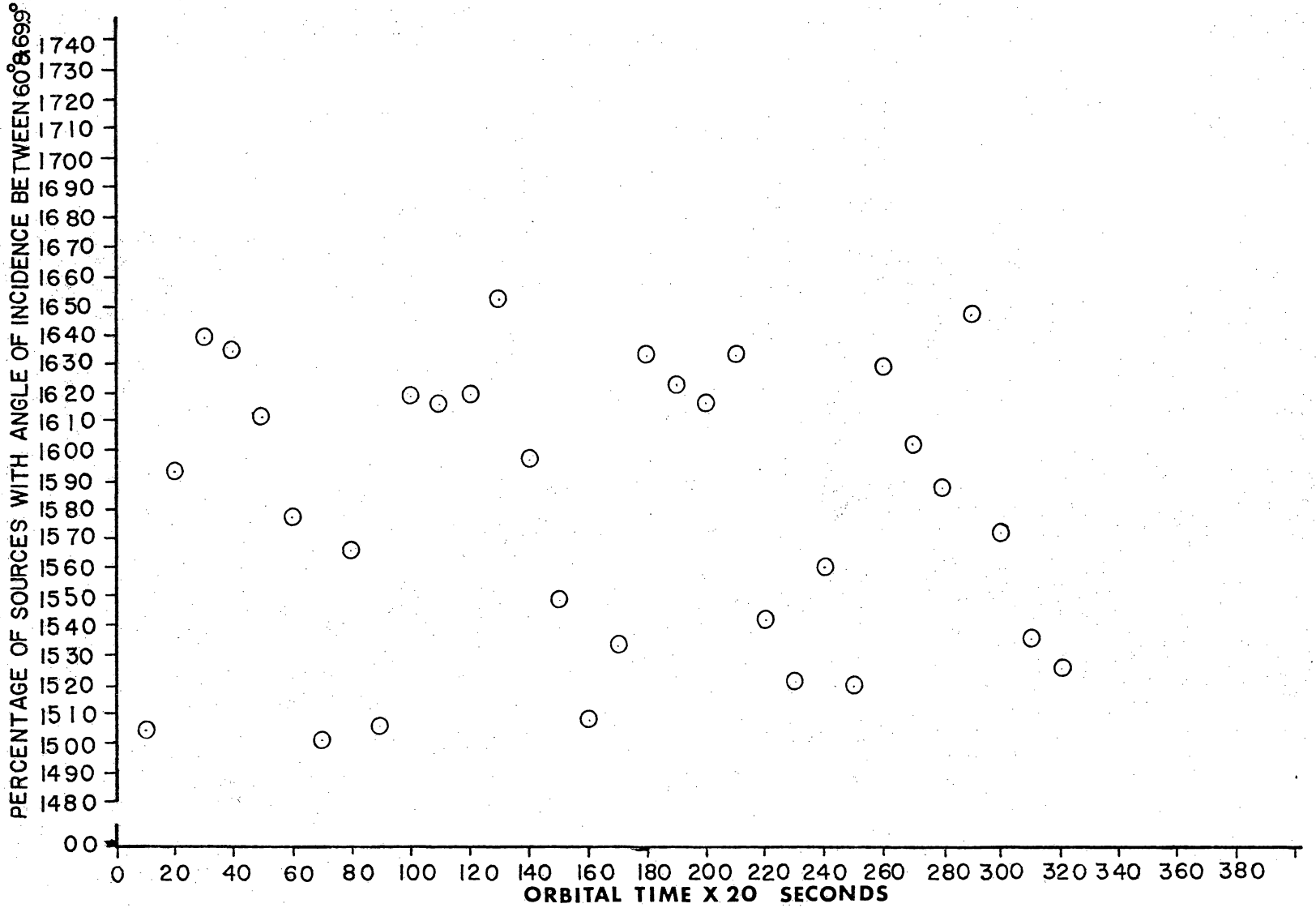

Figure 12. Percentage of all Earth-Emitted Sources with Angle of Incidence Between 60 deg. and 69 deg.

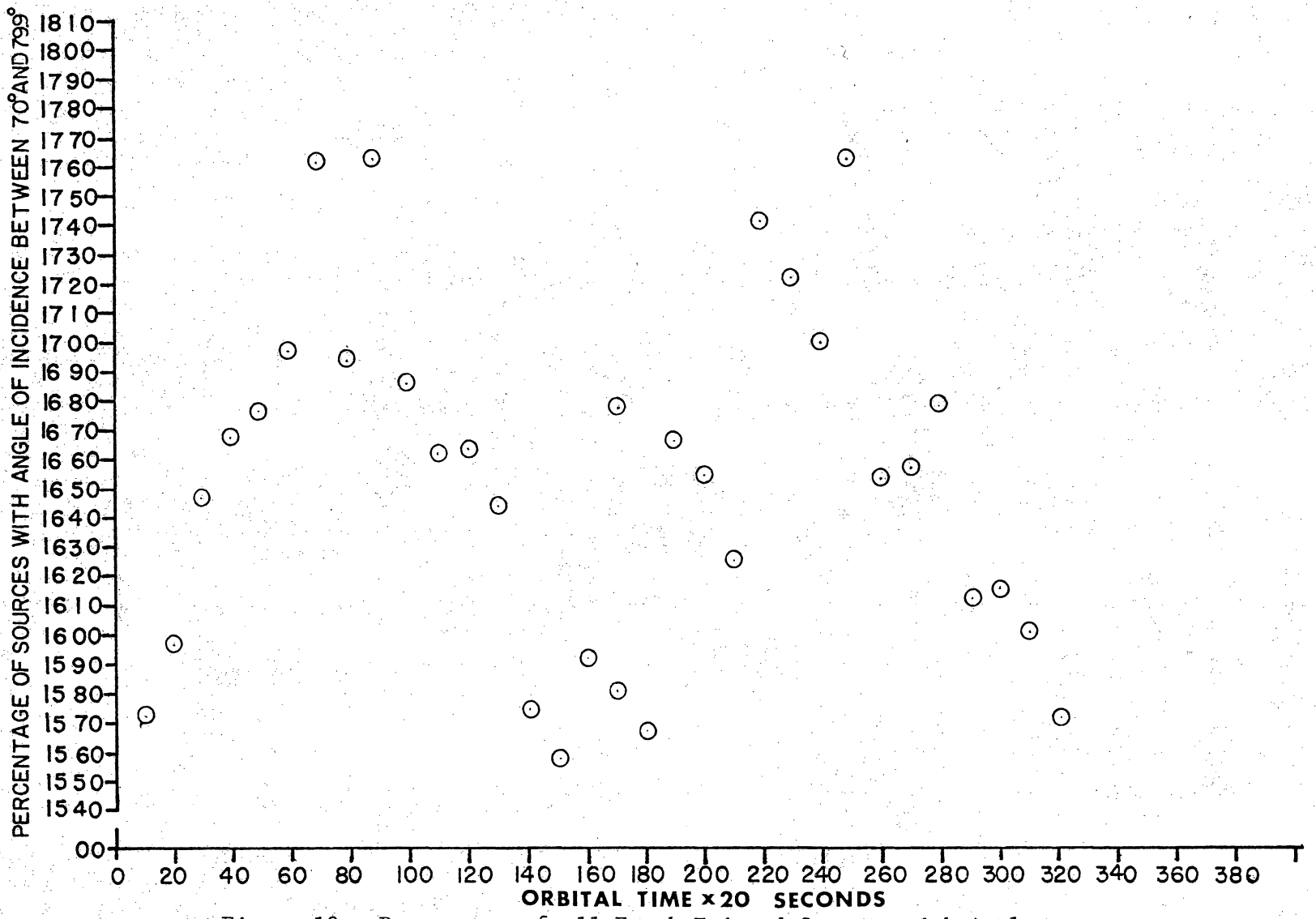

Figure 13. Percentage of all Earth-Emitted Sources with Angle of Incidence Between 70 deg. and 79 deg.

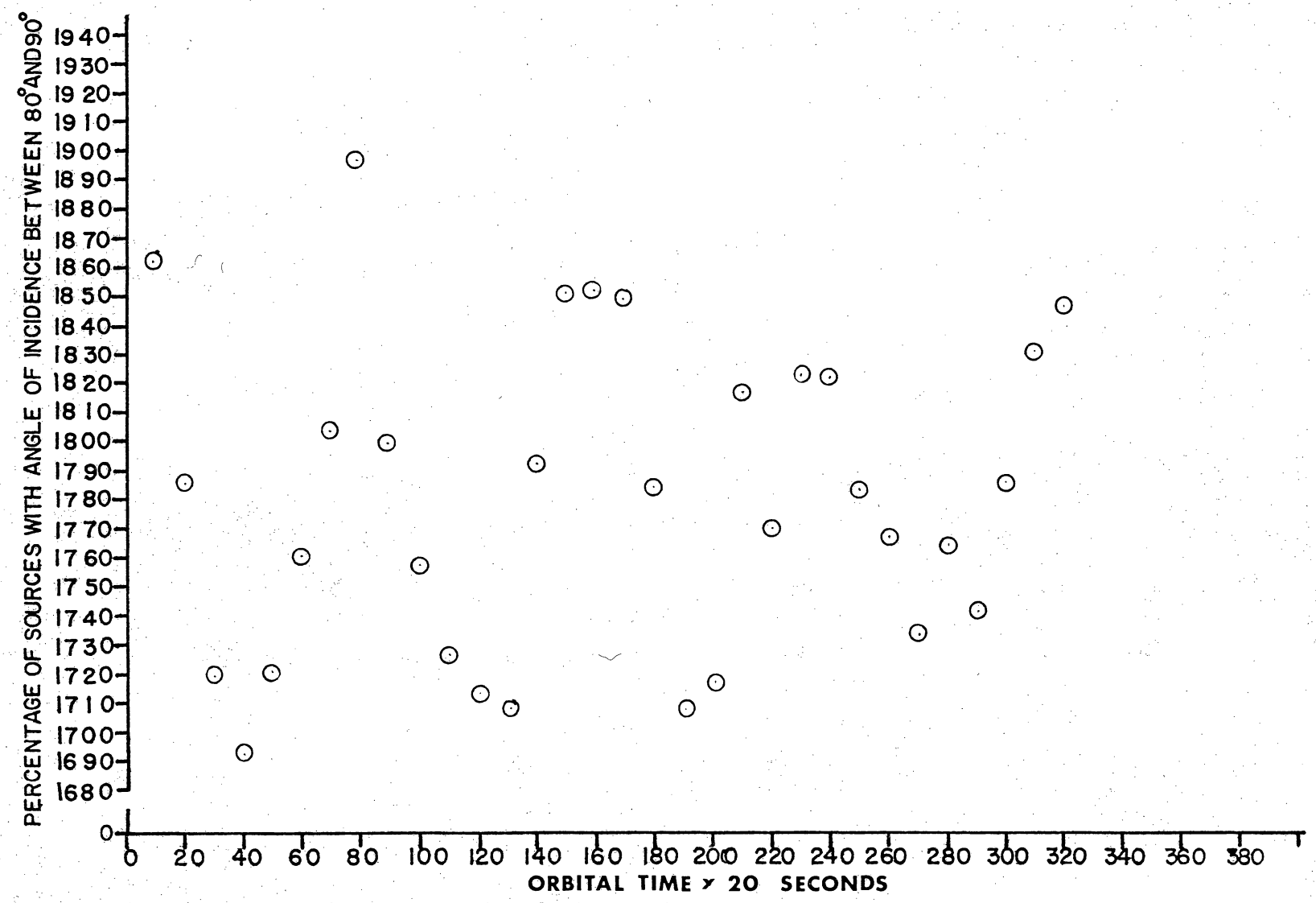

Figure 14. Percentage of all Earth-Emitted Sources with Angle of Incidence Between 80 deg. and 90 deg.

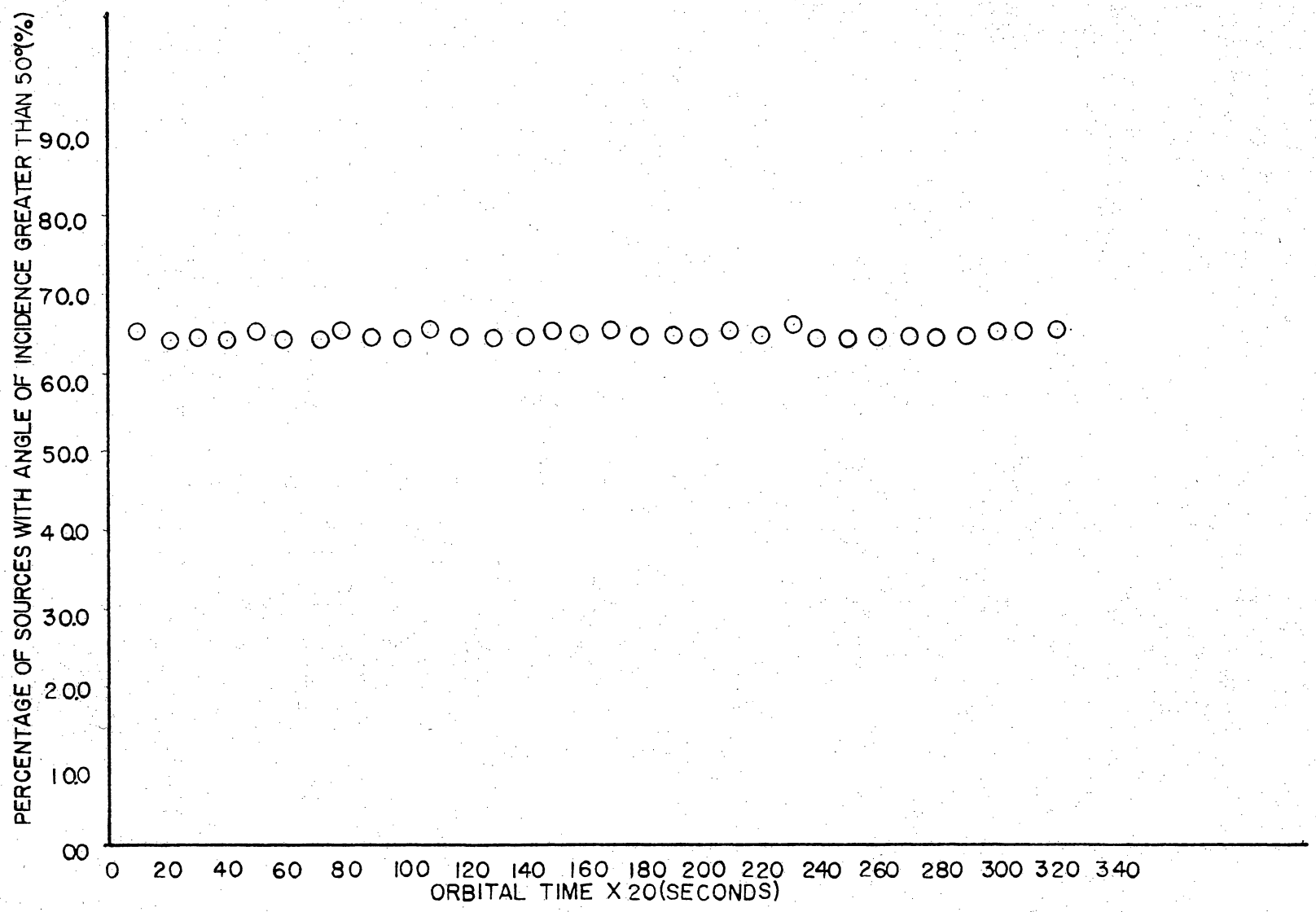

Figure 15. Percentage of all Earth-Emitted Sources with Angle of Incidence Greater Than 50 deg.

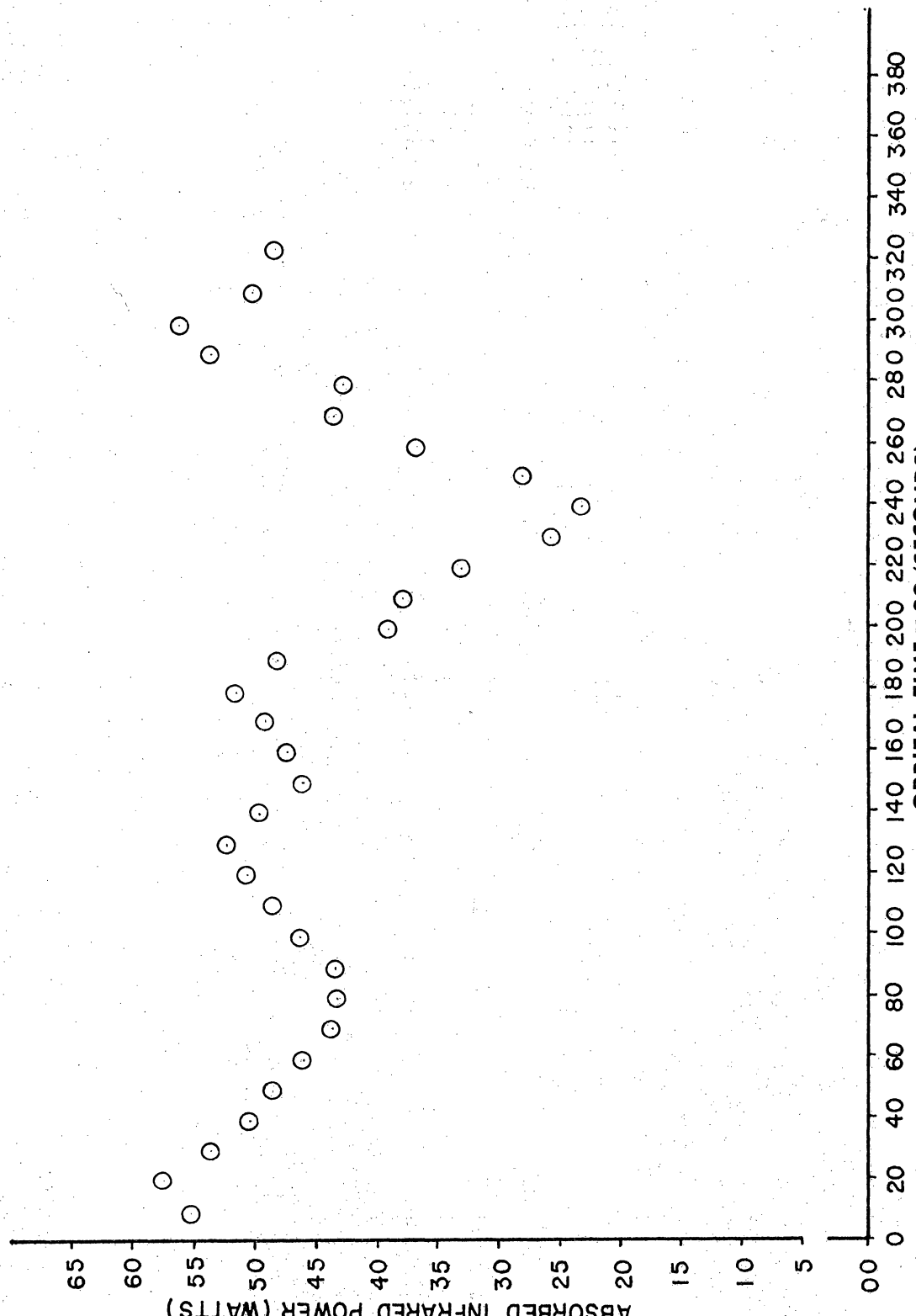

Figure 16. Absorbed Long Wavelength Power for the Orbit

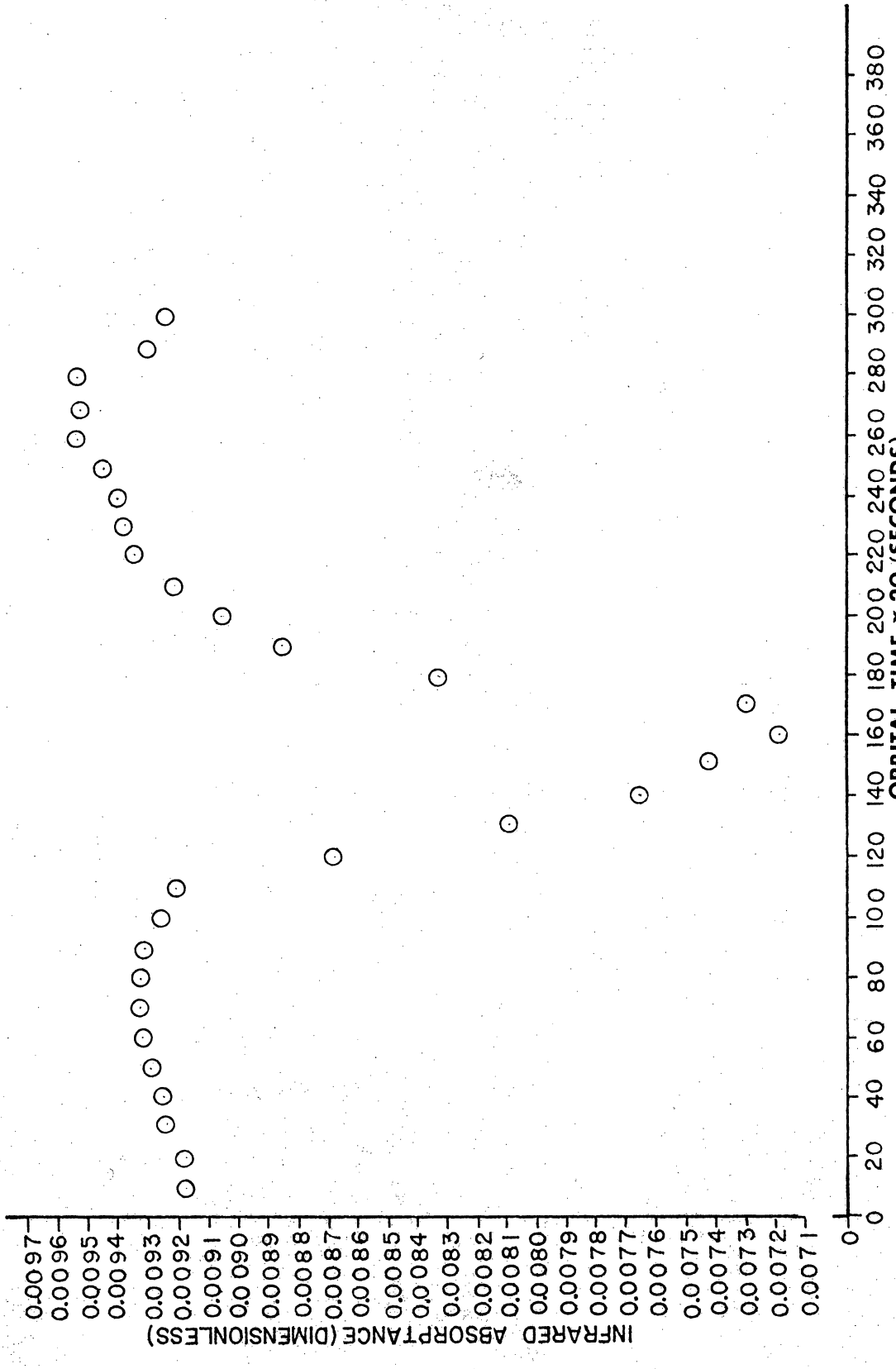

Figure 17. Long Wavelength Absorptance of the Detector for the Orbit

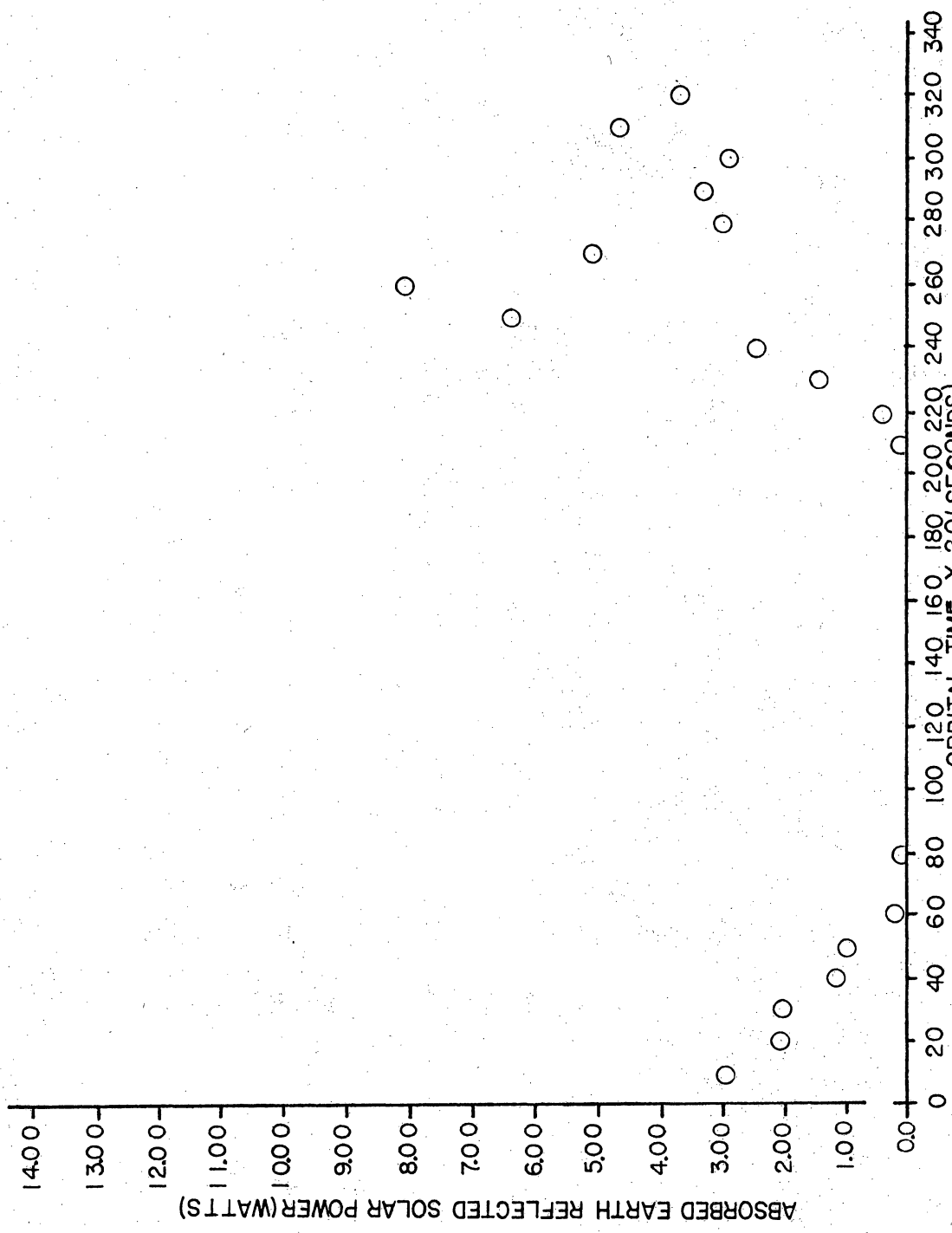

Figure 18. Absorbed Earth-Reflected Solar Power for the Orbit

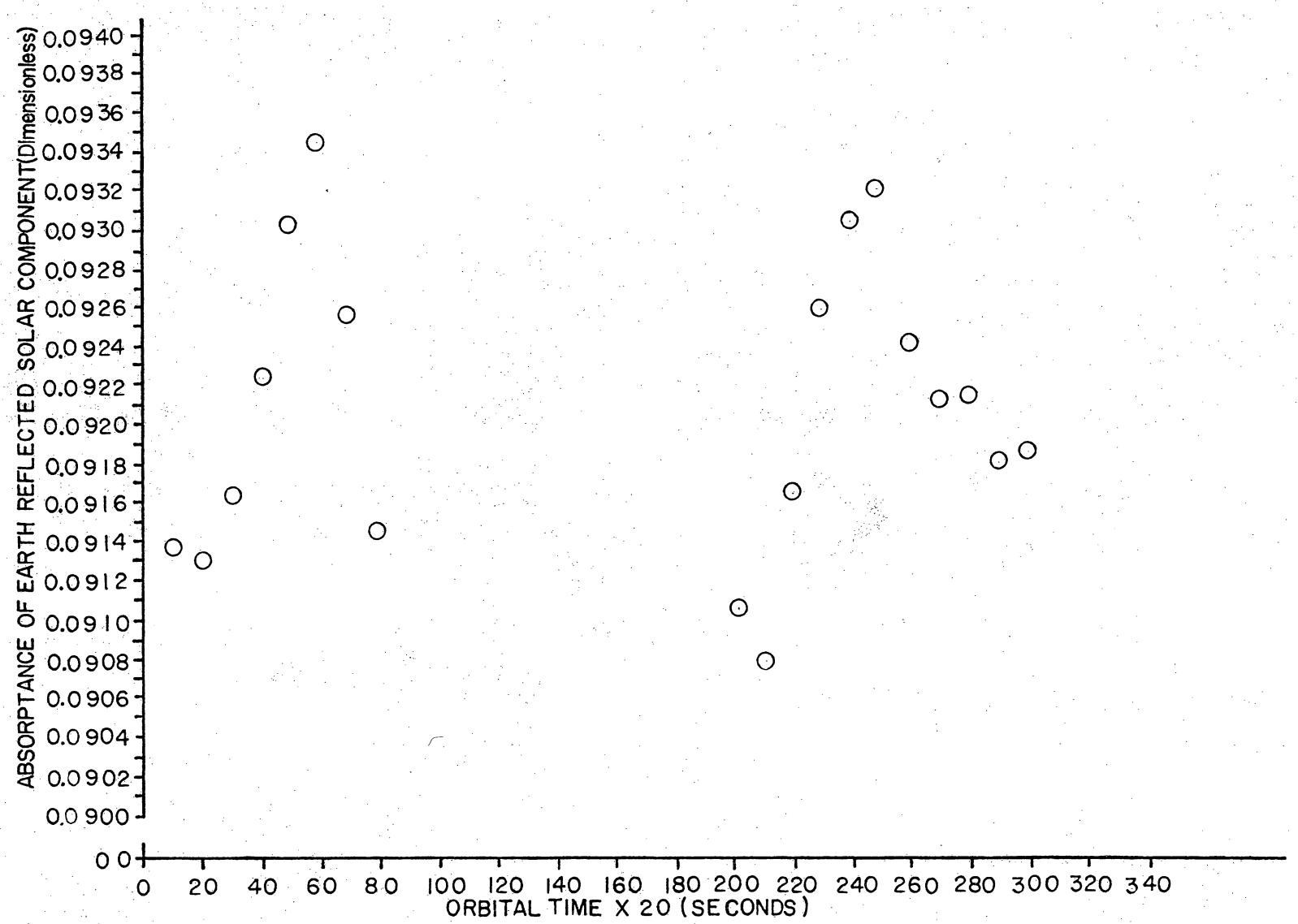

Figure 19. Solar Absorptance for the Orbit

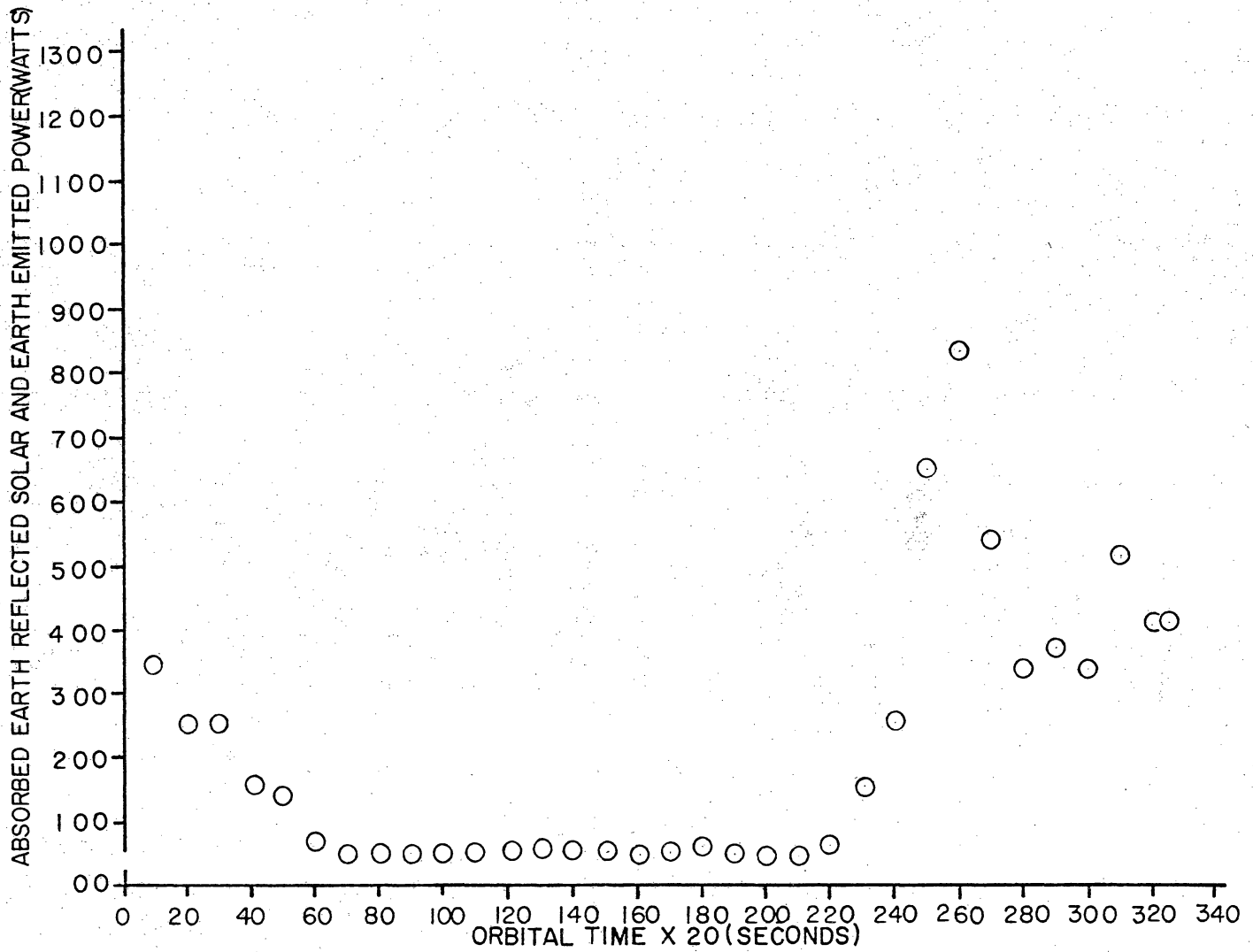

Figure 20. Absorbed Earth-Emitted and Earth-Reflected Solar Power for the Orbit

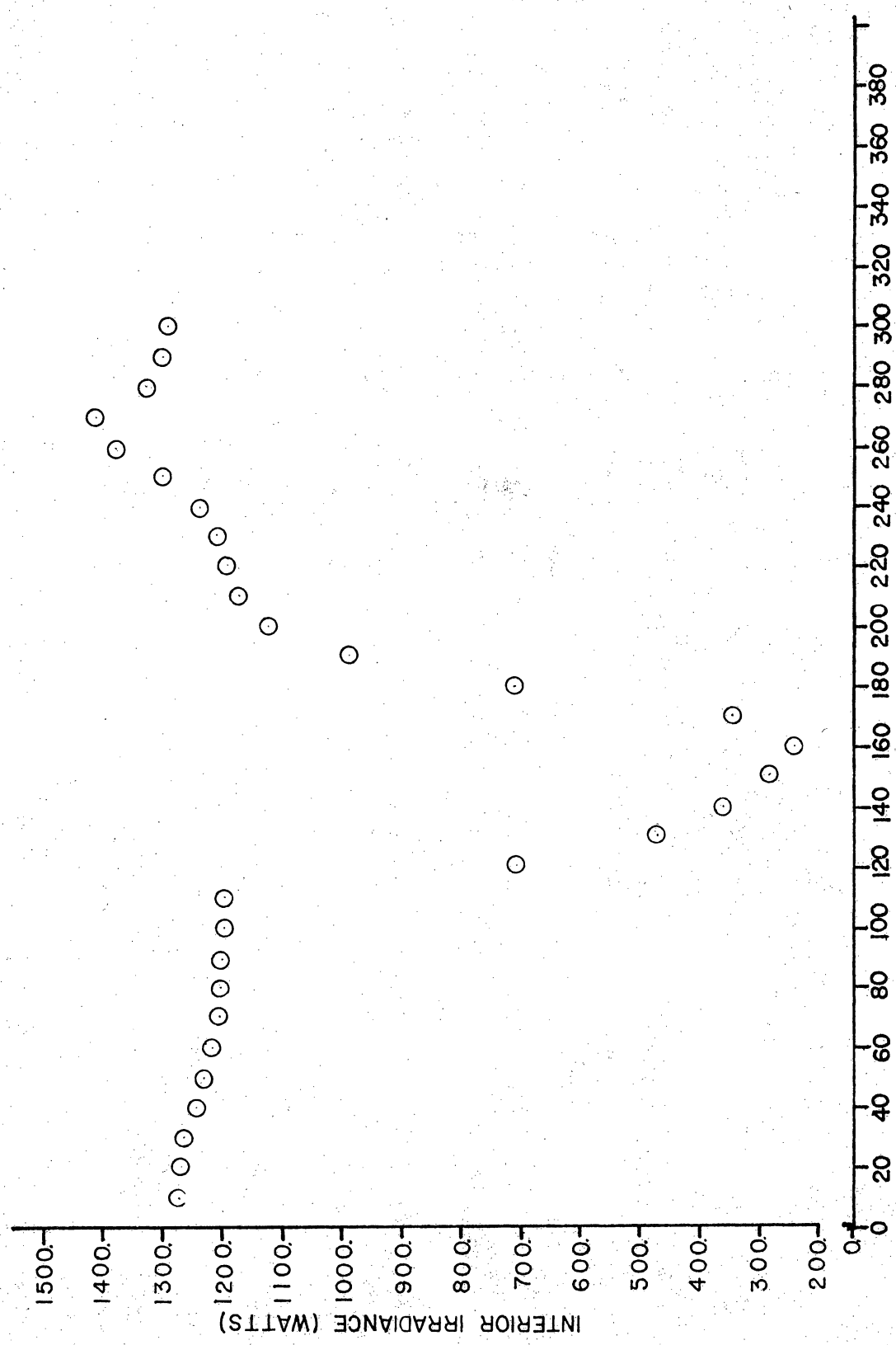

Figure 21. Interior Irradiance of the Detector for the Orbit

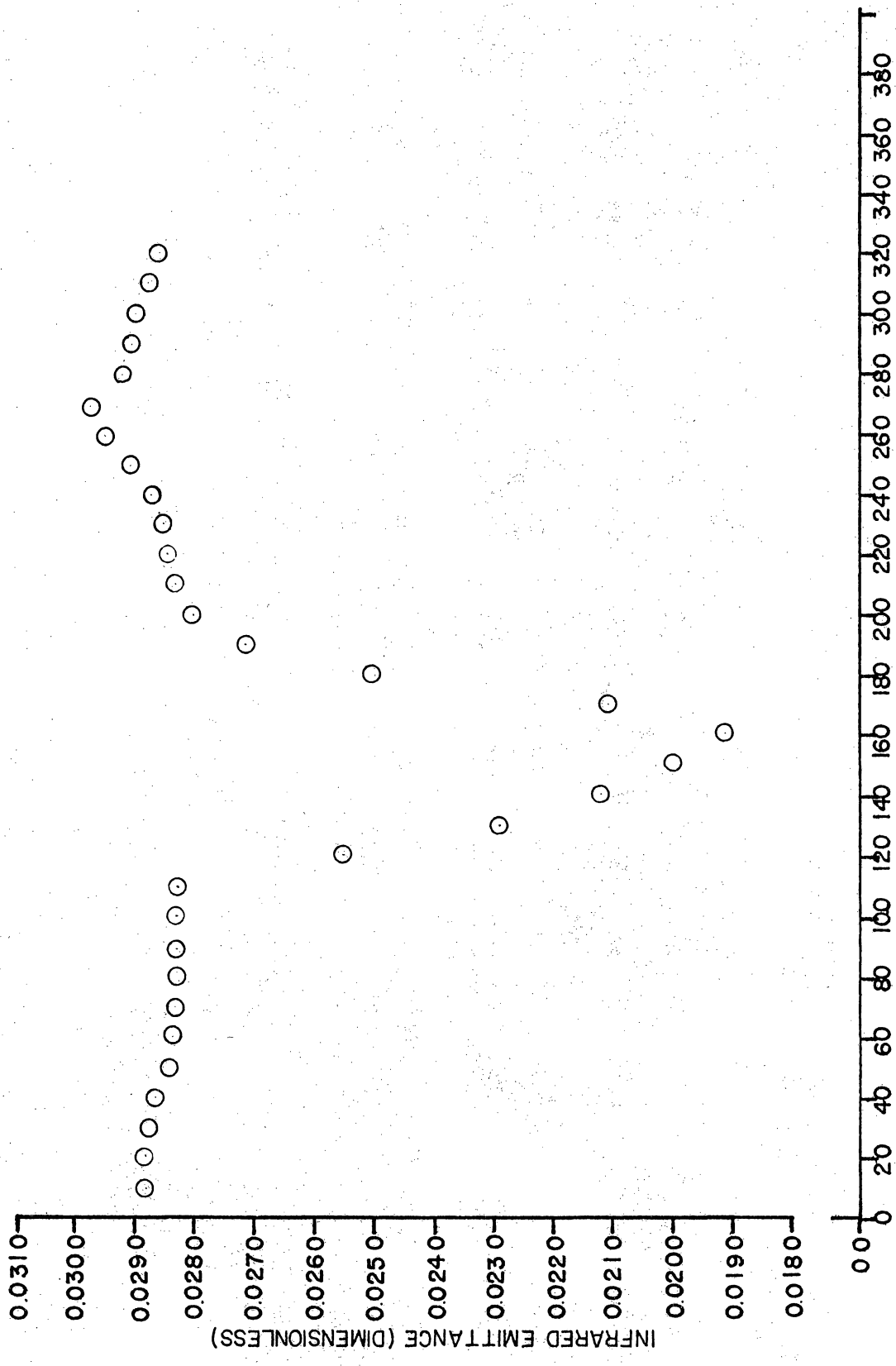

Figure 22. Emittance of the Detector for the Orbit

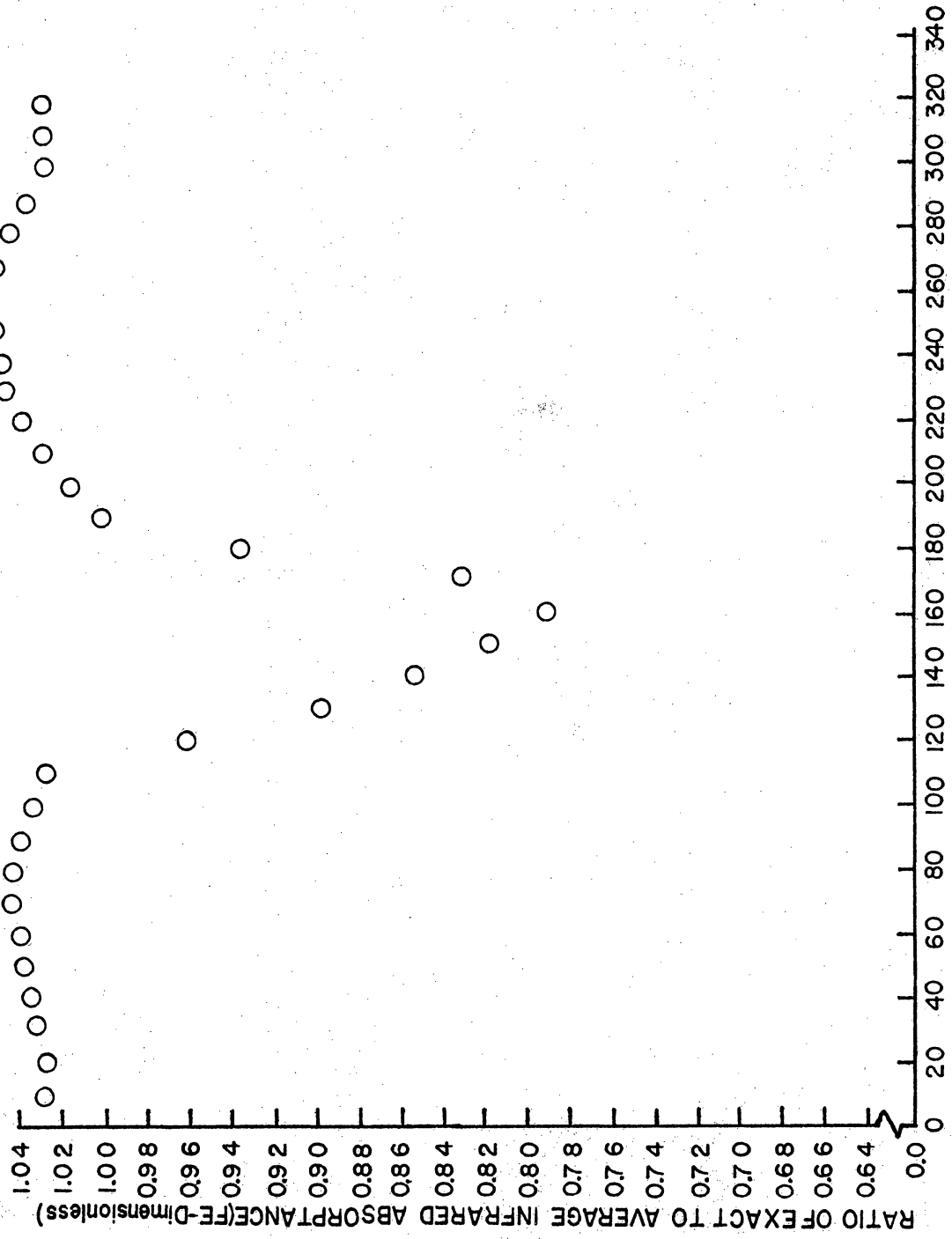

Figure 23. Ratio of Actual Absorbed Earth-Emitted Power to the Average Absorbed Earth-Emitted Power (FE) for the Orbit

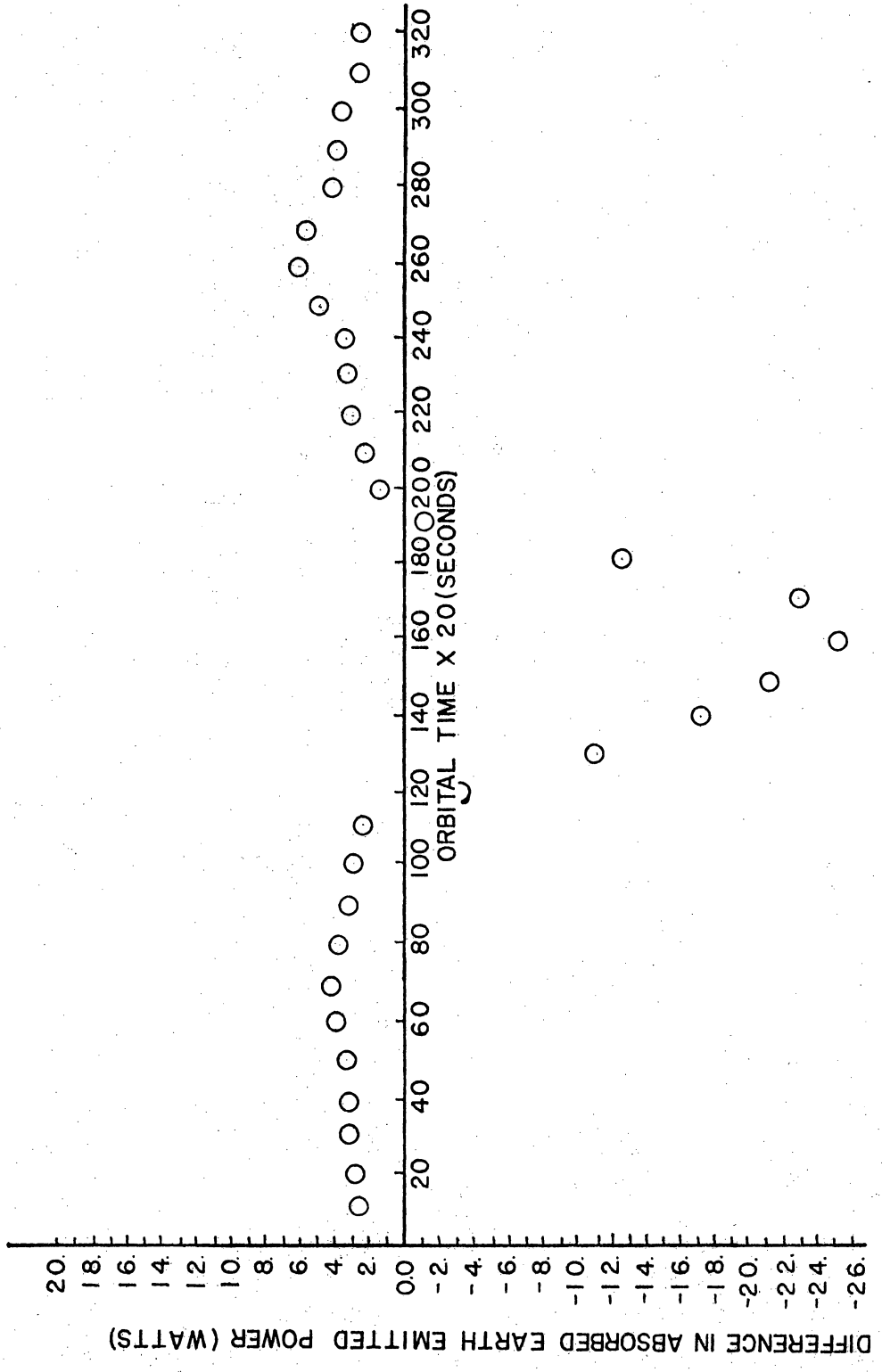

Figure 24. Difference Between the Actual and Average Absorbed Earth-Emitted Power for the Orbit

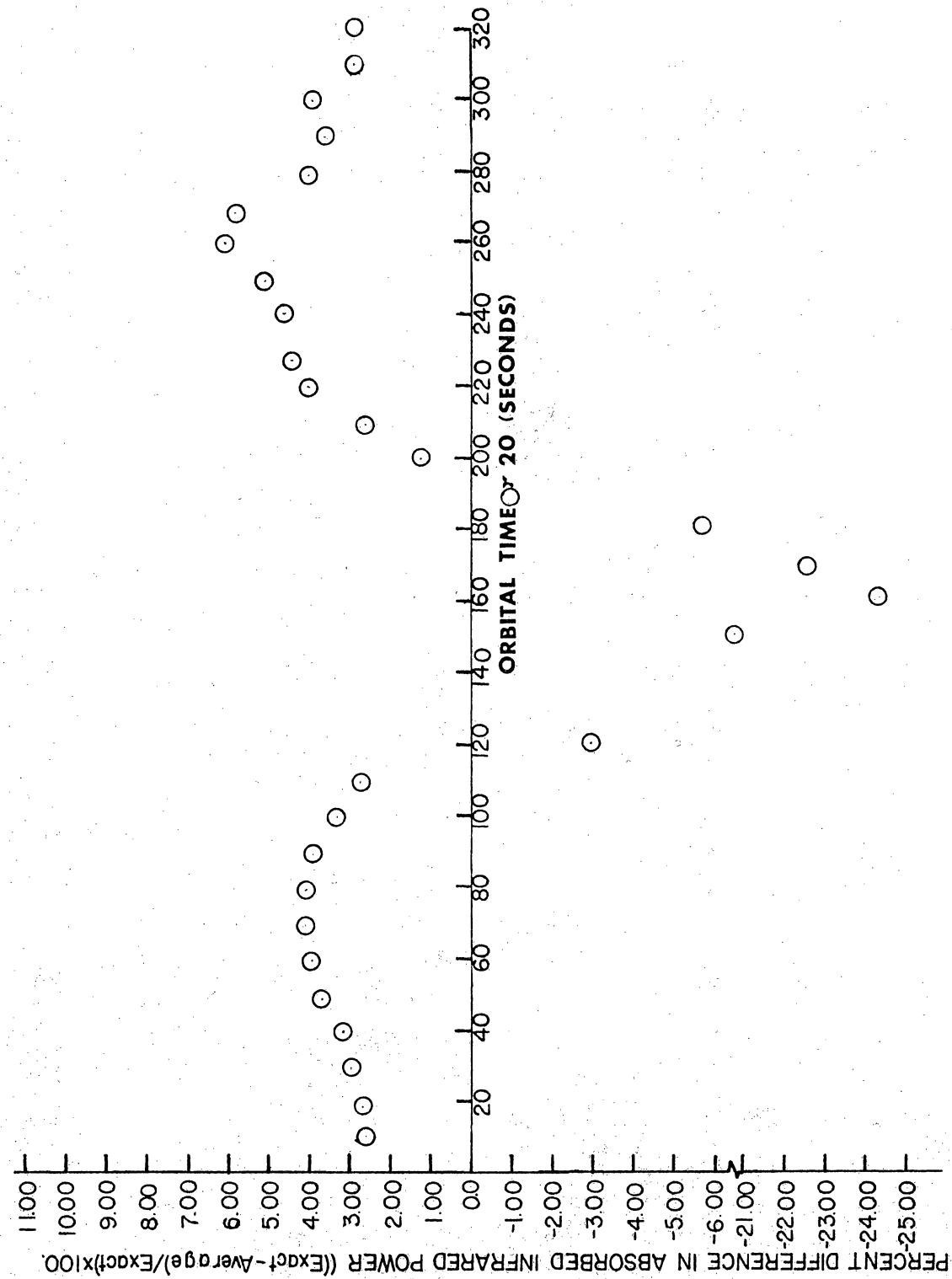

Figure 25. Per Cent Difference Between the Actual and Average Absorbed Earth-Emitted Power for the Orbit

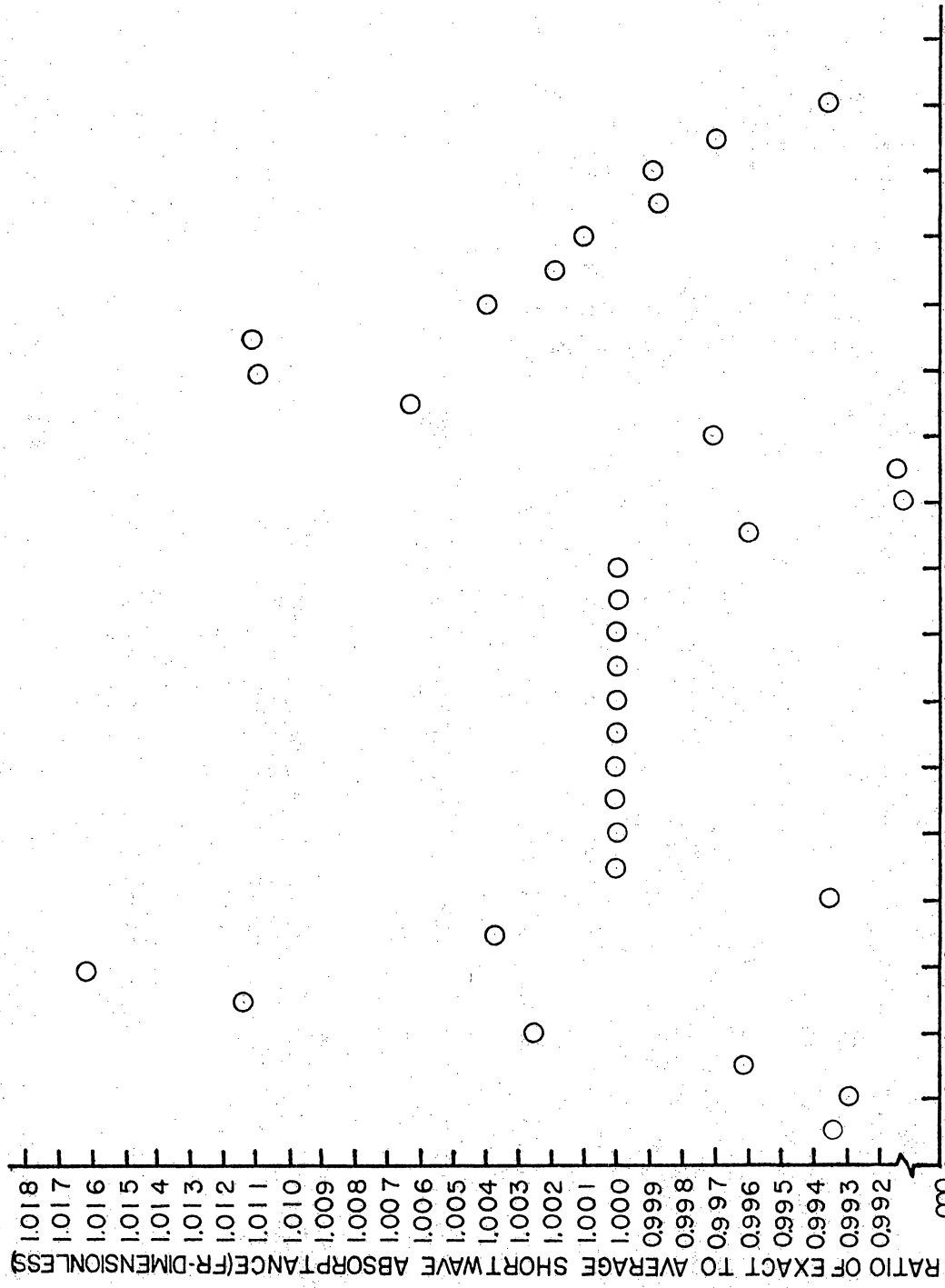

Figure 26. Ratio of the Actual Absorbed Earth-Reflected Solar Power to the Average Absorbed Earth-Reflected Solar Power (FR) for the Orbit

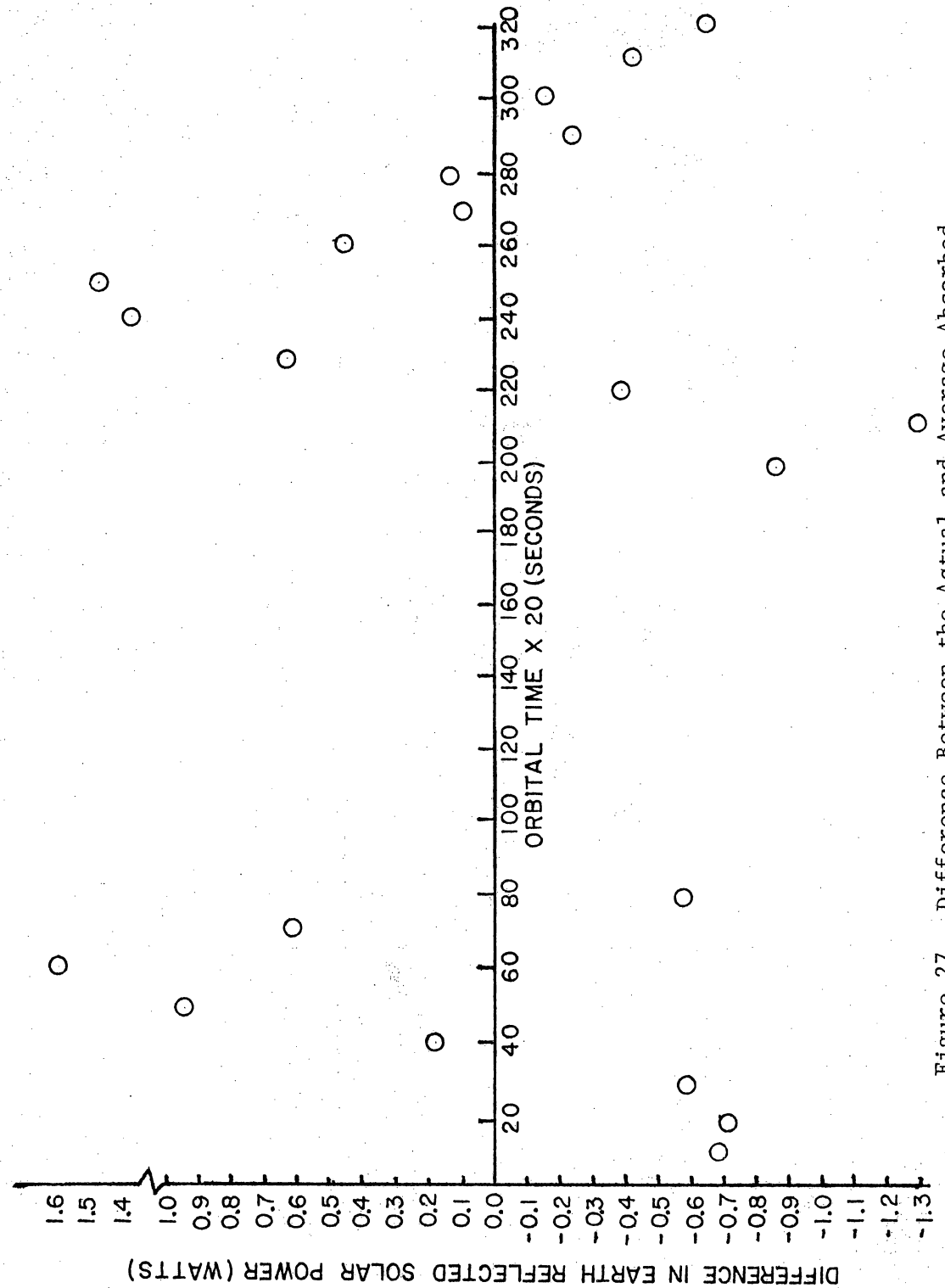

Figure 27. Difference Between the Actual and Average Absorbed Earth-Reflected Solar Power for the Orbit

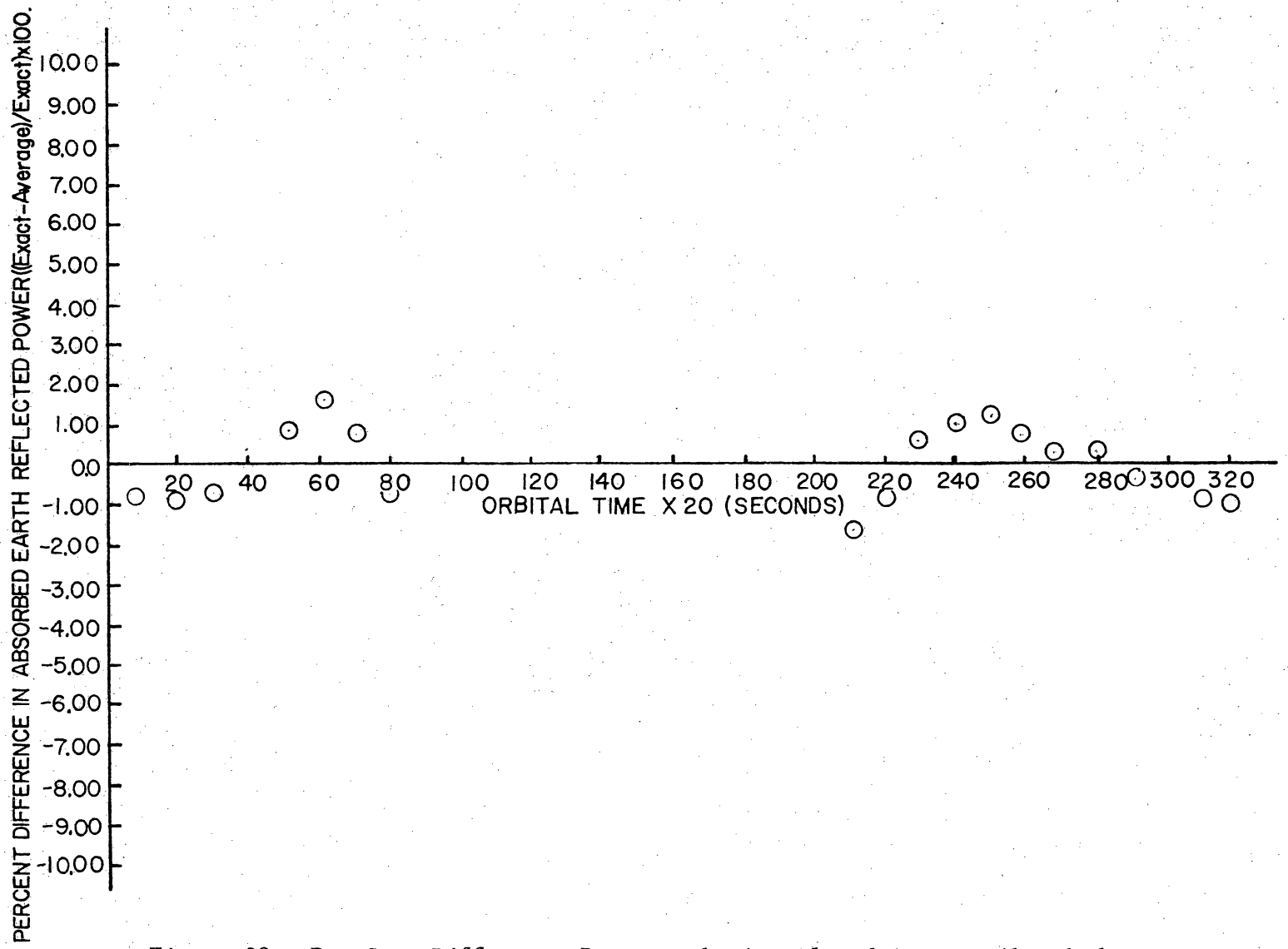

Figure 28. Per Cent Difference Between the Actual and Average Absorbed Earth-Reflected Solar Power for the Orbit

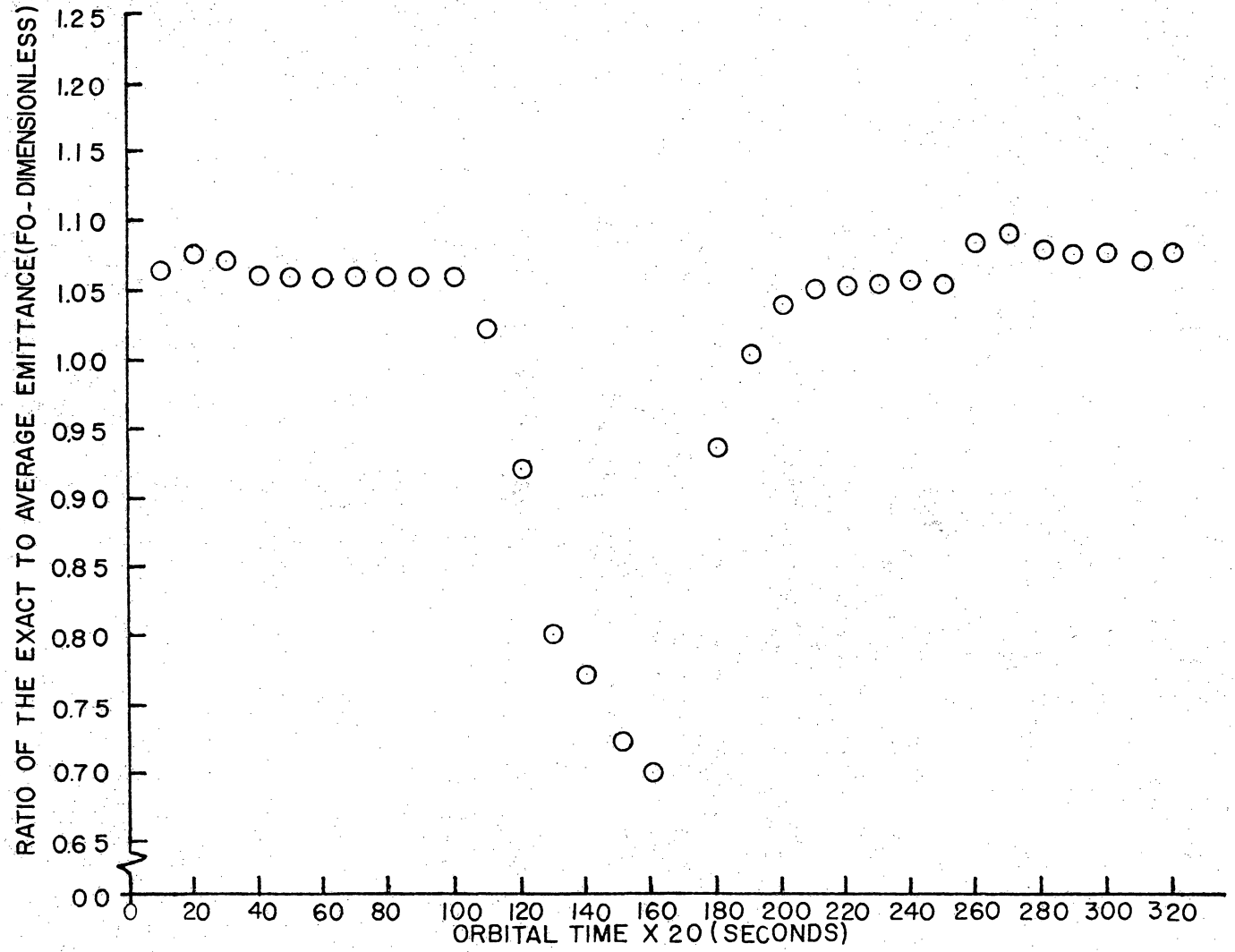

Figure 29. Ratio of the Actual Emittance to the Average Emittance (FO) for the Orbit

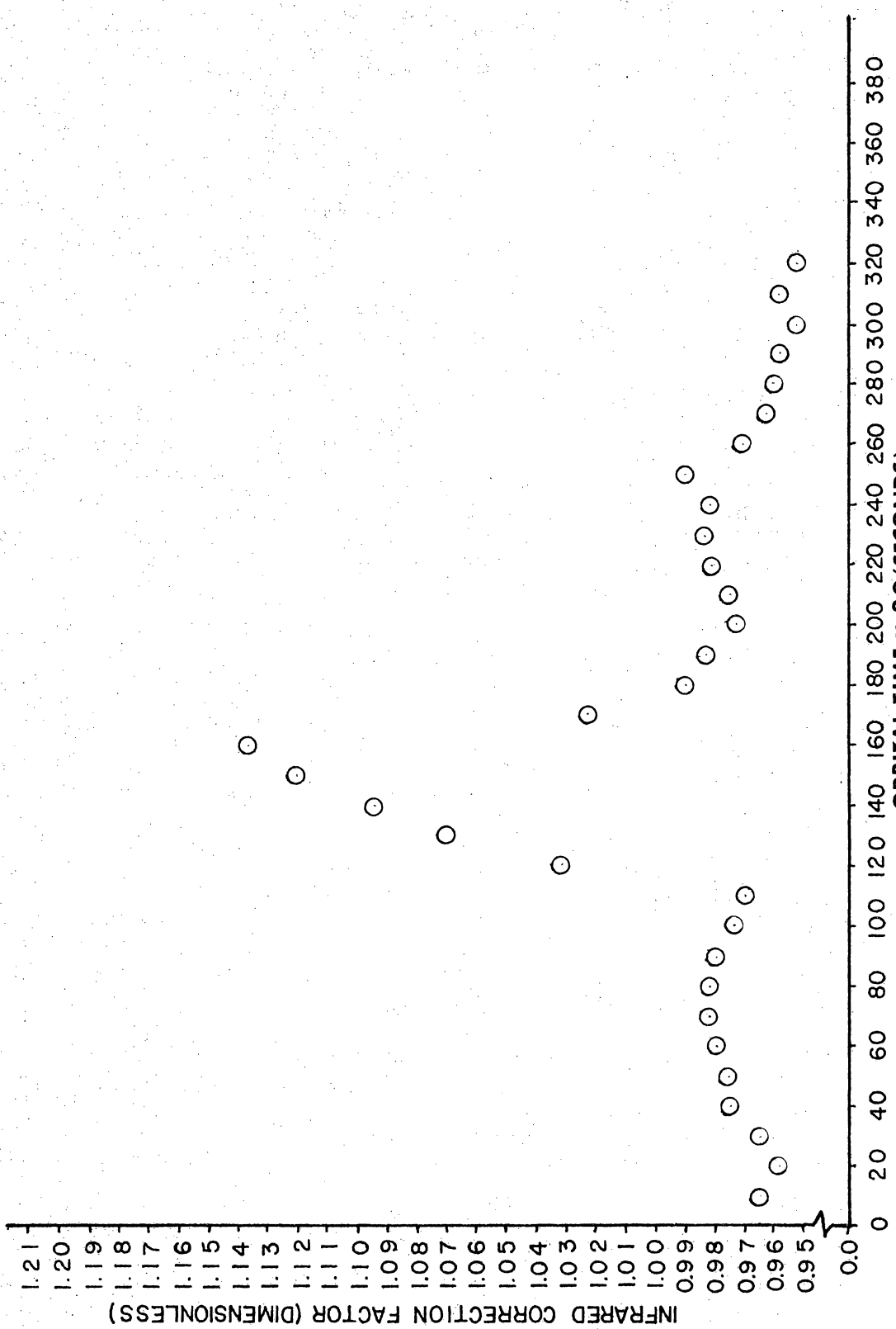

Figure 30. Long Wavelength Correction Factor (CE) for the Orbit

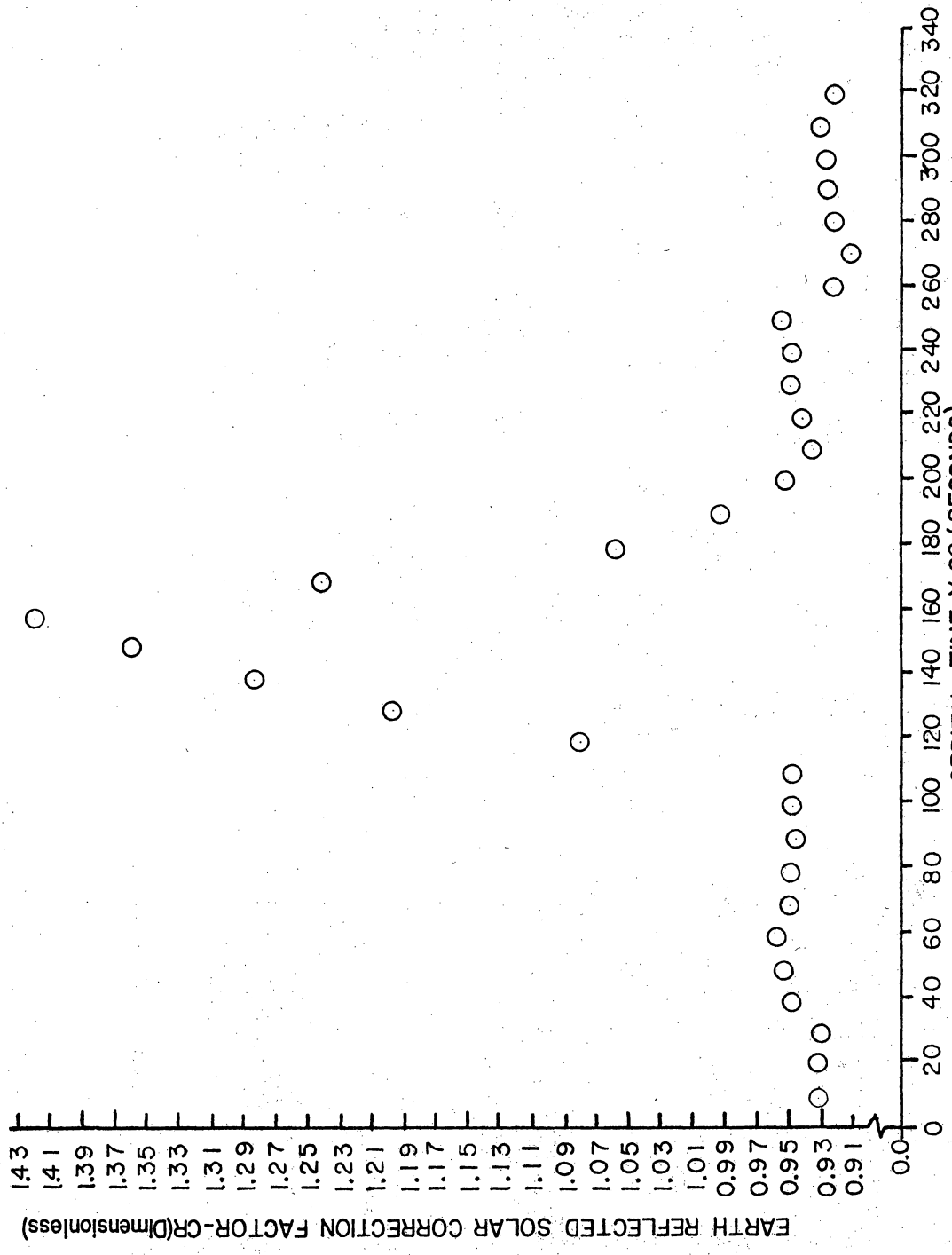

Figure 31. Earth-Reflected Solar Correction Factor (CR) for the Orbit

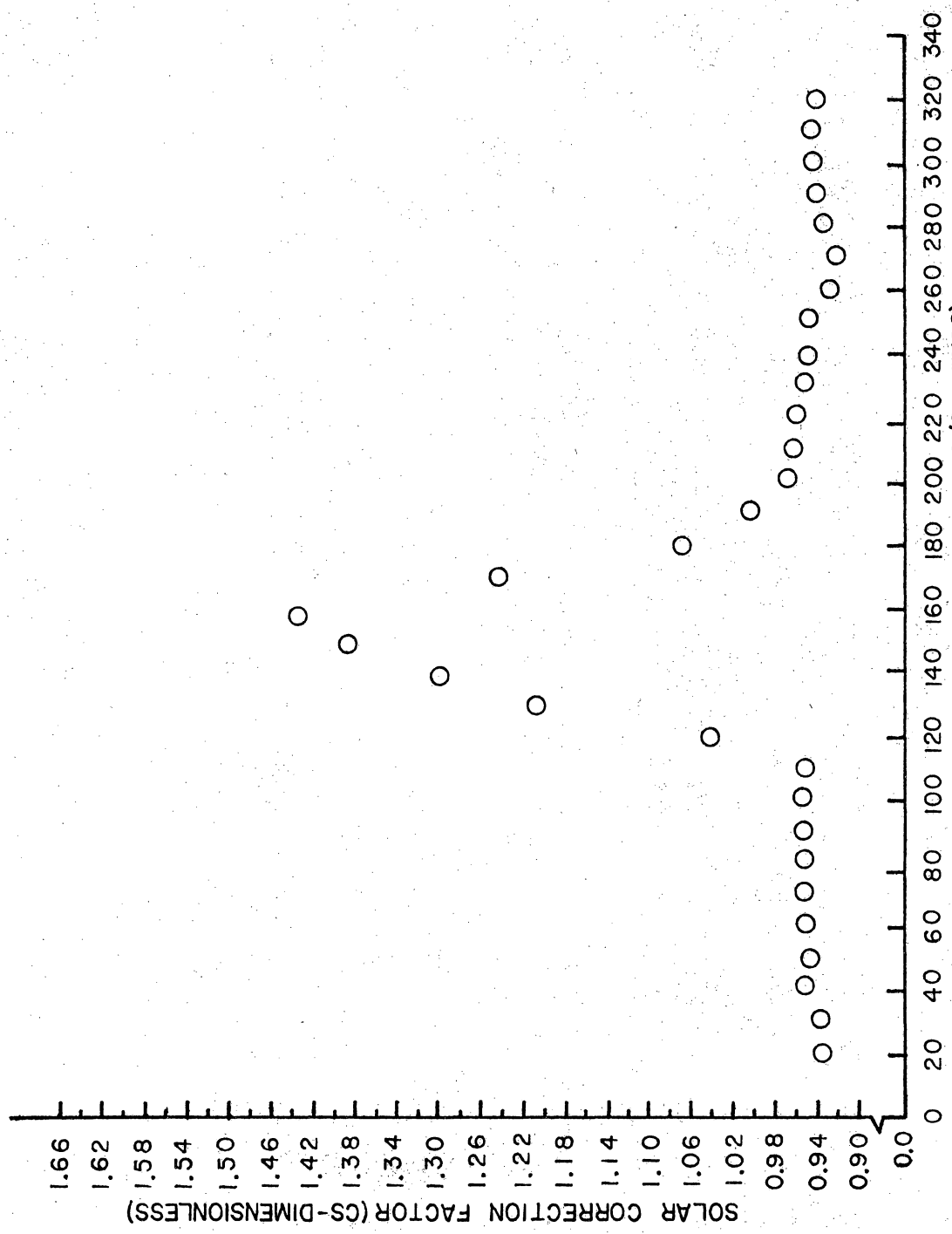

Figure 32. Solar Correction Factor (CS) for the Orbit

```
C      EARTH.  GIVEN IRRADIANCE VALUES FOR THE LONG AND SHORT WAVE        JOP   18
C      EARTH COMPONENTS AND THE SHORT WAVELENGTH SOLAR COMPONENT, THE     JOP   19
C      PROGRAM WILL CALCULATE THE TEMPERATURE DISTRIBUTION ON THE         JOP   20
C      SURFACE OF THE SATELLITE.  FROM THIS DISTRIBUTION, CONCLUSIONS     JOP   21
C      MAY BE DRAWN WITH REGARD TO THE THERMAL RESPONCE OF THE            JOP   22
C      SATELLITE AND ITS SUITABILITY AS AN ENERGY BUDGET SENSOR.          JOP   23
       BLOCK DATA
       IMPLICIT REAL *8(A-H,O-Z)
       DOUBLE PRECISION VERC(5,220),SOURCE(3,211),H(3,92),TINIT(2,92),
      1SOLAR(10,10),DCCOND(92),SOLAB(91),PRCNT(50),XLAMDA(50),BNDENG(50),
      2BPAR(30),BUF(15),STUCK(92),T(10,10),CONTAN(93),TLAM(93)
       INTEGER LIMIT(92)
       COMMON/STORE1/ SOURCE,TINIT,DCCOND,AREATH
       COMMON/STORE2/ STUCK,SOLAB,PRCNT
       COMMON/STORE3/ H,SOLAR,HZ,AVG,ALW,ELW
       COMMON/STORE4/ BNDENG,XLAMDA,XNORML,XPARAL
       COMMON/STORE5/ TLAM,CONTAN
       COMMON/ACCESS/ LIMIT,NPOINT,NVECTR
       COMMON/CNSTNT/ PI,P2,RADIAN,SIGO,SIG,E,XMNEFF,CO,RSAT,NTS,NPS
       COMMON/LABEL/ VERC,BPAR,BUF,POMEGA,RELAXT,TAU2
       COMMON/START/ T,XXH,KKKK
       DATA SIG/5.6693D-08/
       DATAT/100*0.0D0/
       DATA KKKK/0/,XXH/0.D0/
       DATASOURCE/633*0.0D0/,SOLAR/100*0.0D0/,DCCOND/92*0.0D0/,BNDENG/50*
      10.0D0/,LIMIT/92*0/
       DATA PI/3.141592653897/,RADIAN/0.01745329/,E/4.80296D-10/,XMNEFF/2
      1.6D0/,CO/2.997925D14/,XNORML/0.50D0/,XPARAL/0.50D0/
       DATA NTS/10/,NPS/10/
       END
       IMPLICIT REAL *8(A-H,O-Z)
       REAL SNGL
```

```
      DOUBLE PRECISION SOURCE(3,211),VERC(5,220),H(3,92),TINIT(2,92),
     1T(10,10),TT(10,10),SOLAR(10,10),HIN(10,10),DCCOND(92),SOLAB(91),PR
     2CNT(50),XLAMDA(50),BNDENG(50),BPAR(30),BUF(15),STUCK(92),F(4,92),
     3CONTAN(93),TLAM(93)
      INTEGER LIMIT(92)
      REAL LAT,LONG                                                    JOP   34
      COMMON/STORE1/ SOURCE,TINIT,DCCOND,AREATH
      COMMON/STORE2/ STUCK,SOLAB,PRCNT
      COMMON/STORE3/ H,SOLAR,HZ,AVG,ALW,ELW
      COMMON/STORE4/ BNDENG,XLAMDA,XNORML,XPARAL
      COMMON/ACCESS/ LIMIT,NPOINT,NVECTR
      COMMON/CNSTNT/ PI,P2,RADIAN,SIGC,SIG,E,XMNEFF,CO,RSAT,NTS,NPS
      COMMON/LABEL/ VERC,BPAR,BUF,POMEGA,RELAXT,TAU2
      COMMON/START/ T,XXH,KKKK
      BTA(TH)=2.*DARSIN(   DSIN(TH)*DSIN(THR*.5))                      00000080
      A12(T1,T2,A1,A2)=THR-DARCOS(((A2*DSIN(T2))**2+(A1*DSIN(T1))**2
     1-(A1*A1+A2*A2-(A2*DCOS(T2)-A1*DCOS(T1))**2))/(2.*A2*DSIN(T2)
     2*A1*DSIN(T1)))
      BT12(T1,T2,A1,A2)=DARCOS((A2*A2+A1*A1-((A2*DCOS(T2)-A1*DCOS(T1))
     1**2+(A2*DSIN(T2))**2+(A1*DSIN(T1))**2-2.*A2*DSIN(T2)*A1*DSIN(T1)
     2*DCOS(A12(T1,T2,A1,A2))))/(2.*A1*A2))
C     DEFINE BASIC CONSTANTS                                           JOP   42
10000 CONTINUE                                                         JOP   43
      DATA D/3.0CD09/,A/1.0D10/,B/2.0D09/,XKP/13.1700/,RT1/430.0D0/,FRT/
     1375.0D0/,OR/5.68D-05/,PO/2040.0D0/,C/752.17396D0/,AOV/0.0005D0/,TS
     2INK/350.D0/,EI/0.5D0/,REARTH/6.370+06/
      DATA KNUMB/0/,JCONT/0/,JK/0/,IUNIT/8/,ISET/0/
      KKK=2
      LGO=0
      K1=1
      SIGO=3.178D17
      X4V=26.9815D0/2.692D0
```

```
      SUMELW=0.0D0
      SUMALW=0.0D0
      SUMASW=0.0D0
      SUMAVG=0.0D0
      DO 9009 I=1,324
      READ(5,9008) ALW,ELW,ASW,AVGALW
 9008 FORMAT(4D15.8)
      IF(ASW.GT.0.0D0) UADDEM=UADDEM+1.0D0
      SUMELW=SUMELW+ELW
      SUMALW=SUMALW+ALW
      SUMASW=SUMASW+ASW
      SUMAVG=SUMAVG+AVGALW
 9009 CONTINUE
      ASW=SUMASW/UADDEM
      ALW=SUMALW/324.0D0
      ELW=SUMAVG/324.0D0
      WRITE(6,9010) ALW,ASW,ELW
 9010 FORMAT(1H ,4HALW=,F12.6,3X,4HASW=,F12.6,3X,4HELW=,F12.6)
      XNN=6.02D23/XMV
      XMNEFF=2.6D0*XNN
      XLAMD=3.8
      DO 713 K=1,50
      IF(K.EQ.1) XLAMDA(K)=XLAMD+0.2
      IF(K.GT.1.AND.K.LT.7) XLAMDA(K)=XLAMDA(K-1)+0.2
      IF(K.GT.6.AND.K.LT.17) XLAMDA(K)=XLAMDA(K-1)+0.5
      IF(K.GT.16.AND.K.LT.27) XLAMDA(K)=XLAMDA(K-1)+1.0
      IF(K.GT.26.AND.K.LT.32) XLAMDA(K)=XLAMDA(K-1)+2.0
      IF(K.GT.31.AND.K.LT.38) XLAMDA(K)=XLAMDA(K-1)+5.0
      IF(K.GT.37.AND.K.LT.42) XLAMDA(K)=XLAMDA(K-1)+10.0
      IF(K.GT.41) XLAMDA(K)=XLAMDA(K-1)+20.0
  713 CONTINUE
      NN=0
```

```
C***** BUFF(4) - NUMBER OF SATELLITES IN ORBIT
C***** BUFF(5) - NUMBER OF TIME STEPS COVERED IN THE ORBIT
C***** BUFF(6) - BUFF(10) -SATELLITE PARAMETERS
C***** BUFF(11) - ORBIT RADIUS
      IF(LGO.EQ.1) GO TO 502
      NPINT=0
      DO 501 I=1,NTS
      DO 501 J=1,NPS
      NPINT=NPINT+1
      IF(ISET.EQ.0) DCCOND(NPINT)=SIGO*(273.0D0/T(I,J))
      IF(ISET.EQ.1) DCCOND(NPINT)=SIGO*(273.0D0/TINIT(2,NPINT))
      IF(I.EQ.NTS.AND.J.EQ.2) GO TO 502
  501 CONTINUE
  502 CONTINUE
      IF(ISET.EQ.0) KKKJ=KKKK+1
      IF(KKKJ.GT.1) GO TO 812
      DO 810 I=1,NTS
      DO 810 J=1,NPS                                                    JOP   64
      IF(I.EQ.NTS) ASATE=0.5*XNPS                                       JOP   65
      SAS=SAS+T(I,J)**4*ASATE                                           JOP   66
      IF(I.EQ.NTS.AND.J.EQ.2) GO TO 811                                 JOP   67
  810 CONTINUE                                                          JOP   68
  811 XXH=SIG*SAS/(XNPS*XNTS)                                           JOP   69
  812 CONTINUE
      IF(ISET.EQ.1) XXH=XXH1
      RSAT=BUF(11)-REARTH
      THITA=REARTH/BUF(11)
      THEETA=DARCOS(THITA)
      RADEUS=REARTH*DSIN(THEETA)
      SURFAC=PI*RADEUS**2.
      AREATH=SURFAC/BPAR(30)
C*****LCHECK IS THE COMMAND STATEMENT UTILIZED IN THE LOGIC TO DETERMINE
```

```
C*****WHAT SOLUTION TECHNIQUE IS TO BE UTILIZED; IF LCHECK=0,THEN THE
C*****EXACT SOLUTION IS PERFORMED AND IF LCHECK=1,THEN THE AVERAGE
C*****PROPERTY SOLUTION IS PERFORMED
      LCHECK=0
      IF(LGO.EQ.1) LCHECK=1
C*****STIME- START TIME
      STIME=BUF(1)                                                    JOP   83
C*****DTM- A NEW SOURCE FIELD IS PROVIDED EACH DTM TIME INCREMENT
      DTM=BUF(3)                                                      JOP   84
      DT=DTM
      RS=BUF(4)                                                       JOP   85
      NBUF2=BUF(5)
      TIME=BPAR(1)                                                    JOP   89
      HZ=BPAR(25)
      LAT=BPAR(2)                                                     JOP   90
      LONG=BPAR(4)                                                    JOP   91
      N=BPAR(30)
C     THE '7' DO-LOOP IS THE MAIN INTEGRATING LOOP OF THE PROGRAM     JOP  128
C     IT SWEEPS OVER ALL AREA ELEMENTS OF THE SATELLITE AND COMPUTES   JOP  129
C     THE INCIDENT RADIANT FLUX ON EACH                               JOP  130
      NPOINT=0
      DO 6 I1=1,NTS                                                   JOP  135
      PS=-DPS                                                         JOP  136
      TS=DARCOS(1.-DFLOAT(I1)*2./XNTS)
      DO 6 I2=1,NPS                                                   JOP  138
      IF (I1.EQ.NTS.AND.I2.EQ.3) GO TO 7                              JOP  139
      NPOINT=NPOINT+1
C     TINIT(1,NPOINT) IS THE TEMPERATURE DISTRIBUTION STORAGE ARRAY FOR THE
C     INITIAL TEMPERATURE DISTRIBUTION FOR USE WITH THE AVERAGE OPTICAL
C     PROPERTIES
C     TINIT(2,NPOINT) IS THE NEW TEMPERATURE DISTRIBUTION FOR THE AVERAGE
C     OPTICAL PROPERTIES
```

```
C       NPOINT IS THE VARIABLE NAME GIVEN EACH NODE POINT ON THE DETECTOR
        IF(ISET.EQ.1) T(I1,I2)=TINIT(2,NPOINT)
        IF(ISET.EQ.0) TINIT(1,NPOINT)=T(I1,I2)
        PS=PS+DPS
        IF (I1.EQ.NTS.AND.I2.EQ.2) TS=0.                                    JOP  141
        IF (I1.EQ.NTS.AND.I2.EQ.2) PS=0.                                    JOP  142
C       XS,YS,AND ZS ARE THE CARTESIAN COMPONENTS OF THE SATELLITE NODE      JOP  143
C       POINT IN TERMS OF THE SATELLITE FRAME OF REFERENCE.  IT DOES NOT     JOP  144
C       TAKE INTO ACCOUNT SATELLITE ROTATION AND IS NOT RELATIVE TO ANY      JOP  145
C       INERTIAL FRAME OF REFERENCE.                                         JOP  146
C       THR IS THE ANGULAR DISPLACEMENT OF THE SATELLITE ABOUT ITS           JOP  147
C       AXIS OF ROTATION.                                                    JOP  148
        RSSINT=BUF(4)*DSIN(TS)
        XIR=RSSINT*DCOS(PS)
        XS=XIR
        YIR=RSSINT*DSIN(PS)
        YS=YIR
        ZIR=BUF(4)*DCOS(TS)
        ZS=ZIR
        XUIR=XIR/BUF(4)
        YUIR=YIR/BUF(4)
        ZUIR=ZIR/BUF(4)
        XIT=XIR+BPAR(23)*BPAR(5)
        YIT=YIR+BPAR(23)*BPAR(6)
        ZIT=ZIR+BPAR(23)*BPAR(7)
C       THEM IS THE HALF ANGLE OF VIEW RELATIVE TO AN EARTH BASED COORDINAJOP  165
C       SYSTEM                                                               JOP  166
        CBB=1.                                                               JOP  168
C       THE LOGIC FROM STATEMENT 30 TO STATEMENT 31 IS THE EARTH             JOP  169
C       INTEGRATION ROUTINE FOR THE SATELLITE NODE BEING CONSIDERED          JOP  170
C       XE1,YE1,ZE1 ARE THE COMPONENTS OF THE EARTH NODE UNIT VECTOR         JOP  171
C       IN INERTIAL COORDINATES                                              JOP  172
```

```
C      ESX,ESY,ESZ ARE THE COMPONENTS OF THE VECTOR FROM THE EARTH        JOP  173
C      NODE BEING CONSIDERED TO THE SATELLITE NODE BEING CONSIDERED       JOP  174
C      IN INERTIAL COORDINATES                                            JOP  175
C      ESM IS THE MAGNITUDE OF THIS VECTOR                                JOP  176
C      ESXU,ESYU,ESZU ARE THE COMPONENTS OF THE UNIT VECTOR FROM THE      JOP  177
C      EARTH NODE TO THE SATELLITE NODE                                   JOP  178
C      CBB IS THE COSINE OF THE ANGLE BETWEEN THE NEGATIVE OF THE EARTH TJOP  179
C      VECTOR AND THE SAT. NORMAL VECTOR                                  JOP  180
C      CBE IS THE COSINE OF THE ANGLE BETWEEN THE EARTH NODE VECTOR AND TJOP  181
C      TO SAT. VECTOR                                                     JOP  182
C      CES IS THE COSINE OF THE ANGLE BETWEEN THE EARTH NODE (NORMAL) VECJOP  183
C      THE NEGATIVE OF THE SOLAR UNIT VECTOR                              JOP  184
C      NOTE:  ALL VECTORS INVOLVED IN THESE COSINE COMPUTATIONS ARE UNIT  JOP  185
       NVECTR=0
       DO 5 J1=1,N                                                        JOP  188
       SOURCE(1,J1)=0.0
       SOURCE(2,J1)=0.0
       SOURCE(3,J1)=0.0
       CBB=(XUIR*VERC(1,J1)+YUIR*VERC(2,J1)+ZUIR*VERC(3,J1))
       CBB=-CBB                                                           JOP  190
       IF (CBB.GT.1.) CBB=1.                                              JOP  191
       IF (CBB.LT.-1.) CBB=-1.                                            JOP  192
       IF (CBB.LT.0.) GO TO 5                                             JOP  193
       NVECTR=NVECTR+1
C      NVECTR IS THE VARIABLE NAME GIVEN TO EACH POINT SOURCE THAT CAN SEE EACH
C      NODE ON THE DETECTOR SURFACE
C      SOURCE(J,NPOINT,NVECTR) IS THE ARRAY THAT STORES THE ANGLE IN RADIANS OF
C      EACH PARTICULAR SOURCE POINT INCIDENT ON EACH PARTICULAR NODE POINT ON THE
C      DETECTOR,AND THE ASSOCIATED LONG WAVE AND SHORT WAVE ENERGY FROM THE
C      PARTICULAR POINT SOURCE
       ANGLE=DARCOS(CBB)
C*****SOURCE(1,NVECTOR)= THE ANGLE CBB EXPRESSED IN RADIANS
```

```
      SOURCE(1,NVECTR)=ANGLE
C*****SOURCE(2,NVECTOR)= LONG WAVE ENERGY INCIDENT AT EACH NODE
      SOURCE(2,NVECTR)=VERC(5,J1)
C*****SOURCE(3,NVECTOR)= SHORT WAVE COMPONENT INCIDENT AT A NODE
      SOURCE(3,NVECTR)=VERC(4,J1)
      IF(LCHECK.EQ.0) GO TO 5
C     BSW IS THE SHORT WAVELENTH COMPONENT OF THE OUTGOING RADIANT FLUX JOP  194
C     AT THE EARTH NODE BEING CONSIDERED                               JOP  195
C     RIN IS THE EARTH SHORT AND LONG WAVELENGTH COMPONENT OF THE RADIANJOP  196
C     FLUX INCOMING TO THE SATELLITE NODE UNDER CONSIDERATION          JOP  197
5     CONTINUE                                                         JOP  206
C*****LIMIT(NPOINT)= THE NUMBER OF SOURCE POINTS INCIDENT ON A NODE
C*****(NUMBERED NPOINT)
      LIMIT(NPOINT)=NVECTR
      WRITE(1) SOURCE
C     CSS IS THE COSINE OF THE ANGLE BETWEEN THE NEGATIVE OF THE SOLAR  JOP  207
C     UNIT VECTOR AND THE UNIT NORMAL VECTOR AT THE POINT ON THE SATELLIJOP  208
C     BEING CONSIDERED                                                 JOP  209
C     HS IS THE SOLAR COMPONENT OF THE INCOMING FLUX TO THE AREA ON THE JOP  210
C     SATELLITE BEING CONSIDERED                                       JOP  211
C     HIN IS THE ARRAY WHICH STORES THE INCIDENT FLUX VALUE FOR EACH NODJOP  212
 307  CSS=(-1.*(BPAR(11)*XUIR+BPAR(12)*YUIR+BPAR(13)*ZUIR))
      HS= CSS*BPAR(25)
      IF(HS.LE.0.0D0) GO TO 7717
C     THE ARRAY NAME SOLAR(10,10) IS THE STORAGE ARRAY FOR THE ANGLE BETWEEN
C     THE INCIDENT SOLAR ENERGY AND THE NODE POINTUNIT NORMAL VECTOR
      ANGL=DARCOS(CSS)
      SOLAR(I1,I2)=ANGL
      GO TO 6
C*****SOLAR(I1,I2)= THE ANGLE(IN RADIANS) FORMAED BY THE SOLAR COMPONENT
C*****AND THE UNIT NORMAL OF THE NODE POINT
 7717 SOLAR(I1,I2)=(PI/2.)*RADIAN
```

```
6      CONTINUE                                                        JOP  217
7      CONTINUE                                                        JOP  218
       REWIND 1
C***** ISET IS THE LOGIC COMMAND UTILIZED IN THE GETVEC SUBROUTINE SO
C*****THAT THE SUBROUTINE WILL NOT ATTEMPT TO READ FROM CARDS AT THE NEXT
C*****POINT IN ORBIT
       ISET=1
C      THE SOLABS SUBROUTINE DETERMINES THE SOLAR ABSORPTANCE OF THE NODE POINT
C      THAT CAN SEE THE SUN,AND THE ABSORPTANCE IS A FUNCTION ONLY OF THE INCIDEN
C      T ANGLE(NOT OF TEMPERATURE)
C*****SOLABS- CALLS THE SUBROUTINE TO CALCULATE THE SOLAR ABSORPTANCE
C*****AS A FUNCTION OF THE INCIDENT ANGLE OF THE RADIANT ENERGY
       CALL SOLABS(ABSUV,LGO)
C*****REFLEX= CALLS THE SUBROUTINE TO CALCULATE THE ABSORPTANCE FOR THE
C*****ALBEDO COMPONENT OF THE INCIDENT ENERGY
       CALL REFLEX(LGO,ASW)
       IF(LGO.EQ.1) GO TO 333
  303  NPI=0
       SUMEMT=0.0D0
C*****THE 331 DO LOOP CALCULATES THE EMISSIVITY OF EACH NODE AS A FUNCTION
C*****OF THE TEMPERATURE OF THE NODE IN QUESTION
       DO 331 I=1,NTS
       DO 331 J=1,NPS
       NPI=NPI+1
       RAT=(T(I,J)*8.987D11)/DCOND(NPI)
       RAT1=0.751*(RAT)**0.5
       RAT2=0.632*RAT
       RAT3=0.670*RAT**(3./2.)
       RAT4=0.607*RAT**2.
C*****VERC(3,NPI)= THE STORAGE LOCATION OF THE EMISSIVITY OF THE NODE
C*****POINT IN QUESTION
C*****THE SOLUTION FOR THE TOTAL HEMISPHERICAL EMISSIVITY AS A FUNCTION
```

```
C*****OF TEMPERATURE IS A FORMULA BASED ON THE DRUDE THEORY AS MODIFIED BY
C*****SCHMIDT AND ECKERT,AS WELL AS FOOT,DAVISON,AND WEEKS. THIS WAS
C*****OBTAINED FROM THE ARTICLE"THE RELATION BETWEEN THE TOTAL THERMAL
C*****EMISSION POWER OF A METAL AND ITS ELECTRICAL RESISTIVITY"BY
C*****C. DAVISSON AND J.R.WEEKS,JR. FROM THE JOURNAL OF THE OPTICAL SOCIETY
C*****OF AMERICA,VOL. 8,NO. 5,MAY,1924
      VERC(3,NPI)=RAT1-RAT2+RAT3-RAT4
      SUMEMT=SUMEMT+VERC(3,NPI)
      IF(I.EQ.NTS.AND.J.EQ.2) GO TO 332
  331 CONTINUE
  332 CONTINUE
C*****EARTH - CALLS THE SUBROUTINE TO CALCULATE THE ABSORPTANCE OF THE
C*****EARTH EMITTED COMPONENT OF THE TOTAL INCIDENT ENERGY
  333 CONTINUE
      CALL EARTH(LGO)
      IF(LGO.EQ.1) READ(5,43)(VERC(2,LINE),LINE=1,92)
      IF(LGO.EQ.1) READ(5,43)(VERC(3,LINE),LINE=1,92)
      READ(5,99)((SOLAR(I,J),J=1,NTS),I=1,NPS)
      IF(LGO.EQ.1) READ(5,43)(STUCK(LINE),LINE=1,92)
      IF(LGO.EQ.1) READ(5,99)((SOLAR(I,J),J=1,NTS),I=1,NPS)
      TOTRAD=0.0D0
      SUN=0.0
      ALBEDO=0.0
      XINFRA=0.0
      NPT=0
C*****THE 130 DO LOOP WILL CALCULATE THE TOTAL INCIDENT SOLAR,ALBEDO,
C*****AND EARTH EMITTED COMPONENTS ON EACH NODE ON THE DETECTOR SURFACE
      DO 130 I=1,NTS
      DO 130 J=1,NPS
      IF(I.EQ.NTS.AND.J.EQ.3) GO TO 131
      NPT=NPT+1
C*****SUN - THE SUM TOTAL SOLAR ENERGY INCIDENT ON THE SPHERICAL DETECTOR
```

```
      SUN=SUN+SOLAR(I,J)
C*****ALBEDO - THE SUM TOTAL ALBEDO COMPONENT INCIDENT ON THE SPHERICAL DETECTOR
      ALBEDO=ALBEDO+STUCK(NPT)
C*****XINFRA - THE SUM TOTAL EARTH EMITTED COMPONENT INCIDENT ON THE DETECTOR
      XINFRA=XINFRA+VERC(2,NPT)
C*****HIN(I,J) - THE TOTAL INCIDENT ENERGY AT A NODE ON THE DETECTOR SURFACE
      HIN(I,J)=SOLAR(I,J)+VERC(2,NPT)+STUCK(NPT)
  130 CONTINUE
  131 IF(LCHECK.EQ.0) GO TO 158
      TOTRAD=SUN+ALBEDO+XINFRA
      SOLPCT=(SUN/TOTRAD)*100.0D0
      ALBPCT=(ALBEDO/TOTRAD)*100.0D0
      EEMPCT=(XINFRA/TOTRAD)*100.0D0
C***** AVG IS THE AVERAGE ULTRA VIOLET ABSORPTANCE AS A FUNCTION OF INCIDENT
C*****ANGLE; IT IS CALCULATED IN THE REFLEX SUBROUTINE
      AVGALB=0.0D0
      AVGEEM=0.0D0
      AVGSOL=0.0D0
      TOTHIN=0.0D0
      NP=0
      DO 126 I=1,NTS
      DO 126 J=1,NPS
      NP=NP+1
      HIN(I,J)=ASW*(H(1,NP)+H(2,NP))+ALW*H(3,NP)
      TOTHIN=TOTHIN+HIN(I,J)
      AVGSOL=AVGSOL+ASW*H(1,NP)
      AVGALB=AVGALB+ASW*H(2,NP)
      AVGEEM=AVGEEM+ALW*H(3,NP)
      IF(I.EQ.NTS.AND.J.EQ.2) GO TO 158
  126 CONTINUE
C     SAS IS USED TO COMPUTE XXH THE INTERNAL IRRADIANCE WHICH IS CONSTAJOP  219
C     DTM IS THE SUBPOINT TO SUBPOINT TIME INCREMENT                  JOP  220
```

```
C      DT IS ENERGY EQUATION TIME STEP (LESS THAN OR EQUAL TO DTM)        JOP  221
C      TSUM IS THE RUNNING TOTAL OF THE ELAPSED TIME BETWEEN              JOP  222
C      SUBPOINTS                                                          JOP  223
C      TQ IS THE TOTAL ELAPSED TIME                                       JOP  224
  158  ASATE=1.0
       PCTSUN=(AVGSOL/TOTHIN)*100.0D0
       PCTALB=(AVGALB/TOTHIN)*100.0D0
       PCTEEM=(AVGEEM/TOTHIN)*100.0D0
C*****THE NEXT THREE STATEMENTS WILL DETERMINE THE INTEGRATION TIME STEP TO
C*****BE UTILIZED IN THE SOLUTION
       IF(LCHECK.EQ.1) DT=DTM
       IF(LCHECK.EQ.0) DT=DTM/2.0D0
       SAS=0.                                                             JOP  226
       SH=0.0                                                             JOP  227
       AREA=0.0                                                           JOP  228
       NPT=0
       DO 11 I=1,NTS                                                      JOP  229
       DO 11 J=1,NPS                                                      JOP  230
       NPT=NPT+1
C*****FOR THE EXACT SOLUTION WE MUST DEFINE THE TOTAL HEMISPHERICAL EMITTANCE
C*****AS A FUNCTION OF THE NODE TEMPERATURE
       IF(LCHECK.EQ.0) ELW=VERC(3,NPT)
       IF(ELW.EQ.0.0) GO TO 11
       IF (I.EQ.NTS) ASATE=0.5*XNPS                                       JOP  231
       SH=SH+HIN(I,J)*ASATE/ELW                                           JOP  232
       IF(LCHECK.EQ.1) T(I,J)=TINIT(1,NPT)
       IF (I.EQ.NTS.AND.J.EQ.2) GO TO 12                                  JOP  234
11     CONTINUE                                                           JOP  235
12     CONTINUE                                                           JOP  236
       SH=SH/(XNTS*XNPS)                                                  JOP  237
       IF (IEXIT.EQ.0)TR=0.0
       JK=JK+1                                                            JOP  243
```

```
      GO TO 10                                                          JOP  244
8     DT=DT/10.                                                         JOP  245
      TR=0.0D0
9     CONTINUE                                                          JOP  248
      JK=JK+1                                                           JOP  249
10    CONTINUE                                                          JOP  250
      TR=TR+DT                                                          JOP  251
C     THE '45' DO-LOOP COMPUTES THE TEMPERATURE OF EACH SATELLITE NODE  JOP  252
C     AT AN ELAPSED TIME DT GREATER THAN THE PRESENT                    JOP  253
C     TS AND PS ARE THE SATELLITE COORDINATES OF THE NODE BEING CONSIDERJOP  254
C     TSA AND TSB ARE THE MIN AND MAX THETA VALUES OF THE AREA ELEMENT  JOP  255
C     BEING CONSIDERED
      IF(LCHECK.EQ.1.AND.TR.GT.0.0) GO TO 72
      GO TO 71
C*****THE 72 DO LOOP IS ONLY ENTERED TO RESET THE TEMPERATURE DISTRIBUTION
C*****FOR THE AVERAGE PROPERTY SOLUTION
  72  NP=0
      DO 73 I=1,NTS
      DO 73 J=1,NPS
      NP=NP+1
      IF(I.EQ.NTS.AND.J.EQ.3) GO TO 74
      T(I,J)=TINIT(1,NP)
  73  CONTINUE
  74  CONTINUE
  71  NPT=0
C*****THE 26 DO LOOP WILL COMPUTE THE NEW TEMPERATURE DISTRIBUTION
      DO 26 I=1,NTS                                                     JOP  257
      PS=-DPS                                                           JOP  258
      TS=DARCOS(1.-DFLOAT(I)*2./XNTS)
      IF (I.EQ.NTS) GO TO 13                                            JOP  260
      TSA=DARCOS(1.-(DFLOAT(I)-.5)*2./XNTS)
      TSB=DARCOS(1.-(DFLOAT(I)+.5)*2./XNTS)
```

```
      DTH=DABS(TSB-TSA)
13    CONTINUE                                                          JOP  264
      DO 26 J=1,NPS                                                     JOP  265
      IF (I.EQ.NTS.AND.J.EQ.3) GO TO 27                                 JOP  266
      NPT=NPT+1
      IF(LCHECK.EQ.0) ELW=VERC(3,NPT)
      PS=PS+DPS                                                         JOP  267
      IF (I.EQ.NTS.AND.J.EQ.2) TS=0.                                    JOP  268
C     JM1,JP1,J,I,ETC. ARE SUBSCRIPTS USED TO IDENTIFY THE SUBPOINT OF  JOP  269
C     INTEREST                                                          JOP  270
      IF (I.EQ.NTS.AND.J.EQ.2) PS=0.                                    JOP  271
      JM1=J-1                                                           JOP  272
      JP1=J+1                                                           JOP  273
      IF (J.EQ.1) JM1=NPS                                               JOP  274
      IF (J.EQ.NPS) JP1=1                                               JOP  275
      IF (I.EQ.1) GO TO 16                                              JOP  276
      IF (I.EQ.NTS-1) GO TO 17                                          JOP  277
      IF (I.EQ.NTS) GO TO 18                                            JOP  278
      TI1=T(I-1,J)                                                      JOP  279
14    TI2=T(I+1,J)                                                      JOP  280
15    TJ1=T(I,JM1)                                                      JOP  281
      TJ2=T(I,JP1)                                                      JOP  282
      GO TO 23                                                          JOP  283
16    TI1=T(NTS,2)                                                      JOP  284
      GO TO 14                                                          JOP  285
17    TI1=T(I-1,J)                                                      JOP  286
      TI2=T(NTS,1)                                                      JOP  287
      GO TO 15                                                          JOP  288
18    TES=0.                                                            JOP  289
      IF (J.EQ.1) GO TO 20                                              JOP  290
      TFE=0.                                                            JOP  291
      DO 19 I3=1,NPS                                                    JOP  292
```

```
19      TES=TES+T(NTS-1,I3)                                              JOP  293
        GO TO 22                                                         JOP  294
C       IF THE NODE BEING CONSIDERED IS A POLE, A SLIGHTLY DIFFERENT     JOP  295
C       EQUATION MUST BE SOLVED TO COMPUTE THE NEW TEMPERATURE TT AND    JOP  296
C       THE STABILITY COEFFICIENT COF.                                   JOP  297
20      TPE=PI                                                           JOP  298
        DO 21 I3=1,NPS                                                   JOP  299
21      TES=TES+T(1,I3)                                                  JOP  300
22      CONTINUE                                                         JOP  301
        STHPOL=DSIN(THPOLE)
        XMRL1=DT/(RO*C)                                                  JOP  308
        XMRL2=(EI+ELW)*SIG*T(I,J)**3                                     JOP  309
        XMRL3=XKP*STHPOL*XNTS
        XMRL4=BPAR(23)*BPAR(23)*XNPS*2.*THPOLE
        TT(I,J)=T(I,J)+XMRL1*((1./DR*(EI*XXH+HIN(I,J)-(XMRL2*T(I,J))))+  JOP  312
       1XMRL3/XMRL4*(TES-XNPS*T(I,J)))                                   JOP  313
        COF=1.-XMRL1*(XMRL2/DR+XMRL3/XMRL4)                              JOP  314
        GO TO 24                                                         JOP  317
C       FOR ALL STANDARD (NON-POLAR) NODES THE NEW TEMPERATURE AND THE   JOP  318
C       STABILITY COEFFICIENT--TT AND COF--ARE COMPUTED BELOW            JOP  319
 23     SINTS=DSIN(TS)
        DPSINT=DPS*SINTS
        XMRL1=DT/(RO*C)                                                  JOP  328
        XMRL2=(EI+ELW)*SIG*T(I,J)**3                                     JOP  329
        XMRL3=BPAR(23)*BPAR(23)*DTH*DPSINT
        TT(I,J)=T(I,J)+XMRL1*((1./DR*(EI*XXH+HIN(I,J)-(XMRL2*T(I,J))))+XKPJOP  331
       1/XMRL3*(DPSINT/DTH*(TI2+TI1-2.*T(I,J))+DTH/DPSINT*(TJ2+TJ1-2.*T(  JOP  332
       2I,J))))                                                          JOP  333
        COF=-2.*DPSINT/DTH-2.*DTH/DPSINT-XMRL2*XMRL3/(DR*XKP)+           JOP  3
       1XMRL3/(XMRL1*XKP)                                                JOP  335
24      CONTINUE                                                         JOP  338
        IF (COF.GE.0.) GO TO 25                                          JOP  339
```

```
      GO TO 8                                                          JOP  340
25    CONTINUE                                                         JOP  341
26    CONTINUE                                                         JOP  342
27    CONTINUE                                                         JOP  343
C     REVALUE THE OLD TEMPERATURE VALUES  TO THE VALUES COMPUTED AT    JOP  344
C     TIME = OLD ELAPSED TIME + DT                                     JOP  345
C     THEN RETURN AND REPEAT THE PROCESS                               JOP  346
      IEXIT=1
      ASATE=1.0                                                        JOP  347
      SAS=0.                                                           JOP  348
      NP=0
      ICHECK=0
C*****THE 813 DO LOOP WILL CHECK TO DETERMINE THE MEASURE OF CONVERGENCE
C*****FOR THE WARM UP SITUATION
      DO 813 I=1,NTS                                                   JOP  349
      DO 813 J=1,NPS                                                   JOP  350
      NP=NP+1
      IF(I.EQ.NTS) ASATE=0.5*XNPS                                      JOP  351
      DIFF=T(I,J)-TT(I,J)
      IF(LCHECK.EQ.0) GO TO 108
      DELTT=TT(I,J)-T(I,J)
  108 DDIFF=DABS(DIFF)
      IF(DDIFF.GT.90.0D0) ICHECK=1
      IF(LCHECK.EQ.0) DCCOND(NP)=SIGO*(273.D0/TT(I,J))
      IF(LCHECK.EQ.1) TINIT(1,NP) =TT(I,J)
      IF(LCHECK.EQ.0) T(I,J)=TT(I,J)
      SAS=SAS+T(I,J)**4*ASATE                                          JOP  353
      IF(I.EQ.NTS.AND.J.EQ.2) GO TO 814                                JOP  354
  813 CONTINUE                                                         JOP  355
C*****XXH - THE INTERNAL IRRADIANCE
  814 XXH=SIG*SAS/(XNPS*XNTS)                                          JOP  356
      IF(LCHECK.EQ.0) XXH1=XXH
```

```
      IF(LCHECK.EQ.1)XXH2=XXH
      IF(TR.EQ.10.0D0) GO TO 9
      IF(TR.LT.20.0.AND.KKKJ.EQ.1) GO TO 9                              JOP  357
      IF(K1.LT.KKK-1.AND.KKKJ.EQ.1) GO TO 1111                          JOP  359
  831 IF (TR.GE.20.0) GO TO 30                                          JOP  379
      GO TO 9                                                           JOP  380
30    CONTINUE                                                          JOP  381
      IF(LCHECK.EQ.0.AND.ICHECK.EQ.1) GO TO 303
      IF(LCHECK.NE.0) GO TO 44
      WRITE(7,99)((T(I,J),J=1,NTS),I=1,NPS)
   99 FORMAT(5D15.8)
      WRITE(7,98) KKKK,XXH
   98 FORMAT(I3,D15.8)
   44 NP=0
      DO 180 I=1,NTS
      DO 180 J=1,NPS
      NP=NP+1
      IF(LGO.EQ.1) TINIT(2,NP)=TT(I,J)
      IF(LCHECK.EQ.0) TINIT(2,NP)=TT(I,J)
      IF(I.EQ.NTS.AND.J.EQ.2.AND.LCHECK.EQ.1) GO TO 1111
      IF(I.EQ.NTS.AND.J.EQ.2) GO TO 181
  180 CONTINUE
  181 CONTINUE
C***** RECALL THAT LCHECK=1 IS THE LOGIC UTILIZED TO PERFORM THE CALCULATIONS
C*****BASED ON THE AVERAGE PROPERTIES
      LCHECK=1
      IEXIT=0
C*****THE NEXT STATEMENT RECOGNIZES THAT THE EXACT SOLUTION IS COMPLETE
C*****AND WE NOW MUST RETURN TO PERFORM THE AVERAGE PROPERTY SOLUTION
      IF(LCHECK.EQ.1.AND.ICHECK.EQ.0) GO TO 131
1111  K1=K1+1                                                           JOP  472
      LCHECK=0
```

```
      IF(TIME.EQ.STIME.AND.K1.LT.KKK) KKKK =1                          JOP  473
      KKK1=KKK-1                                                       JOP  474
      IF(TIME.EQ.STIME.AND.K1.LT.KKK1) KKKK=0                          JOP  475
      KKKJ=KKKJ+1                                                      JOP  476
      IF(LGO.EQ.1) GO TO 334
      EMITDN=0.0D0
      EMITNU=0.0D0
      I=0
      DO 169 I=1,NP
      EMITNU=EMITNU+VERC(3,I)*SIG*TINIT(1,I)**4
      EMITDN=EMITDN+SIG*TINIT(1,I)**4
  169 CONTINUE
      AVGALW=EMITNU/EMITDN
      WRITE(7,43)(VERC(2,LINE),LINE=1,92)
      WRITE(7,43)(VERC(3,LINE),LINE=1,92)
      WRITE(7,43)(STUCK(LINE),LINE=1,92)
      WRITE(7,99)((SOLAR(I,J),J=1,NTS),I=1,NPS)
   43 FORMAT(4D15.8)
  334 CONTINUE
      I=0
C*****THE 170 DO LOOP WILL COMPUTE THE F(1,NPOINT),F(2,NPOINT),F(3,NPOINT),AND
C*****F(4,NPOINT) FACTORS UTILIZED TO COMPUTE THE CORRECTION FACTORS
      WRITE(6,457) KKKK
  457 FORMAT(1H ,30X,56HTHE FOLLOWING INFORMATION IS FOR ORBITAL POSITIO
     1N NUMBER,I4)
      WRITE(6,458)
  458 FORMAT(1H0,4H    )
      DO 170 J=1,NTS
      DO 170 K=1,NPS
      I=I+1
      F(1,I)=0.0D0
      F(2,I)=0.0D0
```

```
      F(3,I)=0.0D0
      F(4,I)=0.0D0
      IF(H(3,I).EQ.0.0D0) GO TO 441
      F(1,I)=VERC(2,I)/(H(3,I)*ALW)
  441 IF(H(2,I).EQ.0.0D0) GO TO 442
      F(2,I)=STUCK(I)/(H(2,I)*ASW)
  442 IF(H(1,I).EQ.0.0D0) GO TO 443
      F(3,I)=SOLAR(J,K)/(H(1,I)*ASW)
  443 F(4,I)=VERC(3,I)/ELW
      WRITE(6,172) I,F(1,I),I,F(2,I),I,F(3,I),I,F(4,I)
  172 FORMAT(1H ,20X,4HF(1,,I2,2H)=,F8.5,3X,4HF(2,,I2,2H)=,F8.5,3X,4HF(3
     1,,I2,2H)=,F8.5,3X,4HF(4,,I2,2H)=,F8.5)
      IF(J.EQ.NTS.AND.K.EQ.2) GO TO 173
  170 CONTINUE
  173 CONTINUE
      SUMHEN=0.0D0
      SUMHED=0.0D0
      SUMHRN=0.0D0
      SUMHRD=0.0D0
      SUMHSN=0.0D0
      SUMHSD=0.0D0
      FR=0.0D0
      FS=0.0D0
      FD=0.0D0
      FE=0.0D0
      CE=0.0D0
      CR=0.0D0
      CS=0.0D0
      SUMFOD=0.0D0
      SUMFON=0.0D0
      I=0
      DO 371 J=1,NTS
```

```
      DO 371 K=1,NPS
      I=I+1
      SUMHEN=H(3,I)*F(1,I)+SUMHEN
      SUMHED=SUMHED+H(3,I)
      SUMHRN=SUMHRN+F(2,I)*H(2,I)
      SUMHRD=SUMHRD+H(2,I)
      SUMHSN=SUMHSN+F(3,I)*H(1,I)
      SUMHSD=SUMHSD+H(1,I)
      SUMFOD=SUMFOD+SIG*TINIT(1,I)**4
      SUMFON=SUMFON+SIG*TINIT(1,I)**4*F(4,I)
      IF(J.EQ.NTS.AND.K.EQ.2) GO TO 372
  371 CONTINUE
  372 CONTINUE
C*****FE - THE PERCENT DIFFERENCE IN SOLUTION TECHNIQUE,AVERAGE/EXACT FOR
C*****THE EARTH EMITTED COMPONENT
      FE=SUMHEN/SUMHED
C*****FR - THE PERCENT DIFFERENCE IN SOLUTION TECHNIQUE FOR THE ALBEDO
C*****COMPOMENT
      IF(SUMHRD.EQ.0.0D0) GO TO 55
      FR=SUMHRN/SUMHRD
   55 IF(SUMHRD.EQ.0.0D0) FR=1.0D0
C*****FS - THE PERCENT DIFFERENCE IN SOLUTION TECHNIQUE FOR THE SOLAR
      IF(SUMHSD.EQ.0.0D0) GO TO 56
      FS=SUMHSN/SUMHSD
   56 IF(SUMHSD.EQ.0.0D0) FS=1.0D0
C*****FO - THE PERCENT DIFFERENCE SOLUTION TECHNIQUE FOR THE EMITTANCE
      FO=SUMFON/SUMFOD
      WRITE(6,459)
  459 FORMAT(1H0,20X,40HTHE RATIO OF THE TWO SOLUTION TECHNIQUES)
      WRITE(6,421) FE,FR,FS,FO
  421 FORMAT(1H ,2X,3HFE=,F12.6,3X,3HFR=,F12.6,3X,3HFS=,F12.6,3X,3HFO=,
     1F12.6)
```

```
C*****CE - THE CORRECTION FACTOR FACTOR FOR THE EARTH EMITTED COMPONENT
      CE=FE/FO
C*****CR - THE CORRECTION FACTOR FOR THE ALBEDO COMPONENT
      CR=FR/FO
C*****CS - THE CORRECTION FACTOR FOR THE SOLAR COMPONENT
      CS=FS/FO
      WRITE(6,460)
  460 FORMAT(1HO,20X,71HTHE CORRECTION FACTORS FOR THE SOLAR,ALBEDO,AND
     1EARTH EMITTED COMPONENT)
      WRITE(6,509)CE,CR,CS
  509 FORMAT(1HO,4X,3HCE=,F12.6,3X,3HCR=,F12.6,3X,3HCS=,F12.6)
      WRITE(6,314) SUN,ALBEDO,XINFRA
  314 FORMAT(1HO,4X,4HSUN=,F12.6,3X,7HALBEDO=,F12.6,3X,7HXINFRA=,F12.6)
      IF(SUN.EQ.0.0D0) GO TO 467
      DIFSUN=((SUN-AVGSOL)/SUN)*100.0D0
      IF(ALBEDO.EQ.0.0D0) GO TO 467
      DIFALB=((ALBEDO-AVGALB)/ALBEDO)*100.0D0
  467 DIFEEM=((XINFRA-AVGEEM)/XINFRA)*100.0D0
      IF(ALBEDO.EQ.0.0D0) DIFALB=0.0D0
      IF(SUN.EQ.0.0D0) DIFSUN=0.0D0
      WRITE(6,451)
  451 FORMAT(1HO,4X,52HPERCENT DIFFERENCE OF ABSORBED FLUX FROM EACH SOU
     1RCE)
      WRITE(6,450) DIFSUN,DIFALB,DIFEEM
  450 FORMAT(1HO,4X,25HDIFFERENCE IN SOLAR FLUX=,F12.6,3X,26HDIFFERENCE
     1IN ALBEDO FLUX=,F12.6,3X,33HDIFFERENCE IN EARTH EMITTED FLUX=,F12
     2.6)
      WRITE(6,452)
  452 FORMAT(1HO,4X,68HPERCENT OF THE TOTAL ABSORBED FLUX DETERMINED BY
     1THE EXACT TECHNIQUE)
      WRITE(6,453) SOLPCT,ALBPCT,EEMPCT
  453 FORMAT(1HO,4X,16HSOLAR COMPONENT=,F12.6,3X,17HALBEDO COMPONENT=,F1
```

```
     12.6,3X,24HEARTH EMITTED COMPONENT=,F12.6)
      WRITE(6,454)
  454 FORMAT(1HO,4X,70HPERCENT OF THE TOTAL ABSORBED FLUX DETERMINED BY
     1THE AVERAGE TECHNIQUE)
      WRITE(6,453) PCTSUN,PCTALB,PCTEEM
      WRITE(6,9901) ALW,ELW,ASW
 9901 FORMAT(1HO,4X,4HALW=,F12.6,3X,4HELW=,F12.6,3X,4HASW=,F12.6)
      IF(KNUMB.LT.NBUF2) GO TO 1                                        JOP  560
      KNUMB=0                                                           JOP  561
C                                                                       JOP  562
      DEBUG UNIT(6),SUBCHK
      STOP                                                              JOP  627
      END                                                               JOP  628
```

```
      SUBROUTINE GETVEC(IU,ISIT,NVEC,LAST)
      IMPLICIT REAL *8(A-H,O-Z)
C   GETVEC GETS VECTORS WRITTEN BY GENVEC FORMA GENDAT                    JOP  918
C   NEXT SET OF BUF,BPAR,VERR  READ FORM UNIT IU                          JOP  919
C    CALL IF JUST WANT BUF,BPAR,VERC IN SEQUENCE ON TAPE                  JOP  920
      DIMENSION VECTOR(5,220),BPARR(30),BUFF(15),SOLAR(10,10),SOLAB(91),
     1PRCNT(50),H(3,92),STUCK(92),T(10,10),CONTAN(93),TLAM(93)
      COMMON/START/ T,XXH,KKKK
      COMMON/STORE2/ STUCK,SOLAB,PRCNT
      COMMON/STORE3/ H,SOLAR,HZ,AVG,ALW,ELW
      COMMON/STORE5/ TLAM,CONTAN
      COMMON/ LABEL/ VECTOR,BPARR,BUFF,POMEGA,RELAXT,TAU2
      KINK=0
      IF(ISIT.EQ.1) GO TO 1
      READ(5,233)((T(I,J),J=1,10),I=1,10)
  233 FORMAT(5D15.8)
      READ(5,234) KKKK,XXH
  234  FORMAT(I3,D15.8)
      KIP=KKKK
      IF(KKKK.GT.0.AND.LAST.NE.1) KIP=KKKK+1
      READ(5,231) (SOLAB(I),I=1,91)
  231 FORMAT(13F6.4)
      READ(5,100)(TLAM(I),I=1,93)
  100  FORMAT(8D9.3)
      READ(5,101)(CONTAN(I),I=1,93)
  101  FORMAT(13F6.4)
      READ(5,232) (PRCNT(I),I=1,50)
  232 FORMAT(5D9.3)
      READ(IU,888) (BUFF(I),I=1,15)
  888  FORMAT(8E15.8)
    1  READ(IU,889) (BPARR(J),J=1,30)
  889  FORMAT(8E15.8)
```

```
      NVEC=BPARR(30)
      DO 906 J=1,NVEC,3
      L=J+1
      M=J+2
      IF(L.GT.NVEC) GO TO 904
      IF(M.GT.NVEC) GO TO 901
      READ(IU,907) (VECTOR(K,J),K=1,5),(VECTOR(KK,L),KK=1,5),(VECTOR(LL,
     1M),LL=1,5)
  907 FORMAT(3(3(F7.5) ,2(F11.6)))
      GO TO 906
  904 READ(IU,903)(VECTOR(K,J),K=1,5)
  903 FORMAT(3(F7.5),2(F11.6))
      GO TO 906
  901 READ(IU,900)(VECTOR(K,J),K=1,5),(VECTOR(KK,L),KK=1,5)
  900 FORMAT(2(3(F7.5),2(F11.6)))
  906 CONTINUE
      IF(KKKK.GT.0.AND.ISIT.EQ.1) GO TO 2
      IF(KKKK.EQ.0.AND.ISIT.EQ.0) GO TO 2
      IF(KKKK.GT.0.AND.ISIT.EQ.0) KINK=KINK+1
      IF(KINK.EQ.KIP.AND.ISIT.EQ.0) GO TO 2
      GO TO 1
    2 KKKK=KKKK+1
      RETURN
      END                                                          JCP   940
```

```
      SUBROUTINE REFLEX(LAST,ABSALB)
C*****THIS SUBROUTINE WILL DETERMINE THE ULTRA VIOLET ABSORPTANCE FOR THE
C*****DETECTOR AS A FUNCTION OF THE INCIDENT ANGLE OF THE ENERGY SOURCE.
C*****THIS SUBROUTINE IS UTILIZED ONLY FOR THE ALBEDO COMPONENT(REFLECTED
C*****SOLAR ENERGY)
      IMPLICIT REAL *8(A-H,O-Z)
      DIMENSION H(3,92),SOURCE(3,211),SOLAR(10,10),DCCOND(92),SOLAB(9
     11),PRCNT(50),TINIT(2,92),STUCK(92)
      INTEGER LIMIT(92)
      COMMON/STORE1/ SOURCE,TINIT,DCCOND
      COMMON/STORE2/ STUCK,SOLAB,PRCNT
      COMMON/STORE3/ H,SOLAR,HZ,AVG,ALW,ELW
      COMMON/ACCESS/ LIMIT,NPOINT,NVECTR
      COMMON/CNSTNT/ PI,P2,RADIAN,SIGO,SIG,E,XMNEFF,CO,RSAT,NTS,NPS
      TOTINC=0.0D0
      SUMABS=0.0D0
      TAVG=0.0
C*****THE 1 DO LOOP WILL ITERATE OVER ALL NODES ON THE DETECTOR SURFACE
      DO 1 I=1,NPOINT
      TOTSTK=0.0
      TOTIN=0.0
      TOTABS=0.0
      NIN=LIMIT(I)
C*****WE NOW READ FROM THE SCRATCH DISK THE RADIATION FIELD INCIDENT ON
C*****THE PARTICULAR DETECTOR NODE IN QUESTION
      READ(1) SOURCE
C*****THE NEXT STEP CHECKS TO SEE IF NO ENERGY IS INCIDENT ON THE PARTICULAR
C*****DETECTOR NODE
      IF(NIN.EQ.0) GO TO 5
C***** THE 2 DO LOOP NOW WILL ITERATE OVER ALL POINT SOURCES OF ALBEDO
C*****COMPONENT ENERGY INCIDENT ON THE NODE POINT I(DEFINED IN DO LOOP 1)
C*****OF THE DETECTOR SURFACE.
```

```
      DO 2 J=1,NIN
C***** XCOS - THE ANGLE OF INCIDENCE MEASURED FROM THE UNIT NORMAL VECTOR
C*****OF THE NODE POINT IN QUESTION
      XCOS=DCOS(SOURCE(1,J))
      IF(LAST.EQ.1) GO TO 8
      ANGLE=0.0
C***** THE 4 DO LOOP NOW WILL FIND THE ANGLE(IN DEGREES) OF INCIDENCE FOR
C*****THE POINT SOURCE OF ENERGY
      DO 4 K=1,91
      ANGLE1=ANGLE*RADIAN
      IF(ANGLE1.GT.SOURCE(1,J)) GO TO 3
      IF(K.GT.1) ANGLE2=ANGLE1
      ANGLE=ANGLE+1.0
  4   CONTINUE
      ABSALB=0.0
      GO TO 7
C***** THE NEXT FOUR STEPS WILL DETERMINE THE ULTRA VIOLET ABSORPTANCE
C*****FOR THE PARTICULAR SOURCE OF INCIDENT ENERGY. THE VALUE OFABSORPT-
C*****ANCE IS LINEARLY INTERPOLATED FOR ANGULAR VALUES BETWEEN THE KNOWN
C*****VALUES AS A FUNCTION OF ANGLE.
 3    IF(K.EQ.2) ANGLE2=0.0
      DIFF=SOURCE(1,J)-ANGLE2
      RATIO=DIFF/RADIAN
      ABSALB=SOLAB(K-1)+RATIO*(SOLAB(K)-SOLAB(K-1))
  7   TOTABS=TOTABS+ABSALB
C***** XIN - THIS IS THE INCIDENT ALBEDO COMPONENT IN WATTS/METER**2
C*****TIMES THE PROJECTED AREA OF THE NODE POINT IN QUESTION
   8  XIN=XCOS*SOURCE(2,J)
C***** TOTIN - THE SUM OF THE INCIDENT ALBEDO COMPONENTS TIMES THE PROJECTED
C*****AREAS OF THE DETECTOR SURFACE
      TOTIN=TOTIN+XIN
C***** STICK - THE ACTUAL AMOUNT OF ENERGY ABSORBED FROM A PARTICULAR
```

```
C*****SOURCE OF ALBEDO ENERGY
      STICK=ABSALB*XIN
C***** TOTSTK - THE SUM OF THE ABSORBED ENERGY CONTAINED IN EACH POINT
C*****SOURCE VISIBLE TO THE NODE ON THE DETECTOR SURFACE.
      TOTSTK=TOTSTK+STICK
      IF(J.EQ.LIMIT(I)) STUCK(I)=TOTSTK
  2   CONTINUE
C     AVERAGE SHORT WAVE ABSORPTANCE FOR ALL SOURCES INCIDENT ON ONE
C     NODE POINT
C***** TOTINC - THIS IS THE TOTAL ENERGY INCIDENT ON THE DETECTOR
      TOTINC=TOTINC+TOTIN
C***** SUMABS - THE TOTAL ENERGY ABSORBED FROM THE ALBEDO COMPONENT
      SUMABS=SUMABS+TOTSTK
C     INCIDENT ALBEDO AT EACH POINT
      H(2,I)=TOTIN
      GO TO 6
  5   H(2,I)=0.0
      STUCK(I)=0.00
  6   CONTINUE
  1   CONTINUE
      REWIND 1
      IF(LAST.EQ.1) RETURN
C     AVERAGE ABSORPTANCE FOR ALL NODE POINTS
C***** AVG - THE AVERAGE ULTRA VIOLET ABSORPTANCE, THIS VALUE IS OBTAINED
C*****BY A PURE AVERAGE FOR EACH SOURCE INCIDENT ON ALL NODES OF THE
C*****DETECTOR SURFACE
      IF(TOTINC.EQ.0.000.OR.SUMABS.EQ.0.000) GO TO 11
      AVG=SUMABS/TOTINC
      RETURN
  11  AVG=0.000
      RETURN
      END
```

```
      SUBROUTINE EARTH(LAST)
C***** THIS SUBROUTINE WILL CALCULATE THE INFRA RED ABSORPTANCE OF THE
C*****DETECTOR SURFACE AS A FUNCTION OF WAVELENGTH OF THE INCIDENT ENERGY
C*****,THE ANGLE OF INCIDENCE,THE TEMPERATURE OF THE SOURCE,AND THE
C*****TEMPERATURE OF THE DETECTOR SURFACE.
      IMPLICIT REAL *8(A-H,O-Z)
      DIMENSION SOURCE(3,211),H(3,92),LIMIT(92),PRONT(50),BNDENG(50),
     1XLAMDA(50),VERC(5,220),TINIT(2,92),DCCOND(92),SOLAB(91),BPAR(30),B
     2UF(15),SOLAR(10,10),STUCK(92)
      COMMON/STORE1/ SOURCE,TINIT,DCCOND,AREATH
      COMMON/STORE2/ STUCK,SOLAB,PRONT
      COMMON/STORE3/ H,SOLAR,HZ,AVG,ALW,FLW
      COMMON/STORE4/BNDENG,XLAMDA,XNORML,XPARAL
      COMMON/ACCESS/ LIMIT,NPOINT,NVECTR
      COMMON/CNSTNT/ PI,P2,RADIAN,SIGO,SIG,E,XMNEFF,CO,RSAT,NTS,NPS
      COMMON/LABEL/ VERC,BPAR,BUF,POMEGA,RELAXT,TAU2
C***** THE NEXT 5 STEPS INITIALIZE COUNTERS
      COUNT=0.0D0
      TINCID=0.0D0
      TTALW=0.0D0
      SUMIN=0.0D0
      TOTAVG=0.0D0
C***** THE 1 DO LOOP WILL ITERATE OVER ALL OF THE NODE POINTS ON THE
C*****DETECTOR SURFACE TO DETERMINE THE INCIDENT ENERGY TO EACH NODE.
      DO 1 I=1,NPOINT
      WRITE(6,40) I
   40 FORMAT(1H ,3X,48HTHE FOLLOWING ARE POINT SOURCES INCIDENT ON NODE,
     1I3)
C***** WE NOW READ FROM THE SCRATCH DISK THE RADIATION FIELD INCIDENT TO
C*****EACH NODE ON THE DETECTOR SURFACE
      READ (1) SOURCE
      COUNT=COUNT+1.0D0
```

```
C***** TOTABS - THIS INITIALIZES THE COUNTER FOR THE TOTAL ABSORBED ENERGY
C*****FROM THE INFRA RED COMPONENT AT EACH NODE ON THE DETECTOR SURFACE.
      TOTABS=0.0D0
C***** TOTIN - THIS INITIALIZES THE COUNTER FOR THE INCIDENT INFRA RED
C*****ENERGY AT EACH NODE ON THE DETECTOR SURFACE.
      TOTIN=0.0D0
C***** NVCTOR - THE NUMBER OF POINT SOURCES OF INFRA RED ENERGY
      NVCTOR=LIMIT(I)
      IF(NVCTOR.EQ.0) GO TO 6
C***** THE 2 DO LOOP WILL ITERATE OVER EACH NODE POINT SOURCE OF INFRA
C*****RED ENERGY INCIDENT ON A PARTICULAR DETECTOR NODE POINT
      DO 2 J=1,NVCTOR
C***** XCOS - THE ANGLE OF INCIDENCE OF THE POINT SOURCE OF INFRA RED ENERGY
      XCOS=DCOS(SOURCE(1,J))
C***** THE NEXT TWO STEPS WILL DETERMINE WHAT THE EFFECTIVE TEMPERATURE
C*****OF THE AREA ON THE EARTH MUST BE TO PRODUCE THE AMOUNT OF  ENERGY
C*****THAT WOULD PASS THROUGH THE ORBITAL PLANE
      T4=(SOURCE(3,J)*PI*(RSAT)**2)/(SIG*AREATH*XCOS)
      TSOURC=T4**0.25
      CALL BLACKBD(TSOURC)
      IF(J.GT.LIMIT(I)) GO TO 1
C***** XXEN - THE PRODUCT OF THE INFRA RED ENERGY INCIDENT AND THE PROJECTED
C*****AREA OF THE DETECTOR SURFACE
      XXEN=XCOS*SOURCE(3,J)
      IF(LAST.EQ.1) VERC(1,J)=XXEN*ALW
      IF(LAST.EQ.1) GO TO 8
C***** THE 4 DO LOOP WILL BREAK UP THE INCIDENT POINT SOURCE INTO A
C*****MONOCHROMATIC BLACK BODY DISTRIBUTION AT THE TEMPERATURE THAT
C*****CORRESPONDS TO THAT OF THE EFFECTIVE EARTH TEMPERATURE
      DO 4 K=1,50
      BNDENG(K)=XXEN*PRCNT(K)
  4   CONTINUE
```

```
C***** THE DRUDE SUBROUTINE WILL CALCULATE THE INFRA RED ABSORPTANCE OF
C*****THE DETECTOR NODE POINT AS A FUNCTION OF WAVELENGTH OF THE INCIDENT
C*****ENERGY(CONSEQUENTLY,THE TEMPERATURE OF THE SOURCE),THE TEMPERATURE
C*****OF THE DETECTOR NODE POINT,AND ANGLE OF INCIDENCE OF THE PARTICULAR
C*****POINT SOURCE OF INFRA RED ENERGY
      CALL DRUDE(I,J)
C***** VERC(1,J) - THIS IS RETURNED FROM THE DRUDE SUBROUTINE. THIS
C*****QUANTITY IS THE ACTUAL ABSORBED INFRA RED COMPONENT FROM ONE POINT
C*****SOURCE ON THE EARTH TO ONE POINT ON THE DETECTOR SURFACE. THE COUNTER
C*****J IS THE NUMBER OF DISCRETE POINTS ON THE EARTH VISIBLE TO THE
C*****DETECTOR NODE.
C***** TOTABS - THE TOTAL INFRA RED ENERGY ABSORBED BY A PARTICULAR NODE
C*****POINT ON THE DETECTOR SURFACE. THIS QUANTITY IS USED TO OBTAIN THE
C*****INFRA RED ABSORPTANCE FOR THE ENTIRE DETECTOR
    8 TOTABS=TOTABS+VERC(1,J)
C***** TOTIN - THE TOTAL INFRA RED ENERGY INCIDENT ON THE DETECTOR SURFACE
C*****THIS QUANTITY IS USED TO DETERMINE THE INFRA RED ABSORPTANCE FOR
C*****THE DETECTOR SURFACE.
      TOTIN=TOTIN+XXEN
  2   CONTINUE
C***** TINCID - THE COUNTER FOR THE TOTAL INCIDENT INFRA RED ENERGY OVER
C*****THE ENTIRE DETECTOR SURFACE.
      TINCID=TINCID+TOTIN
C***** VERC(4,I) - THE STORAGE LOCATION FOR THE INFRA RED ABSORPTANCE FOR
C*****THE DETECTOR NODE IDENTIFIED BY I
      VERC(4,I)=TOTABS/TOTIN
      EMIT=0.0D0
      TOTAL=0.0D0
      NIN=LIMIT(I)
      IF(NIN.EQ.0) GO TO 6
      TOTAL=TOTABS
C     THE AVERAGE ABSORPTION=EMITTANCE OF ONE NODE POINT FOR ALL SOURCES
```

```
C       OF INFRARED ENERGY INCIDENT ON THE NODE POINT
        TOTAVG=TOTAVG+VERC(3,I)
        TTALW=TTALW+VERC(4,I)
C       THE TOTAL ABSORBED INFRARED ENERGY AT A NODE POINT
        VERC(2,I)=TOTAL
        SUMIN=SUMIN+VERC(2,I)
C       TOTAL INCIDENT INFRARED AT ONE NODE POINT
        H(3,I)=TOTIN
        GO TO 1
    6   VERC(4,I)=0.0D0
        VERC(2,I)=0.0
        H(3,I)=0.0
  1     CONTINUE
        REWIND 1
        IF(LAST.EQ.1) RETURN
C       THE AVERAGE ABSORPTION=EMITTANCE FOR ALL NODE POINTS ON THE DETECTOR
        ELW=TOTAVG/DFLOAT(NPOINT)
C***** ALW - THE INFRA RED ABSORPTANCE OF THE DETECTOR SURFACE FOR ONE
C*****POINT IN ORBIT. THIS VALUE WILL CHANGE AS A RESULT OF THE CHANGING
C*****RADIATION FIALD,TEMPERATURE OF THE DETECTOR,ETC.
        ALW=SUMIN/TINCID
        RETURN
        END
```

```
      SUBROUTINE CRUDE(II,JJ)
C***** THIS SUBROUTINE DETERMINES THE INFRA RED ABSORPTANCE OF THE DETECTOR
C*****SURFACE AS A FUNCTION OF INCIDENT ANGLE OF RADIATION, THE TEMPERATURE
C*****OF THE SOURCE AND THE TEMPERATURE OF THE DETECTOR SURFACE. THIS
C*****SUBROUTINE IS CALLED FROM SUBROUTINE EARTH AND IS ENTERED FOR EACH
C*****DISCRETE POINT SOURCE OF INFRA RED ENERGY INCIDENT ON THE DETECTOR.
      IMPLICIT REAL *8(A-H,O-Z)
      DIMENSION SOURCE(3,211),VERC(5,220),DCCOND(92),BNDEN
     1G(50),XLAMDA(50),TINIT(2,92),BPAR(30),BUF(15),STUCK(92),SOLAB(91),
     2PRCNT(50)
      INTEGER LIMIT(92)
      COMMON/STORE1/ SOURCE,TINIT,DCCOND,AREATH
      COMMON/ STORE2/ STUCK,SOLAB,PRCNT
      COMMON/STORE4/ BNDENG,XLAMDA,XNORML,XPARAL
      COMMON/ACCESS/ LIMIT,NPOINT,NVECTR
      COMMON/CNSTNT/ PI,P2,RADIAN,SIGO,SIG,E,XMNEFF,CO,RSAT,NTS,NPS
      COMMON/LABEL/ VERC,BPAR,BUF,POMEGA,RELAXT,TAU2
      TOTEMT=0.0
C***** THE RELAXATION TIME FOR THE ELECTRONS OF THE CONSTITUENT ATOMS THAT
C*****COMPRISE THE SURFACE. THE RELAXATION TIME IS A FUNCTION OF EFFECTIVE
C*****ELECTRONS PER ATOM(XMNEFF),THE D.C. CONDUCTIVITY OF THE MATERIAL
C*****AND AS A FUNCTION OF TEMPERATURE
      RELAXT=(DCCOND(II)*9.1090-28)/(XMNEFF*E**2)
      TAU2=1./(RELAXT*RELAXT)
      XSIN=DSIN(SOURCE(1,JJ))
      THETA=XSIN*XSIN
      XCOSTH=DCOS(SOURCE(1,JJ))
      ENRIN=XCOSTH*SOURCE(3,JJ)
      COSQRD=XCOSTH*XCOSTH
      XXDIFF=PI*0.5-SOURCE(1,JJ)
      IF(XXDIFF.LT.0.0001) GO TO 2
      XTANTH=DTAN(SOURCE(1,JJ))
```

```
      TANSQD=XTANTH*XTANTH
      TOTEN=0.0
C***** THE 1 DO LOOP WILL ITERATE OVER THE FIFTY DISCRETE WAVELENGTH
C*****BANDS THAT THE INCIDENT POINT SOURCE HAS BEEN DECOMPOSED TO, SO AS
C*****TO ATTEMPT TO MODEL THE MONOCHROMATIC BEHAVIOR OF THE INFRA RED
C*****ABSORPTANCEOF THE SURFACE.
      DO 1 I=1,50
      XOMEGA=CO/XLAMDA(I)
      XOMEG2=XOMEGA**2
      XN2K2=1.0D0-(POMEGA/(XOMEG2+TAU2))
      XNK=(1.0D0/(2.0D0*XOMEGA*RELAXT))*(POMEGA/(XOMEG2+TAU2))
      RADICL=(XN2K2-THETA)**2+4.0D0*XNK**2
      RADSQT=DSQRT(RADICL)
      PART=XN2K2-THETA
      ASQURD=0.5D0*(RADSQT+PART)
      A=DSQRT(ASQURD)
      BSQURD=0.5D0*(RADSQT-PART)
      SUMSQD=ASQURD+BSQURD
      PROD=2.0D0*A*XCOSTH
      XNUMER=SUMSQD-PROD+COSQRD
      DENOM=SUMSQD+PROD+COSQRD
      REFNML=XNUMER/DENOM
      XPROD=2.0D0*A*XSIN*XTANTH
      SQRPRD=THETA*TANSQD
      YNUMER=SUMSQD-XPROD+SQRPRD
      YDENOM=SUMSQD+XPROD+SQRPRD
      REFPAR=REFNML*(YNUMER/YDENOM)
      TOTREF=REFNML*XNORML+REFPAR*XPARAL
C***** ABSIR - THE INFRA RED ABSORPTANCE(ASSUMING THE TRANSMITTANCE IS ZERO)
C*****IS 1- REFLECTANCE,AND THE EQUATION YIELDS THE REFLECTANCE FOR THE SURFACE
      ABSIR=1.0D0-TOTREF
      TOTEMT=TOTEMT+ABSIR*PRCNT(I)
```

```
C***** ENERGY - THE ABSORBED ENERGY WITHIN EACH WAVELENGTH BAND.
      ENERGY=BNDENG(I)*ABSIR
C***** TOTEN - THE COUNTER FOR THE SUMMATION OF THE ABSORBED ENERGY IN
C*****EACH WAVELENGTH BAND.
      TOTEN=TOTEN+ENERGY
  1   CONTINUE
C     VERC(3,JJ) THE AVERAGE EMITTANCE=ABSORPTION OF ONE NODE POINT OVER
C     THE WAVELENGTH BANDS
C     VERC(1,II) IS THE TOTAL ENERGY(INFRARED) ABSORBED BY A NODE POINT
      VERC(1,JJ)=TOTEN
      ABSORB=VERC(1,JJ)/ENRIN
      RETURN
  2   VERC(1,JJ)=0.0
      RETURN
      END
```

```
      SUBROUTINE SOLABS(ABSW,LAST)
C***** THIS SUBROUTINE CALCULATES THE SOLAR ABSORPTANCE FOR THE DETECTOR
C*****SURFACE AS A FUNCTION OF INCIDENT ANGLE OF THE SOLAR ENERGY
      IMPLICIT REAL *8(A-H,O-Z)
      DIMENSION H(3,92),SOLAR(10,10),SOLAB(91),PRCNT(50),STUCK(92)
      INTEGER LIMIT(92)
      COMMON/STORE2/ STUCK,SOLAB,PRCNT
      COMMON/STORE3/ H,SOLAR,HZ,AVG,ALW,ELW
      COMMON/ACCESS/ LIMIT,NPOINT,NVECTR
      COMMON/CNSTNT/ PI,P2,RADIAN,SIGO,SIG,E,XMNEFF,CO,RSAT,NTS,NPS
      XNINTY=PI*0.5*RADIAN
      SUMSOL=0.0D0
      SOLABS=0.0D0
      NP=0
      DO 1 K=1,NTS
C***** THE 1 DO LOOP WILL ITERATE OVER THE NODE POINTS ON THE DETECTOR
C*****SURFACE
      DO 1 I=1,NPS
      NP=NP+1
      IF(K.EQ.NTS.AND.I.EQ.3.AND.LAST.EQ.1) RETURN
      IF(K.EQ.NTS.AND.I.EQ.3) GO TO 11
      IF(HZ.EQ.0.0D0) GO TO 4
      IF(SOLAR(K,I).EQ.XNINTY) GO TO 4
      IF(LAST.EQ.1) GO TO 8
      ANGLE=0.0
      ANGLE2=0.0
C***** THE 10 DO LOOP WILL DETERMINE THE ANGLE OF INCIDENCE(IN DEGREES),
C*****WHICH WILL BE USED TO DETERMINE THE ULTRA VIOLET(SOLAR)ABSORPTANCE
C*****OF THE DETECTOR AS A FUNCTION OF INCIDENT ANGLE
      DO 10 J=1,91
      ANGLE1=ANGLE*RADIAN
      IF(ANGLE1.GT.SOLAR(K,I)) GO TO 2
```

```
      IF(J.GT.1) ANGLE2=ANGLE1
      ANGLE=ANGLE+1.0
   10 CONTINUE
      RETURN
    2 CONTINUE
      DIFF=SOLAR(K,I)-ANGLE2
      RATIO=DIFF/RADIAN
C***** THE SOLAR ABSORPTANCE OF THE NODE POINT ON THE DETECTOR SURFACE
      ASW=SOLAB(J-1)+(SOLAB(J)-SOLAB(J-1))*RATIO
C     INCIDENT SOLAR AT EACH NODE POINT
C***** COSSIN - THE COSINE OF THE INCIDENT ANGLE OF THE SOLAR COMPONENT
    8 COSSIN=DCOS(SOLAR(K,I))
C***** H(1,NP) - THE INCIDENT SOLAR ENERGY AT EACH NODE
      H(1,NP)=COSSIN*HZ
      IF(H(1,NP).LT.0.0D0) H(1,NP)=0.0D0
C***** STIX - THE ABSORBED SOLAR ENERGY AT EACH NODE IN QUESTION
      IF(LAST.EQ.1) ASW=ABSW
      STIX=ASW*H(1,NP)
C***** SOLAR(K,J) - THE STORAGE LOCATION FOR THE ABSORBED SOLAR ENERGY AT
C*****THE NODES ON THE DETECTOR SURFACE DEFINED BY K,I.
      SOLAR(K,I)=STIX
C***** SUMSOL - THE TOTAL INCIDENT SOLAR ENERGY ON THE ENTIRE DETECTOR
      SUMSOL=SUMSOL+H(1,NP)
C***** SULABS - THE ABSORBED SOLAR ENERGY ON THE ENTIRE DETECTOR SURFACE
      SULABS=SULABS+STIX
      GO TO 1
    4 SOLAR(K,I)=0.0
      H(1,NP)=0.0D0
    1 CONTINUE
C***** ABSW - THE EFFECTIVE SOLAR ABSORPTANCE FOR THE ENTIRE DETECTOR
   11 IF(SUMSOL.EQ.0.0D0) GO TO 12
      ABSW=SULABS/SUMSOL
```

```
      RETURN
   12 ABSW=0.0D0
      RETURN
      END
```

```
      SUBROUTINE BLACKB(TEMP)
C***** THIS SUBROUTINE IS USED TO DETERMINE THE BLACKBODY ENERGY
C*****DISTRIBUTION FOR THE INFRA RED ENERGY EMITTED BY AN AREA ON THE EARTH AT
C*****A TEMPERATURE TEMP.
      IMPLICIT REAL *8(A-H,O-Z)
      DIMENSION PRCNT(50),STUCK(92),SOLAB(91),TLAM(93),CONTAN(93),XLAMDA
     1(50)
      COMMON/STORE2/ STUCK,SOLAB,PRCNT
      COMMON/STORE4/ BNDENG,XLAMDA,XNORML,XPARAL
      COMMON/STORE5/ TLAM,CONTAN
      SUM=0.0D0
      DO 1I=1,50
      TLAMDA=XLAMDA(I)*TEMP
      DO2 J=1,93
      IF(TLAM(J).GT.TLAMDA) GO TO 3
  2   CONTINUE
    3 PRCNT(I)=CONTAN(J)-SUM
      SUM=SUM+PRCNT(I)
  1   CONTINUE
      WRITE(6,10) SUM
 10   FORMAT(1H ,4HSUM=,E15.8)
      RETURN
      END
```

0.91873043D-02 0.29052589D-01 0.91695162D-01 0.28791192D-01
0.92027743D-02 0.29055710D-01 0.91638972D-01 0.28792307D-01
0.92107165D-02 0.29063847D-01 0.91631314D-01 0.28805372D-01
0.92237103D-02 0.29082463D-01 0.91589290D-01 0.28819337D-01
0.92227393D-02 0.29092802D-01 0.91700163D-01 0.28841779D-01
0.92352819D-02 0.29109933D-01 0.91594667D-01 0.28858069D-01
0.92377270D-02 0.29118972D-01 0.91577898D-01 0.28877395D-01
0.92469219D-02 0.29130039D-01 0.91582065D-01 0.28888877D-01
0.92506304D-02 0.29135753D-01 0.91588255D-01 0.28906638D-01
0.92438056D-02 0.29143089D-01 0.91504687D-01 0.28912114D-01
0.92305317D-02 0.29151872D-01 0.91526102D-01 0.28931073D-01
0.92215111D-02 0.29156169D-01 0.91466944D-01 0.28926273D-01
0.92314038D-02 0.29155046D-01 0.91426680D-01 0.28935243D-01
0.92344713D-02 0.29150305D-01 0.91391076D-01 0.28922116D-01
0.92375268D-02 0.29146209D-01 0.91380660D-01 0.28926593D-01
0.92371305D-02 0.29138369D-01 0.91486243D-01 0.28909998D-01
0.92249145D-02 0.29126392D-01 0.91500728D-01 0.28901523D-01
0.92302133D-02 0.29109948D-01 0.91511623D-01 0.28875605D-01
0.92248928D-02 0.29093743D-01 0.91439859D-01 0.28868433D-01
0.92293544D-02 0.29091721D-01 0.91400300D-01 0.28854066D-01
0.91336621D-02 0.28876621D-01 0.91619523D-01 0.28634692D-01
0.91631611D-02 0.28880069D-01 0.91564435D-01 0.28634412D-01
0.91747457D-02 0.28889571D-01 0.91552934D-01 0.28645264D-01
0.91861690D-02 0.28892794D-01 0.91579952D-01 0.28645495D-01
0.91924268D-02 0.28893913D-01 0.91525914D-01 0.28651009D-01
0.91967581D-02 0.28888171D-01 0.91387879D-01 0.28645581D-01
0.91854107D-02 0.28892209D-01 0.91401737D-01 0.28649506D-01
0.91967308D-02 0.28891523D-01 0.91312725D-01 0.28655466D-01
0.91953882D-02 0.28897249D-01 0.91353149D-01 0.28657827D-01
0.92035473D-02 0.28908023D-01 0.91379628D-01 0.28672530D-01
0.92014514D-02 0.28916264D-01 0.91424294D-01 0.28678040D-01
0.91919494D-02 0.28919626D-01 0.91408518D-01 0.28687688D-01

0.919563240-02 0.289322540-01 0.914795520-01 0.287086420-01
0.920192640-02 0.289496570-01 0.914211140-01 0.287292970-01
0.919696930-02 0.289575770-01 0.915411020-01 0.287261740-01
0.918800510-02 0.289583670-01 0.915100840-01 0.287323190-01
0.919705490-02 0.289539770-01 0.915503730-01 0.287195300-01
0.921195110-02 0.289445860-01 0.914088320-01 0.287135460-01
0.920279740-02 0.289348890-01 0.913208770-01 0.286989030-01
0.920533520-02 0.289221530-01 0.913323070-01 0.286880970-01
0.920442780-02 0.289096130-01 0.913549040-01 0.286735480-01
0.919068350-02 0.288995750-01 0.913363660-01 0.286671850-01
0.921565180-02 0.288880340-01 0.912780600-01 0.286515910-01
0.921136720-02 0.288780550-01 0.913490830-01 0.286452180-01
0.921490980-02 0.288707700-01 0.913655120-01 0.286355290-01
0.921419510-02 0.288642470-01 0.914090590-01 0.286312950-01
0.921415720-02 0.288570440-01 0.914429570-01 0.286196240-01
0.923038590-02 0.288509760-01 0.914642610-01 0.286178780-01
0.923465620-02 0.288457520-01 0.914434920-01 0.286093120-01
0.924699670-02 0.288439120-01 0.916231500-01 0.286147300-01
0.924571670-02 0.288441030-01 0.916370960-01 0.286099680-01
0.924447300-02 0.288367830-01 0.916949020-01 0.285980390-01
0.924927630-02 0.288239880-01 0.917716150-01 0.285825290-01
0.924762500-02 0.287996580-01 0.918074890-01 0.285571600-01
0.925252410-02 0.288116610-01 0.917721790-01 0.285717080-01
0.933021670-02 0.285954870-01 0.929617330-01 0.283380950-01
0.932561770-02 0.286030370-01 0.930502910-01 0.283463150-01
0.931175960-02 0.286285020-01 0.934820600-01 0.283733250-01
0.931342980-02 0.286197060-01 0.933508710-01 0.283640700-01
0.931712730-02 0.286374020-01 0.934558230-01 0.283833790-01
0.931894110-02 0.286464310-01 0.934868290-01 0.283927700-01
0.931487720-02 0.286554670-01 0.934994910-01 0.284032950-01
0.930854580-02 0.286641990-01 0.934779010-01 0.284125220-01
0.929952710-02 0.286725580-01 0.934253570-01 0.284224380-01

0.918730400-02 0.290525890-01 0.916951620-01 0.287910920-01
0.920207430-02 0.290557100-01 0.916389720-01 0.287923070-01
0.921071650-02 0.290638470-01 0.916313140-01 0.288053720-01
0.922371030-02 0.290824600-01 0.915892900-01 0.288193370-01
0.922273930-02 0.290926020-01 0.917001630-01 0.288417790-01
0.923528190-02 0.291099330-01 0.915946670-01 0.288580690-01
0.923772700-02 0.291189720-01 0.915778980-01 0.288773950-01
0.924692190-02 0.291300300-01 0.915820650-01 0.288888770-01
0.925063040-02 0.291357530-01 0.915882550-01 0.289066380-01
0.924380560-02 0.291430890-01 0.915046870-01 0.289121140-01
0.923053170-02 0.291518720-01 0.915261020-01 0.289310730-01
0.922151110-02 0.291561690-01 0.914669440-01 0.289262730-01
0.923140380-02 0.291550460-01 0.914206800-01 0.289352430-01
0.923447130-02 0.291508050-01 0.913910760-01 0.289221160-01
0.923752680-02 0.291462090-01 0.913806600-01 0.289265930-01
0.923713050-02 0.291383690-01 0.914862430-01 0.289099980-01
0.922491450-02 0.291263920-01 0.915007280-01 0.289015230-01
0.923021330-02 0.291099480-01 0.915116230-01 0.288756050-01
0.922489280-02 0.290937430-01 0.914398590-01 0.288684330-01
0.922935440-02 0.290917210-01 0.914003000-01 0.288540660-01
0.913366210-02 0.288766210-01 0.916195230-01 0.286346920-01
0.916316110-02 0.288800690-01 0.915644350-01 0.286344120-01
0.917474570-02 0.288895710-01 0.915529340-01 0.286452640-01
0.918616900-02 0.288927940-01 0.915799520-01 0.286454950-01
0.919242680-02 0.288939130-01 0.915259140-01 0.286510090-01
0.919675810-02 0.288881710-01 0.913878790-01 0.286455810-01
0.918541070-02 0.288922090-01 0.914017370-01 0.286495060-01
0.919673080-02 0.288915230-01 0.913127250-01 0.286554660-01
0.919588820-02 0.288972490-01 0.913531490-01 0.286578270-01
0.920354780-02 0.289080230-01 0.913796280-01 0.286725300-01
0.920145140-02 0.289162640-01 0.914242940-01 0.286780400-01
0.919194940-02 0.289196260-01 0.914085180-01 0.286876380-01

```
0.92440472D-02 0.29083254D-01 0.91879973D-01 0.28820244D-01
0.92628831D-02 0.29091402D-01 0.91837912D-01 0.28826772D-01
0.92716271D-02 0.29103378D-01 0.91787553D-01 0.28839311D-01
0.92629665D-02 0.29115469D-01 0.91855056D-01 0.28843763D-01
0.92819562D-02 0.29121872D-01 0.91816820D-01 0.28850936D-01
0.92891473D-02 0.29121259D-01 0.91844132D-01 0.28851952D-01
0.92991314D-02 0.29134169D-01 0.91778484D-01 0.28865461D-01
0.93074074D-02 0.29146076D-01 0.91812187D-01 0.28871683D-01
0.93282470D-02 0.29160218D-01 0.91848669D-01 0.28887644D-01
0.93338823D-02 0.29173554D-01 0.91915045D-01 0.28899182D-01
0.93331349D-02 0.29186667D-01 0.91846879D-01 0.28914802D-01
0.93594861D-02 0.29209221D-01 0.91941551D-01 0.28933154D-01
0.93799512D-02 0.29233027D-01 0.91999532D-01 0.28958019D-01
0.93549669D-02 0.29248970D-01 0.91953603D-01 0.28971001D-01
0.93459671D-02 0.29260606D-01 0.92002643D-01 0.28991684D-01
0.93664369D-02 0.29293298D-01 0.92091935D-01 0.29020454D-01
0.93678612D-02 0.29335343D-01 0.92120909D-01 0.29058721D-01
0.93886227D-02 0.29356404D-01 0.92039342D-01 0.29082483D-01
0.93933658D-02 0.29394993D-01 0.91946204D-01 0.29124189D-01
0.94094943D-02 0.29442348D-01 0.92004002D-01 0.29128255D-01
0.94231192D-02 0.29493212D-01 0.91966080D-01 0.29241848D-01
0.94390050D-02 0.29527981D-01 0.92084267D-01 0.29207745D-01
0.94405128D-02 0.29573167D-01 0.92081986D-01 0.29321656D-01
0.94504562D-02 0.29636961D-01 0.92206978D-01 0.29308907D-01
0.94758858D-02 0.29694678D-01 0.92295478D-01 0.29426523D-01
0.95144308D-02 0.29747949D-01 0.92163420D-01 0.29407604D-01
0.95310405D-02 0.29803356D-01 0.92091908D-01 0.29535101D-01
0.95361442D-02 0.29835671D-01 0.92236594D-01 0.29462888D-01
0.95369799D-02 0.29862125D-01 0.92354268D-01 0.29467012D-01
0.95386542D-02 0.29819414D-01 0.92508185D-01 0.29477672D-01
0.95321693D-02 0.29827717D-01 0.92521595D-01 0.29429445D-01
0.95341220D-02 0.29775003D-01 0.92461157D-01 0.29411008D-01
```

0.92890839D-02 0.28680760D-01 0.93368327D-01 0.28430812D-01
0.92913237D-02 0.28688165D-01 0.93258853D-01 0.28440496D-01
0.92953201D-02 0.28694396D-01 0.93208750D-01 0.28447049D-01
0.93273888D-02 0.28611134D-01 0.93182693D-01 0.28354597D-01
0.92988906D-02 0.28699847D-01 0.93140184D-01 0.28454237D-01
0.92966325D-02 0.28704890D-01 0.93077738D-01 0.28458967D-01
0.92935171D-02 0.28709954D-01 0.93046472D-01 0.28465499D-01
0.93029165D-02 0.28714732D-01 0.92860829D-01 0.28469823D-01
0.92955501D-02 0.28718904D-01 0.92780761D-01 0.28476135D-01
0.92905486D-02 0.28722622D-01 0.92740947D-01 0.28478999D-01
0.92667800D-02 0.28726463D-01 0.92700643D-01 0.28484548D-01
0.92535689D-02 0.28730680D-01 0.92616447D-01 0.28487364D-01
0.92692633D-02 0.28734668D-01 0.92573286D-01 0.28493414D-01
0.92752900D-02 0.28739249D-01 0.92514433D-01 0.28495900D-01
0.92735541D-02 0.28744682D-01 0.92437635D-01 0.28503609D-01
0.92654483D-02 0.28750676D-01 0.92334336D-01 0.28507562D-01
0.92589748D-02 0.28756906D-01 0.92219578D-01 0.28516950D-01
0.92494022D-02 0.28763564D-01 0.92145714D-01 0.28521031D-01
0.92517459D-02 0.28770880D-01 0.92049877D-01 0.28531770D-01
0.92441317D-02 0.28779089D-01 0.91969577D-01 0.28536764D-01
0.92461653D-02 0.28788620D-01 0.91906660D-01 0.28549102D-01
0.93441946D-02 0.28629332D-01 0.92725824D-01 0.28336331D-01
0.93626520D-02 0.28611098D-01 0.92574952D-01 0.28321654D-01
0.93670743D-02 0.28591033D-01 0.92581804D-01 0.28305128D-01
0.93593348D-02 0.28577297D-01 0.92428413D-01 0.28295361D-01
0.93533640D-02 0.28565681D-01 0.92368985D-01 0.28283281D-01
0.92159900D-02 0.29037647D-01 0.91848855D-01 0.28776106D-01
0.92232376D-02 0.29041127D-01 0.91861788D-01 0.28776501D-01
0.92314689D-02 0.29047260D-01 0.91844378D-01 0.28785185D-01
0.92269432D-02 0.29053406D-01 0.91858925D-01 0.28788624D-01
0.92343090D-02 0.29060897D-01 0.91884330D-01 0.28799815D-01
0.92353543D-02 0.29071929D-01 0.91886712D-01 0.28806869D-01

```
0.89869465D-02 0.27759289D-01 0.91631144D-01 0.27461862D-01
0.89908481D-02 0.27670866D-01 0.91823875D-01 0.27374318D-01
0.89742247D-02 0.27572641D-01 0.91629695D-01 0.27270339D-01
0.89393239D-02 0.27464354D-01 0.91799454D-01 0.27157811D-01
0.88834222D-02 0.27344208D-01 0.91799450D-01 0.27032833D-01
0.88695990D-02 0.27211901D-01 0.91799447D-01 0.26895503D-01
0.88329204D-02 0.27066423D-01 0.91799443D-01 0.26746579D-01
0.87732306D-02 0.26906998D-01 0.91799439D-01 0.26578732D-01
0.87318927D-02 0.26733053D-01 0.91799436D-01 0.26397460D-01
0.86844085D-02 0.26543553D-01 0.91799432D-01 0.26199905D-01
0.86275141D-02 0.26337682D-01 0.91799428D-01 0.25985138D-01
0.85808695D-02 0.26114933D-01 0.91799424D-01 0.25752193D-01
0.85199836D-02 0.25874716D-01 0.91799421D-01 0.25500771D-01
0.84555409D-02 0.25615858D-01 0.91799417D-01 0.25230012D-01
0.83869684D-02 0.25338918D-01 0.91799413D-01 0.24939612D-01
0.83152289D-02 0.25044935D-01 0.91799409D-01 0.24629423D-01
0.82397205D-02 0.24733135D-01 0.91799406D-01 0.24299413D-01
0.81562630D-02 0.24404015D-01 0.91799402D-01 0.23949763D-01
0.80752178D-02 0.24058384D-01 0.91799398D-01 0.23580980D-01
0.79756989D-02 0.23697159D-01 0.91799395D-01 0.23193870D-01
0.78646740D-02 0.23321067D-01 0.91799391D-01 0.22789437D-01
0.77689854D-02 0.22930015D-01 0.91799388D-01 0.22368891D-01
0.76600344D-02 0.22521686D-01 0.91799385D-01 0.21933493D-01
0.75420375D-02 0.22088909D-01 0.91799383D-01 0.21483714D-01
0.74237399D-02 0.21616726D-01 0.91799380D-01 0.21017462D-01
0.73119309D-02 0.21079249D-01 0.91799377D-01 0.20525700D-01
0.72121412D-02 0.20439185D-01 0.91799374D-01 0.19984840D-01
0.71213696D-02 0.19647651D-01 0.91799371D-01 0.19353436D-01
0.70821848D-02 0.18637219D-01 0.91799368D-01 0.18633155D-01
0.70976332D-02 0.18704524D-01 0.0             0.18703135D-01
0.71132922D-02 0.18773175D-01 0.0             0.18772399D-01
0.71361970D-02 0.18843118D-01 0.0             0.18843158D-01
```

0.95104268D-02 0.29727776D-01 0.92475151D-01 0.29341053D-01
0.95224913D-02 0.29671445D-01 0.92473499D-01 0.29317338D-01
0.95288550D-02 0.29636947D-01 0.92349899D-01 0.29260783D-01
0.95380947D-02 0.29589095D-01 0.92399388D-01 0.29235303D-01
0.95263056D-02 0.29557281D-01 0.92465584D-01 0.29184577D-01
0.95158720D-02 0.29517885D-01 0.92551781D-01 0.29157021D-01
0.92891672D-02 0.28523710D-01 0.91799165D-01 0.28264233D-01
0.92817439D-02 0.28523564D-01 0.91799168D-01 0.28262527D-01
0.92736127D-02 0.28523450D-01 0.91799171D-01 0.28263781D-01
0.92849450D-02 0.28523898D-01 0.91799162D-01 0.28262628D-01
0.92934971D-02 0.28524125D-01 0.91799159D-01 0.28264899D-01
0.92991433D-02 0.28524728D-01 0.91799154D-01 0.28265834D-01
0.93095282D-02 0.28525132D-01 0.91799151D-01 0.28263191D-01
0.93352207D-02 0.28533117D-01 0.91386081D-01 0.28273221D-01
0.93228329D-02 0.28534769D-01 0.91427007D-01 0.28274421D-01
0.93356262D-02 0.28536635D-01 0.91458427D-01 0.28276916D-01
0.93339730D-02 0.28538728D-01 0.91505310D-01 0.28278432D-01
0.93244757D-02 0.28540996D-01 0.91596568D-01 0.28281601D-01
0.93345669D-02 0.28543517D-01 0.91699392D-01 0.28283313D-01
0.93337252D-02 0.28546321D-01 0.91829133D-01 0.28287237D-01
0.93125038D-02 0.28549413D-01 0.91970422D-01 0.28289338D-01
0.93262191D-02 0.28552822D-01 0.92049156D-01 0.28294163D-01
0.93363337D-02 0.28556601D-01 0.92185445D-01 0.28296649D-01
0.93434619D-02 0.28560760D-01 0.92328860D-01 0.28302635D-01
0.93381029D-02 0.28565322D-01 0.92472859D-01 0.28305557D-01
0.93373818D-02 0.28570346D-01 0.92554370D-01 0.28312875D-01
0.93276326D-02 0.28575850D-01 0.92639465D-01 0.28316291D-01
0.93304742D-02 0.28581851D-01 0.92764321D-01 0.28325251D-01
0.93307146D-02 0.28588418D-01 0.92853538D-01 0.28329074D-01
0.93302167D-02 0.28595487D-01 0.92961733D-01 0.28340063D-01
0.90344234D-02 0.27911633D-01 0.91526350D-01 0.27619931D-01
0.90110275D-02 0.27839942D-01 0.91627721D-01 0.27548683D-01

```
0.9202563D-02 0.2836793D-01 0.9075034D-01 0.2809213D-01
0.9196089D-02 0.2834889D-01 0.9074966D-01 0.2807271D-01
0.9186477D-02 0.2832778D-01 0.9077486D-01 0.2805034D-01
0.9180159D-02 0.2830336D-01 0.9080696D-01 0.2802575D-01
0.9171879D-02 0.2827624D-01 0.9086542D-01 0.2799754D-01
0.9106664D-02 0.2824621D-01 0.9090058D-01 0.2796727D-01
0.9098136D-02 0.2821323D-01 0.9081023D-01 0.2793213D-01
0.9118188D-02 0.2817479D-01 0.9112100D-01 0.2789386D-01
0.9092465D-02 0.2813335D-01 0.9118457D-01 0.2785005D-01
0.9072358D-02 0.2808761D-01 0.9120904D-01 0.2780327D-01
0.9069123D-02 0.2803501D-01 0.9136681D-01 0.2774745D-01
0.9040575D-02 0.2797594D-01 0.9146979D-01 0.2768874D-01
0.9336806D-02 0.2852506D-01 0.9204557D-01 0.2824684D-01
0.9331316D-02 0.2851613D-01 0.9193513D-01 0.2824233D-01
0.9333051D-02 0.2850756D-01 0.9183263D-01 0.2823260D-01
0.9312181D-02 0.2849879D-01 0.9172869D-01 0.2822486D-01
0.9339783D-02 0.2849130D-01 0.9164620D-01 0.2821746D-01
0.9299065D-02 0.2848315D-01 0.9155984D-01 0.2820959D-01
0.9292883D-02 0.2847494D-01 0.9147437D-01 0.2820162D-01
0.9285679D-02 0.2846638D-01 0.9138706D-01 0.2819311D-01
0.9266203D-02 0.2845752D-01 0.9129808D-01 0.2818425D-01
0.9344568D-02 0.2855467D-01 0.9232960D-01 0.2827594D-01
0.9343969D-02 0.2854445D-01 0.9222269D-01 0.2826435D-01
0.9347158D-02 0.2853432D-01 0.9214249D-01 0.2825826D-01
0.7148597D-02 0.1891443D-01 0.0       0.1891553D-01
0.7159969D-02 0.1898693D-01 0.0       0.1898956D-01
0.7173153D-02 0.1906054D-01 0.0       0.1906533D-01
0.7180231D-02 0.1913655D-01 0.0       0.1914291D-01
0.7208946D-02 0.1921585D-01 0.0       0.1922228D-01
0.7240396D-02 0.1929723D-01 0.0       0.1930367D-01
0.7264723D-02 0.1938063D-01 0.0       0.1938695D-01
0.7282374D-02 0.1946653D-01 0.0       0.1947258D-01
```

0.83587220D-02 0.24067043D-01 0.91799213D-01 0.24080336D-01
0.84014698D-02 0.24318677D-01 0.91799213D-01 0.24331606D-01
0.84731684D-02 0.24586672D-01 0.91799213D-01 0.24599248D-01
0.85354010D-02 0.24873004D-01 0.91799213D-01 0.24885129D-01
0.86029979D-02 0.25179944D-01 0.91799213D-01 0.25191647D-01
0.86842841D-02 0.25510169D-01 0.91799213D-01 0.25521434D-01
0.87569819D-02 0.25866949D-01 0.91799213D-01 0.25877733D-01
0.88348588D-02 0.26254168D-01 0.91799213D-01 0.26264588D-01
0.89124368D-02 0.26676396D-01 0.91799213D-01 0.26686683D-01
0.90028973D-02 0.27140470D-01 0.91799213D-01 0.27150166D-01
0.90964188D-02 0.27658091D-01 0.91799213D-01 0.27662940D-01
0.91764353D-02 0.28525733D-01 0.91799213D-01 0.28266845D-01
0.91992026D-02 0.28525403D-01 0.91799213D-01 0.28264924D-01
0.92083238D-02 0.28524960D-01 0.91799210D-01 0.28265305D-01
0.92105123D-02 0.28524689D-01 0.91799208D-01 0.28264140D-01
0.92028115D-02 0.28524444D-01 0.91799205D-01 0.28264828D-01
0.92055111D-02 0.28524172D-01 0.91799202D-01 0.28263506D-01
0.92112343D-02 0.28523962D-01 0.91799199D-01 0.28264481D-01
0.92123330D-02 0.28523816D-01 0.91799196D-01 0.28262909D-01
0.92158572D-02 0.28523693D-01 0.91799193D-01 0.28264354D-01
0.91971669D-02 0.28523561D-01 0.91799190D-01 0.28262424D-01
0.92308734D-02 0.28523449D-01 0.91799188D-01 0.28264323D-01
0.92473603D-02 0.28523374D-01 0.91799185D-01 0.28261891D-01
0.92552648D-02 0.28523305D-01 0.91799182D-01 0.28264489D-01
0.92584392D-02 0.28523267D-01 0.91799179D-01 0.28261371D-01
0.92588810D-02 0.28523283D-01 0.91799176D-01 0.28264837D-01
0.92551346D-02 0.28448028D-01 0.91208159D-01 0.28174552D-01
0.92333978D-02 0.28437851D-01 0.91142964D-01 0.28164174D-01
0.92235427D-02 0.28426428D-01 0.91085329D-01 0.28152470D-01
0.92229139D-02 0.28414150D-01 0.90944004D-01 0.28139925D-01
0.92123438D-02 0.28400516D-01 0.90747754D-01 0.28125692D-01
0.92146858D-02 0.28385410D-01 0.90779356D-01 0.28110118D-01

0.931924210-02	0.285267500-01	0.0	0.282665720-01
0.932540220-02	0.285283660-01	0.0	0.282682980-01
0.932751550-02	0.285292360-01	0.0	0.282689290-01
0.932465770-02	0.285303140-01	0.914513390-01	0.282702560-01
0.932711040-02	0.285316360-01	0.913816830-01	0.282712280-01
0.919498830-02	0.290477320-01	0.917572760-01	0.287855680-01
0.944845610-02	0.291431710-01	0.931906690-01	0.287775220-01
0.919772060-02	0.290440580-01	0.917824210-01	0.287787840-01
0.920483260-02	0.290427600-01	0.917837500-01	0.287799780-01
0.920902710-02	0.290388680-01	0.918255940-01	0.287739830-01
0.955735220-02	0.294798890-01	0.925822030-01	0.291004960-01
0.950758860-02	0.294207510-01	0.926941270-01	0.290601630-01
0.950813680-02	0.293778500-01	0.928094870-01	0.290084120-01
0.949620930-02	0.293206940-01	0.928424860-01	0.289743840-01
0.949233210-02	0.293088150-01	0.928448360-01	0.289365520-01
0.943187130-02	0.292653440-01	0.930712880-01	0.288956200-01
0.946874830-02	0.292122070-01	0.930256600-01	0.288333460-01
0.944641900-02	0.290844920-01	0.932006310-01	0.287181640-01
0.943781660-02	0.290018560-01	0.931702120-01	0.286606280-01
0.943619240-02	0.289474820-01	0.931428900-01	0.286246270-01
0.942295570-02	0.289225110-01	0.929755620-01	0.286023240-01
0.938935430-02	0.289045340-01	0.929983330-01	0.285831410-01
0.940917650-02	0.288812050-01	0.930240390-01	0.285603880-01
0.940418450-02	0.288520520-01	0.930561600-01	0.285375060-01
0.939436050-02	0.288295310-01	0.930140450-01	0.285180370-01
0.939594280-02	0.288135250-01	0.929951340-01	0.285014950-01
0.939065310-02	0.287909800-01	0.930446050-01	0.284820470-01
0.938558160-02	0.287703310-01	0.930061080-01	0.284653350-01
0.938834030-02	0.287582510-01	0.929756000-01	0.284488700-01
0.937354310-02	0.287363540-01	0.930738690-01	0.284295630-01
0.937223190-02	0.287078830-01	0.929884620-01	0.284037980-01
0.936815790-02	0.286954950-01	0.927966770-01	0.283946820-01

```
0.73023520D-02 0.19554575D-01 0.0              0.19560442D-01
0.73318269D-02 0.19645140D-01 0.0              0.19650584D-01
0.73554513D-02 0.19738103D-01 0.0              0.19743338D-01
0.73801684D-02 0.19833416D-01 0.0              0.19838391D-01
0.73972264D-02 0.19931302D-01 0.0              0.19936080D-01
0.74230884D-02 0.20031997D-01 0.0              0.20036624D-01
0.74367179D-02 0.20135298D-01 0.0              0.20140084D-01
0.74501351D-02 0.20241530D-01 0.0              0.20246312D-01
0.74722190D-02 0.20350684D-01 0.0              0.20355652D-01
0.75081415D-02 0.20463015D-01 0.0              0.20468134D-01
0.75317181D-02 0.20578644D-01 0.0              0.20583936D-01
0.95366204D-02 0.29832165D-01 0.92302981D-01 0.29511749D-01
0.75579850D-02 0.20697864D-01 0.0              0.20703277D-01
0.75814180D-02 0.20820773D-01 0.0              0.20826525D-01
0.76114924D-02 0.20947530D-01 0.0              0.20953838D-01
0.76370198D-02 0.21078173D-01 0.0              0.21085347D-01
0.76694208D-02 0.21212755D-01 0.0              0.21221408D-01
0.76969870D-02 0.21352536D-01 0.0              0.21362267D-01
0.77368244D-02 0.21498595D-01 0.0              0.21508300D-01
0.77814685D-02 0.21650229D-01 0.0              0.21659815D-01
0.78226969D-02 0.21807864D-01 0.0              0.21817282D-01
0.78498158D-02 0.21971925D-01 0.0              0.21981237D-01
0.78986870D-02 0.22142828D-01 0.0              0.22152007D-01
0.79470206D-02 0.22321150D-01 0.0              0.22330196D-01
0.79932040D-02 0.22507513D-01 0.0              0.22516388D-01
0.80417459D-02 0.22702557D-01 0.0              0.22711245D-01
0.80927717D-02 0.22907641D-01 0.0              0.22915528D-01
0.81360540D-02 0.23121728D-01 0.0              0.23130114D-01
0.81868159D-02 0.23347480D-01 0.0              0.23356046D-01
0.82445801D-02 0.23584493D-01 0.0              0.23594268D-01
0.83147869D-02 0.23830873D-01 0.0              0.23846082D-01
0.92700832D-02 0.28527521D-01 0.0              0.28267097D-01
```

```
0.100D+040.120D+040.140D+040.160D+040.180D+040.200D+040.220D+040.240D+04
0.260D+040.280D+040.300D+040.320D+040.340D+040.360D+040.380D+040.400D+04
0.420D+040.440D+040.460D+040.480D+040.500D+040.520D+040.540D+040.560D+04
0.580D+040.600D+040.620D+040.640D+040.660D+040.680D+040.700D+040.720D+04
0.740D+040.760D+040.780D+040.800D+040.820D+040.840D+040.860D+040.880D+04
0.900D+040.920D+040.940D+040.960D+040.980D+040.100D+050.102D+050.104D+05
0.106D+050.108D+050.110D+050.112D+050.114D+050.116D+050.118D+050.120D+05
0.122D+050.124D+050.126D+050.128D+050.130D+050.132D+050.134D+050.136D+05
0.138D+050.140D+050.142D+050.144D+050.146D+050.148D+050.150D+050.160D+05
0.170D+050.180D+050.190D+050.200D+050.210D+050.220D+050.230D+050.240D+05
0.250D+050.260D+050.270D+050.280D+050.290D+050.300D+050.400D+050.500D+05
0.600D+050.700D+050.800D+050.900D+050.100D+06
0.00000.00000.00000.00010.00030.00090.00250.00530.00980.01640.02540.03680.0506
0.06670.08500.10510.12670.14960.17340.19790.22290.24810.27330.29830.32300.3474
0.37120.39450.41710.43910.46040.48090.50070.51990.53810.55580.57270.58900.6045
0.61950.63370.64740.66060.67310.68510.69660.70760.71810.72820.73780.74740.7559
0.76430.77240.78020.78760.79470.80150.80810.81440.82040.82620.83170.83700.8421
0.84700.85170.85630.86060.86480.86880.88680.90170.91420.92470.93350.94110.9475
0.95310.95890.96210.96570.96890.97180.97420.97650.98810.99410.99630.99810.9987
0.99900.99921.0000
4.560D-040.674D-030.950D-031.286D-031.681D-03
2.130D-032.610D-033.127D-023.512D-023.896D-02
2.243D-022.530D-022.278D-012.296D-012.307D-01
0.315D-010.635D-010.618D-010.586D-010.544D-01
0.499D-010.452D-010.408D-010.367D-010.328D-01
0.294D-010.499D-010.431D-010.323D-010.263D-01
0.214D-010.387D-010.249D-010.166D-010.114D-01
0.081D-010.063D-010.078D-010.046D-010.029D-01
0.021D-010.023D-010.012D-010.007D-010.004D-01
0.003D-010.002D-010.001D-010.001D-010.001D-01
```

```
 0.93750163D-02 0.28676157D-01 0.92839691D-01 0.28374797D-01
 0.93647262D-02 0.28651904D-01 0.92775345D-01 0.28355606D-01
 0.92916032D-02 0.28524399D-01 0.91799156D-01 0.28262841D-01
 0.93175990D-02 0.28525575D-01 0.91799148D-01 0.28267157D-01
 0.37635037D 03 0.37634424D 03 0.38044477D 03 0.38651613D 03 0.38969362D 03
 0.39079004D 03 0.38969496D 03 0.38652717D 03 0.38046105D 03 0.37635137D 03
 0.37637102D 03 0.37635986D 03 0.37636094D 03 0.38630902D 03 0.39052220D 03
 0.39211766D 03 0.39051208D 03 0.38632864D 03 0.37637907D 03 0.37637472D 03
 0.37639029D 03 0.37637708D 03 0.37635872D 03 0.38572926D 03 0.39058953D 03
 0.39289333D 03 0.39060297D 03 0.38575191D 03 0.37638556D 03 0.37638994D 03
 0.37640756D 03 0.37639391D 03 0.37638063D 03 0.38507188D 03 0.39025360D 03
 0.39226067D 03 0.39026981D 03 0.38509428D 03 0.37640831D 03 0.37641463D 03
 0.37643123D 03 0.37641281D 03 0.37639525D 03 0.38424093D 03 0.38952055D 03
 0.39155919D 03 0.38953722D 03 0.38426709D 03 0.37642100D 03 0.37643175D 03
 0.37644996D 03 0.37643415D 03 0.37641609D 03 0.38223490D 03 0.38848457D 03
 0.39048161D 03 0.38850366D 03 0.38226943D 03 0.37644391D 03 0.37645725D 03
 0.37647346D 03 0.37645668D 03 0.37643509D 03 0.37927997D 03 0.38713147D 03
 0.38887878D 03 0.38714904D 03 0.37931731D 03 0.37646749D 03 0.37647988D 03
 0.37649614D 03 0.37648063D 03 0.37645829D 03 0.37644320D 03 0.38517732D 03
 0.38684352D 03 0.38519594D 03 0.37646845D 03 0.37649060D 03 0.37650341D 03
 0.37651031D 03 0.37650223D 03 0.37648543D 03 0.37647079D 03 0.38027413D 03
 0.38335984D 03 0.38029007D 03 0.37649540D 03 0.37650797D 03 0.37651212D 03
 0.37651209D 03 0.38538776D 03 0.32000000D 03 0.32000000D 03 0.32000000D 03
 0.32000000D 03 0.32000000D 03 0.32000000D 03 0.32000000D 03 0.32000000D 03
 00 0.12005187D 04
0.08000.07990.07970.07950.07930.07900.07870.07850.07840.07820.07800.07820.0782
0.07820.07830.07840.07850.07860.07870.07880.07900.07910.07920.07930.07940.0795
0.07960.07970.07980.07990.08000.08050.08100.08130.08170.08200.08220.08260.0830
0.08350.08370.08400.08420.08480.08520.08560.08600.08650.08710.08800.08850.0890
0.09000.09100.09150.09250.09350.09420.09600.09700.09800.09900.10100.10200.1035
0.10500.10650.10850.11100.11400.11620.12000.12500.12800.13000.13300.13400.1350
0.13500.13500.13450.13400.13200.12950.12600.12300.11500.08000.05900.01800.0000
```

The vita has been removed from the scanned document

DETAILED THERMAL ANALYSIS OF A THIN-SHELL, SPHERICAL RADIOMETER IN EARTH ORBIT

by

John Oliver Passwaters, III

(ABSTRACT)

An exact energy balance is conducted on a spherical thermal radiation detector. The thermal radiation heat transfer to the spherical detector is computed utilizing models of the surface optical properties that vary with surface temperature, wavelength and angle of incidence. Studies have been conducted to analyze the detector under the assumptions of gray, diffuse radiation and constant thermophysical properties. The previous studies have been helpful in developing the theory of operation of such detectors. However, the extreme accuracy required in the experiment necessitates an assessment of the effects of non-gray and non-diffuse radiation and surfaces on the detector behavior.

The effects of non-gray and non-diffuse radiation and surfaces on the detector behavior is assessed by non-dimensionalizing the energy balance. Three correction factors are developed to describe the behavior of the three components of radiant flux incident to the detector. The correction factors are developed to equal unity for a perfectly diffuse gray radiation and surfaces.

The realistic model of the surface optical properties for an aluminum detector consists of independent models of emittance, long wavelength absorptance, and solar absorptance. The emittance as a function of temperature was determined from the Davisson and Weeks analytical expression. The long wavelength absorptance as a function of incident angle, wavelength, and temperature was determined by utilizing Fresnel's equations in conjunction with the Drude-Zener theory to obtain the complex index of refraction. The solar absorptance as a function of incident angle was determined from the experimental results of M. G. Hoke.

The results of the analysis reveals that the earth radiation field is not diffuse. The polar ice caps were found to reflect incident solar radiant flux specularly to the spherical detector. The absorptance of the earth-reflected solar component as a function of incident angle is important and responded to the specularly reflected solar flux as the detector passed over the ice caps. The model for the long wavelength absorptance of the aluminum detector is incorrect. The model produced values of absorptance one-third of the value of emittance. The temperature dependence of the emittance is found to be significant in the detector behavior. The results of the non-dimensional correction factors are found to be inconclusive. The error in the long wavelength absorptance distorts the correction factors and renders them useless.